Wavelength reconfigurability for next generation optical access networks

DOI:
10.6100/IR751519

Document status and date:
Published: 01/01/2013

Document Version:
Publisher's PDF, also known as Version of Record (includes final page, issue and volume numbers)

Wavelength Reconfigurability for Next Generation Optical Access Networks

PROEFSCHRIFT

ter verkrijging van de graad van doctor aan de
Technische Universiteit Eindhoven, op gezag van de
rector magnificus, prof.dr.ir. C.J. van Duijn, voor een
commissie aangewezen door het College voor
Promoties in het openbaar te verdedigen
op woensdag 27 maart 2013 om 16.00 uur

door

Trần Nguyên Các

geboren te Hanoi, Vietnam

Dit proefschrift is goedgekeurd door de promotor:
prof.ir. A.M.J. Koonen

Copromotor:
dr. C.M. Okonkwo

This Ph.D. thesis has been approved by a committee with the following members:

prof.dr.ir. A.C.P.M. Backx (chairman), Eindhoven University of Technology (TU/e)
prof.ir. A.M.J. Koonen (first promoter), Eindhoven University of Technology (TU/e)
dr. C.M. Okonkwo (co-promoter), Eindhoven University of Technology (TU/e)
prof.dr.ir. M.K. Smit, Eindhoven University of Technology (TU/e)
prof.dr. M. Gagnaire, Télécom ParisTech University
dr. M. Popov, Acreo Swedish ICT AB
prof.dr. A. Stavdas, University of Peloponnese (UoP)
dr. B. Lannoo, Ghent University (UGent)

The work described in this thesis was performed in the Electro-optical Communications Systems Group, the Department of Electrical Engineering of the Eindhoven University of Technology, The Netherlands. It was financially partly supported by the European Commission (EC) funded 7th Framework project ALPHA – Architectures for fLexible Photonic Home and Access networks.

A catalogue record is available from the Eindhoven University of Technology Library

Nguyen-Cac Tran

Wavelength reconfigurability for next generation optical access networks / by Nguyen-Cac Tran - Eindhoven: Technische Universiteit Eindhoven, 2013.
Proefschrift - ISBN: 978-90-386-3354-1
NUR 959
Trefw.: optische telecommunicatie / breedbandcommunicatie / mobiele radiocommunicatie
Subject headings: optical fiber communications / optical access networks / wavelength reconfigurability / radio-over-fiber

Printed in The Netherlands.

"Nguyên Các của cha đã chào đời
Oa oa tiếng khóc giữa đất trời
Thế gian thêm một người trung nghĩa
Con góp với đời một nhành hoa"

Trần Văn Phú, 18-06-1982

Literal English Translation:

"Nguyen-Cac, my little son, just was born
Oa oa, you declare yourself to the world
One more faithful person, the world has
A flower branch, you will contribute to the society"

Van-Phu Tran, 18-06-1982

WAVELENGTH RECONFIGURABILITY FOR NEXT GENERATION OPTICAL ACCESS NETWORKS

The global Internet traffic has increased exponentially in recent years and the trend is set to continue growing at a rate of 32% per year [1]. Besides the volume, busy hours are busier because of a new mix of traffic types. The higher level of traffic surge in conjunction with a sharp growth of the mobile generated traffic results in new patterns in the network traffic in which large temporal and spatial variations are observed. To cope with new patterns, next generation optical access networks should not only have larger capacity but also be able to redistribute the network capacity on the fly. Wavelength reconfigurability is the instrument to create such redistribution capability since it allows the dynamic sharing of both wavelengths and timeslots. Wavelengths no longer act as disjointed bandwidth pools which could be congested while the others are largely free. However, wavelength reconfigurability requires a substantial addition to capital expenditure (CAPEX) per user, which is certainly prohibitive for an access network technology. Therefore, this thesis investigates methods to implement wavelength reconfigurability in WDM-TDM optical access networks in an economically-viable manner.

A parameter designated as the degree of flexibility is proposed to indicate the level of reconfigurability of networks. Existing architectures based on wavelength selection (wavelength flexibility is performed at the user side) and wavelength routing (wavelength flexibility is performed by the remote node) are reviewed and positioned in the degree of flexibility scale. By analytical and simulation analyses, the blocking probability and the power consumption are shown to be significantly reduced by increasing the degree of flexibility from the static to a limited degree. A highly or fully flexible architecture can further improve the performance but with smaller margins. To illustrate how the limited flexibility can help to reduce network cost, Broadcast-and-Select, which is a well-known reconfigurable architecture, is modified to reduce the requirement of power loss budget.

The concept of limited flexibility is further developed to the concept of cyclically-linked flexibility. In cyclically-linked networks, the ONU needs to switch only within a subset of two wavelengths, however, the cyclically-linked structure of wavelengths allows free bandwidth blocks to be moved from one wavelength to any other wavelength by a rearrangement process. The cyclically-linked flexibility can reduce the CAPEX since wavelength tuning can be avoided by employing a low-cost dual non-tunable transceiver at the ONU. Heuristic rearrangement algorithms are developed and implemented by C/C++ in the OPNET network simulator to demonstrate that the cyclically-linked flexibility closely performs to the full flexibility in terms of blocking probability, packet delay, and packet loss. Furthermore, the rearrangement process is demonstrated to have a minimum impact to in-service ONUs.

To implement the concept of cyclically-linked flexibility, a family of four physical implementations is proposed, each addressing a different deployment scenario. The first architecture, Passive-components-based Reconfigurable Optical Access network architecture (PRO-Access), achieves the wavelength flexibility by using dual remote-seeded transceivers, a carefully designed wavelength plan, and a unique configuration of the passive remote node (RN). This architecture is implemented as a proof-of-concept demonstration with bidirectional 10Gbps transmission using reflective electro-absorption modulators (REAM). In the wavelength dimension, the architecture is scalable because this architecture only requires 3-dB more in the power loss budget in comparison to the static architecture regardless of the number of wavelengths.

The second architecture, Wavelength Converted Long-reach architecture (WCL-Access), is designed for long-reach PONs with the objective of using readily available components in the ONU. The ONU interfaces with the network through GPON and XGPON wavelength windows, hence it can employ similar optics and electronics as designed for GPON and XGPON. In the RN, the broad wavelength windows are converted to DWDM wavelengths by all-optical wavelength converters or O/E/O transponders. Since one converter is shared by many ONUs, its cost is justified by the reduced cost of ONUs.

The third architecture, a Power-Splitter-Based architecture (PSB-Access), is designed with an objective of implementing wavelength reconfigurability for NG-PON2 (four TDM-PONs on the power-splitter-based outside plant). Wavelength reconfigurability is realized by a dual fixed transceiver and a pluggable passive wavelength selector at the ONU. The performance comparison between PSB-Access and the wavelength-tuned NG-PON2 reveals that no significant difference is observed while PSB-Access can avoid the cumbersome wavelength tuning.

The forth architecture, a cyclically-linked protection architecture, shows that the concept of cyclically-linked flexibility can be exploited not only for wavelength reconfigurability but also for network protection. Multiple legacy PONs are joined together in the cyclically-linked configuration to provide a full and cost-effective protection. The cyclically-linked protection is demonstrated to be fully resilient in the event of a feeder fiber cut or a line card failure. The cyclically-linked protection can be applied directly to current PON standards since it can be regarded as a modified type C protection specified in ITU-T 983.5.

Therefore, PRO-Access is suitable for new deployments and disruptive upgrades in which the network reach is not longer than 20 km. WCL-Access is suitable for metro-access merger with the reach up to 100 km. PSB-Access is suitable to implement directly on power-splitter-based PON deployments, which allows coexistence with current technologies. The cyclically-linked protection architecture can be used with current and future PON standards when network protection is required.

To natively support radio signals, I propose two application-specific reconfigurable architectures for radio signal delivery. The active routing architecture is designed for dynamic cell capacity assignment in cellular networks. This architecture is proof-of-concept demonstrated in which an additional radio channel is dynamically assigned to the remote antenna unit by means of wavelength switching at the RN. The result shows that the allocation time is less than 450 ns and the impact to the existing radio channel is negligible. The second architecture is designed to provide reliable and high speed network connections to train passengers using the concept of moving cell. It employs inexpensive slowly-tunable lasers in the central office and passive add/drop multiplexers in the field. Proof-of-concept is carried out with bidirectional transmission of OFDM signals in which the handover time between remote antenna units is set to be 1ms and can be adjustable.

CONTENTS

CHAPTER 1

THE ROAD TO FUTURE SMART ACCESS NETWORKS

Communication networks have been a key enabler of the information age in which the access part up until recently is the bandwidth bottleneck. Fiber-optics is thought to ultimately solve the access bottleneck since it has essentially unlimited bandwidth potential with much longer reach than other technologies. The available bandwidth should be used in smart ways in order to reduce the power consumption and to cope with traffic dynamics driven by user demands. In particular, this thesis promotes wavelength reconfigurability as a crucial feature for future access networks by investigating and validating novel cost-effective reconfigurable architectures. Using a top-down approach, the performance analysis in the logical layer inspires new architectural designs which subsequently are demonstrated by proof-of-concept experiments in the physical layer.

This introductory chapter identifies the driving force behind the need for more capacity and more intelligence in the network in Section 1.1. Section 1.2 presents a brief overview of current access technologies while requirements and candidates for next generations are described in Section 1.3. WDM-TDM optical access networks, as a prominent candidate, are elaborated in detail in this section. Finally, the contribution and the scope of this thesis are outlined in Section 1.4.

1.1. Entering the Cloud Computing Era

1.1.1. Bandwidth Demand – Bandwidth Availability Innovation Cycle

Storing huge collections of songs, images, and videos in local machines for playback is gradually becoming obsolete. Why do we have to store those files locally when there are plenty of free or cheap online storage services? We can upload and retrieve multimedia files by any device with a decent Internet connection. In fact, the availability of broadband (few Mbps) Internet connection has transformed not only our file storing habit but also brought us to the start of the cloud computing era. The Internet becomes a global computer where your processing and storing power are located somewhere else (in the cloud) while your local devices such as laptops, smartphones or tablets just function as content renderers as shown in Fig. 1.1 [2]. Users gradually change from desktop-based applications to cloud-based ones. As the computer cannot work without high-speed data bus, a broadband Internet connection is one of the prerequisites for cloud computing.

The acceleration of cloud computing was triggered in late 1990's when digital subscriber line (DSL) technology was massively installed. Coexisting on the legacy telephone twisted pair copper wires, the first generation of DSL can provide always-on Internet connection in a range of hundreds of kbps to 1 or 2 Mbps. That bandwidth is enough to flourish early cloud-based services, e.g., Gmail and Rapidshare services. Video sharing and streaming did not enter the mainstream yet because of the limited bandwidth in both core and access networks. The network capacity continues to grow in response to demands and new ideas for services started to flourish on the new level of bandwidth availability. YouTube, the most popular video-sharing platform, is a prominent example of businesses that successfully took the chance and continues to improve the service quality according to the bandwidth availability. The first YouTube video, entitled “me at the zoo”, was uploaded on April 23, 2005. The clip was 19 seconds long at a poor resolution of 320x240 pixels. In 2012, YouTube allows hour-long clips with 1080p high definition (HD) and 3D videos to be uploaded and streamed. Therefore, bandwidth demands lead to a higher level of bandwidth availability that in turn creates a better condition for developers to come up with even higher bandwidth-intensive applications. The innovation cycle for bandwidth demand and bandwidth availability has been formed and steadily revolved.

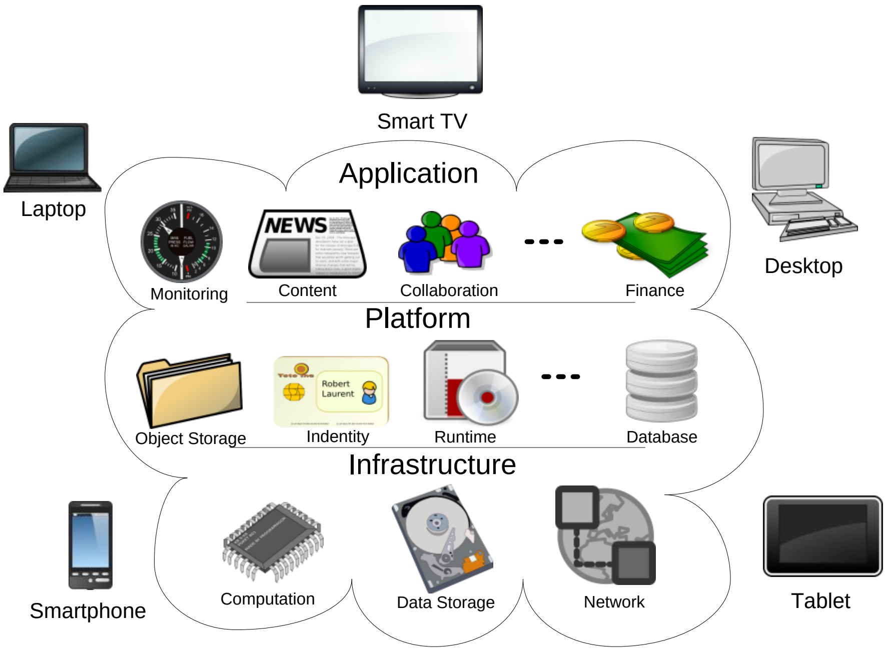

Fig. 1.1. Cloud computing conceptual diagram where storage and processing powers are in the cloud and used by networked devices

The demand side is well reflected by the exponential growth of traffic volume. Cisco has estimated the global IP traffic volume to evolve from 2000 to 2015 as shown in Fig. 1.2 [1][3]. The volume has increased eightfold over the past 5 years, and will increase fourfold over the next 5 years. In 2015, global IP networks will deliver 7.3 petabytes every 5 minutes, which is equivalent to 1.55 million DVD disks. The spectacular growth could not happen and maintain its pace without innovations in network technologies. In order to server more users with new services and better quality, installations of more network equipments and fibers are not enough. Network operators require new technologies since they are also under a heavy pressure to reduce capital expenditure (CAPEX) and operational expenditure (OPEX). Furthermore, higher deployed capacity leads to higher chance of the inefficient use of network resources, which eventually results in unnecessary high CAPEX and OPEX. Therefore, smart technologies are inevitably desirable for traffic engineering and network engineering to guarantee efficiency since demands are not constant in terms of time and location.

1.1.2. **Temporal Traffic Variations**

The rapid increase of network traffic volume is driven by new services, new networked

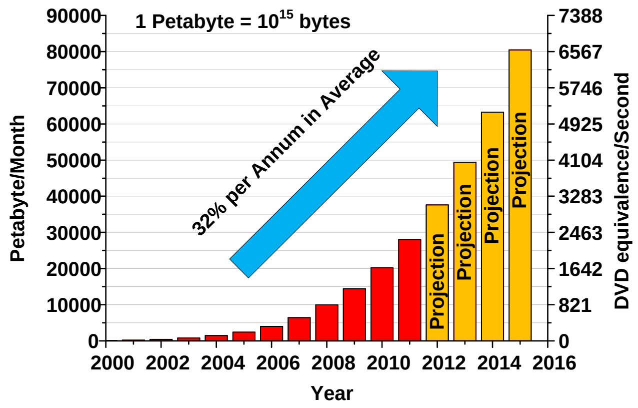

Fig. 1.2. Global IP traffic from 2000 to 2015, compiled from Cisco VNI index and Wikipedia.

TABLE 1.1. PEAK VERSUS AVERAGE FROM APPLICATION CATEGORIES, 3RD QUARTER 2010.

	Volatility*	**Peak-Hour-to-Average Ratio***
Gaming Consoles	63%	2.19
Voice and Video Communications	56%	1.87
Data Communications	54%	2.14
Online Video	53%	1.91
Data	49%	1.71
Other File Sharing	42%	1.77
P2P	33%	1.61

* Volatility is calculated as the standard deviation of hourly volumes, divided by the hourly average. Peak to average is the ratio of the volume of the maximum hour to the volume of the average hour.

devices, and newly-joined users. This evolution of the network ecosystem has made a great impact to traffic patterns. Peer-to-Peer (P2P) traffic, for example, is relatively constant over time as a result of the usage pattern where computers automatically run 24/7 for exchange of files. Therefore, P2P traffic expresses a small peak hour to average hour ratio and volatility as shown in Table 1.1. The low volatility means that the traffic spreads more evenly over 24 hours. Other types of network usages show more dynamic traffic patterns than P2P. Traffic from gaming consoles is highly variable because consoles only generate traffic with the user attendance. The variation in video traffic can be explained in a similar way where users tend to watch videos during the prime time in the evening. Therefore, busy hours are busier on a network that carries more traffic generated from applications in upper rows of Table 1.1 than from those in the lower rows.

Although P2P is still growing in absolute terms, for the first time in 10 years, it was surpassed in 2010 by online video as the most dominant Internet traffic. The share of P2P was 38% of the global broadband traffic in 2009 and sharply decreased to 24.9% in 2010 while online video reached 26.2% in 2010 [4]. The video traffic is expected to expand its share in the coming years. Therefore, it is forecasted that the busy-hour traffic will increase fivefold in the period between 2010 to 2015, while the average traffic will increase at a slower pace of fourfold [1].

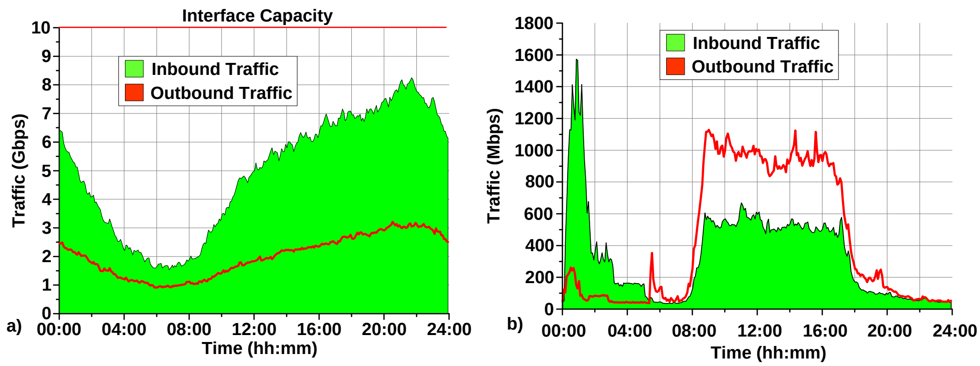

Fig. 1.3. Daily traffic profiles from central offices of Dutch royal telecoms KPN recorded in 2012, a) mixed consumers and businesses in Amsterdam, b) businesses in Rotterdam.

As an example of traffic variation in 24 hours, typical access traffic profiles from the Dutch telecoms KPN network operator are shown in Fig. 1.3. The profile in Fig. 1.3.a) reflects closely the user behavior as 9am is the start of office hours for business users and 11pm is the start of bedtime for consumer users. The low traffic between 4am to 8am is mainly attributed to P2P as the application keeps working without the user being present. The profile of business users in Fig. 1.3.b) shows a higher magnitude of variation because of the smaller diversity in the types of users. The office hours from 9am to 5pm experience a stable traffic level while outside that period almost no traffic is observed since there is no P2P traffic in this network. An exception is observed for 2 hours after the midnight, a steep peak occurs because of database backups. Since these profiles are at a relatively high aggregation level of more than one thousand subscribers, peaks and notches from individual subscribers are already averaged out. If these profiles are broken down to lower aggregation levels, we could see larger variation magnitudes.

1.1.3. Spatial Traffic Variations

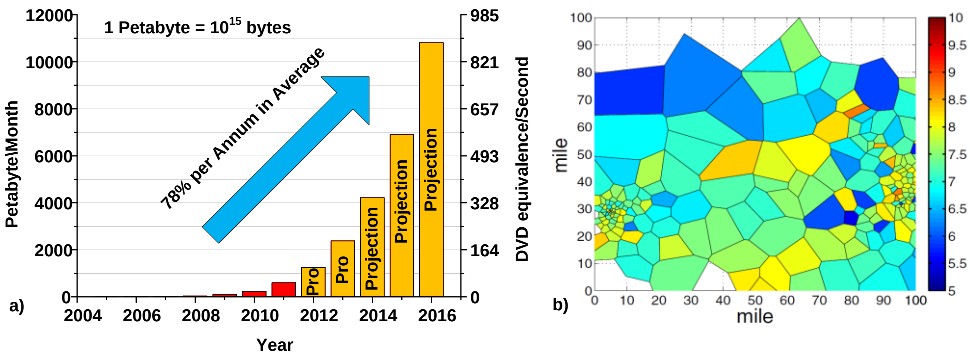

Fig. 1.4. a) Global data mobile traffic from 2005 to 2016, compiled from Cisco VNI mobile and Wikipedia, b) Spatial distribution of total load in a mobile network, the color bar on the right hand side indicates the load level in bytes in $\log_{10}$ scale (courtesy Utpal Paul, INFOCOM 2011).

As discussed in the previous section, traffic temporal variations can be seen in any aggregation level. An analogous phenomenon can also be observed in the geographical dimension. For example, business or industrial areas have high demands during the office time while residential areas have high demands in the evening. If we further zoom in on a residential area, small events such as a birthday party can generate substantial traffic due to the popularity of smartphones and tablets. In the party, some people can record clips and upload to social networks while others show their friends photos from an online storage. As a result, traffic dynamics in location are not only caused by area types but also by the popularity of portable networked devices.

The trend in rapid adoption of smartphones and tablets is clearly seen in the global mobile traffic as shown in Fig. 1.4.a) [3][5]. The mobile traffic in 2011 was eight times the size of the entire global Internet in 2000. Over the period between 2011 and 2016, the mobile traffic will experience an 18-fold increase resulting in a spectacular growth of 78% annually. The traffic growth is not only due to the number of devices but also to the average traffic volume generated by a device. The average amount of traffic per smartphone in 2011 was 150 MB per month, up from 55 MB per month in 2010. In fact, Fig. 1.4.a) only shows traffic transited on cellular mobile networks but not all traffic originated from mobile devices. It is estimated that 33% of the mobile-device-generated traffic was offloaded onto the fixed network through Wi-

Fi or femtocell in 2011. Without offload, the traffic would have been 217 petabytes per month rather than 147 petabytes per month in 2011 [5]. Note that after the wireless transmission in cellular networks, mobile backhaul access networks subsequently carry the mobile traffic. Therefore, future full service access networks have to adequately transport both offloaded traffic as well as cellular mobile traffic.

Traffic originated from mobile devices are highly location dependent leading to hotspots in the geographical dimension. Traffic jams, football matches, and the like potentially create hotspots as shown in Fig. 1.4.b) [6]. Users in the hotspot will experience severe degradation in service quality if network capacity serving the hotspot is not adjusted according to the demand.

1.1.4. Implications of Traffic Dynamics

High temporal and spatial variations of network traffic pose a great challenge for access network operators in capacity planning. Over-provisioning is a popular method to solve the network congestion. However, as the peak traffic from a hotspot reaches a regime of several Gbps or more, over-provisioning becomes extremely inefficient. Any location could be a hotspot leading to massive over-provisioned capacity. To avoid huge network resources wasted for most of the time, smart access networks, which can divert capacity to any hotspot location on demand, are an essential requirement to sustainably evolve further in the cloud computing era.

1.2. Broadband Access Networks: Current Technologies

1.2.1. Copper-Based and Wireless Access Technologies

Telephone local loops were the most widely deployed access networks in early days since telephone was the only consumer telecommunication service for many decades. When the data service entered the mainstream along with the development of Internet, exploiting existing telephone wires to deliver data was a natural choice. The very first technology, called dial-up, modulates data within the telephone frequency band between 300 Hz to 3.3 kHz. The modulated data from the user modem is treated as a normal voice call and routed via the public switched telephone network (PSTN) to the internet service provider (ISP). Dial-up provides a maximum of 56 kbps access rate but in the most cases 40 to 50 kbps is the norm due to various impairments.

When rich-media web contents require higher bit rates, the 56 kbps fundamental limit of Dial-up was not enough leading to the need for broadband access technologies. The term "broadband" was originally designated to any access technology that can deliver better bit rates than Dial-up [7].

Digital Subscriber Line

To transfer higher data rates, the digital subscriber line (DSL) technology was proposed by using the upper frequency band above the voice band of the twisted pair as shown in Fig. 1.5.a). The upstream (towards the network) and the downstream (towards the user) data are modulated to fit within this upper band. Since local loops were originally engineered for the telephone service (<4 kHz), its frequency response at higher frequencies heavily depends on the loop length and the loop quality. The DSL usable bandwidth drops quickly in longer loops. In addition, the unshielded twisted pair is subjected to crosstalk from other pairs in the same cable and electromagnetic interference (EMI) from radio ingress. Very high speed DSL 2 (VDSL2), the highest speed version of DSL, deteriorates quickly from a theoretical maximum rate of 250 Mbps at 0 km to 100 Mbps at 0.5 km [8].

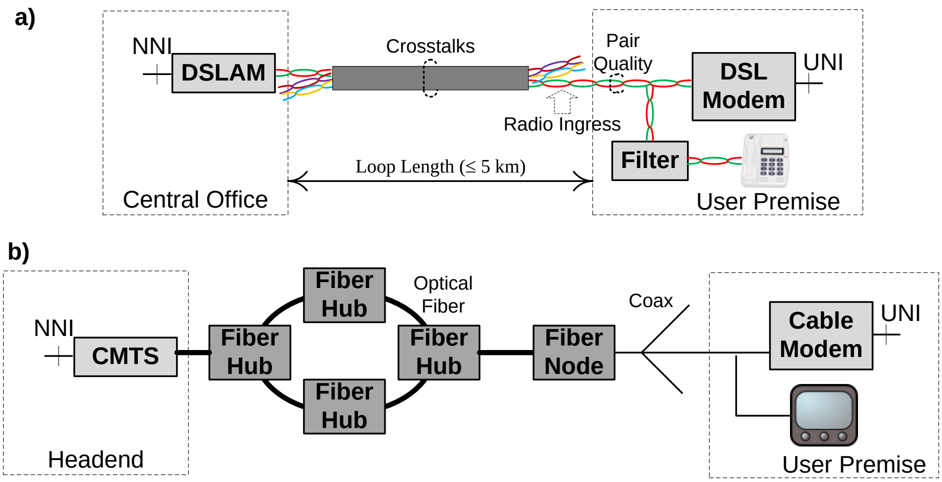

DSLAM – Digital Subscriber Line Access Multiplexer; CMTS – Cable Modem Termination System;
UNI – User Network Interface; NNI – Network Network Interface

Fig. 1.5. Copper-based technologies, a) Digital subscriber line technology, b) Hybrid fiber coax technology.

Asymmetrical DSL (ADSL) and its extension ADSL2+, the most widely deployed versions of DSL, can offer a theoretical downstream rate between 8 and 24 Mbps and a upstream rate between 1 to 3.3 Mbps while the practical speed is in a range of 2.5 to 3.5 Mbps for downstream and lower for upstream [9]. In order to provide the triple play service (voice, video, and data) via DSL, many service providers have to shorten the loop length by using fiber-optics in conjunction with DSL. Those schemes are referred as Fiber to the Curb (FTTC) or Fiber to the Node (FTTN), which is discussed in detail in Section 1.2.2. The DSL loop length (VDSL2) has to be shorted to around 1km to achieve 50Mbps [10]. The DSL power consumption increases rapidly with the bit rate and the loop length because of high attenuation, especially the high frequency region. Therefore, shortening the loop length also helps to reduce the DSL power consumption [11][12].

Hybrid Fiber Coax

Another copper-based major access technology is hybrid fiber coax (HFC), which was originally designed for the cable TV industry. The coaxial cable runs from the user cable modem to the fiber node located in the neighborhood and after that point the optical fiber is used to connect to the operator cable headend as depicted in Fig. 1.5.b). The downstream and upstream data channels are embedded in spectrum segments, which are not occupied by TV channels. The bandwidth limitation of HFC is determined by the coax segment. However, the bandwidth and impairments of TV coaxial cables are much better than those of unshielded twisted pairs. HFC can provide a higher aggregate bit rate than DSL by using larger bandwidth and high-order modulation formats up to 256-QAM (Quadrature Amplitude Modulation). However, that capacity is shared among users in the same coax branch, e.g., 32 data users per branch, resulting in a lower speed for each individual user. Data over cable service interface specification (DOCSIS), the standard for data transfer over HFC, typically can provide in a range of 8 to 11 Mbps downstream and 1 to 4 Mbps upstream speed per user [9]. DOCSIS 3.0, the latest DOCSIS version, allows higher speeds by bonding multiple TV channels together and other advanced signal processing techniques.

Broadband Powerline

Broadband powerline access (BPL) leverages existing electrical power distribution networks to provide broadband services. It is argued to have a high potential because powerlines are installed virtually everywhere. However, power distribution networks were not engineered for communication leading to a large variation and unpredictable in BPL performance. BPL speeds are comparable to that of DSL and HFC in networks with favorable physical characteristics. Since data is transferred through powerlines in a high frequency band, unwanted radiations to environment create concerns among aviation, commercial, amateur radio, and other sectors of spectrum users. Therefore, BPL is a higher risk business than other fixed access technologies that prevents BPL to be fostered [13].

Fixed Wireless Access

There is a range of wireless access technologies including worldwide interoperability for microwave access (WiMAX), satellite, cellular network, even Wi-Fi. Among them, WiMAX and satellite are two popular methods which technically can deliver bit rates in the regime of hundreds Mbps but practical speeds are around 1.3 Mbps [9].

Surplus capacity from mobile cellular networks also can be used for fixed access. 4G cellular networks can offer peak rates in a range of hundreds Mbps but drop sharply when the air gets congested. Therefore, cellular networks only can be regarded as an alternative for other fixed access technologies in some special circumstances [14]. Wi-Fi also can be used for the last leg between the utility pole to the user home with a distance typically below 100 m. It can deliver bit rates typically around 100 Mbps and up to 300 Mbps with MIMO (multiple input multiple output) but the actual rate depends on the backhauling technology.

Wireless access is an economical method to provide broadband access in low populated areas. However, it is expected to have a small share in comparison to other mainstream access technologies due to the shortage of frequency spectrum. Mobile services certainly have higher priority to use this limited resource than fixed access services.

1.2.2. **Fiber-Optic Access Technologies**

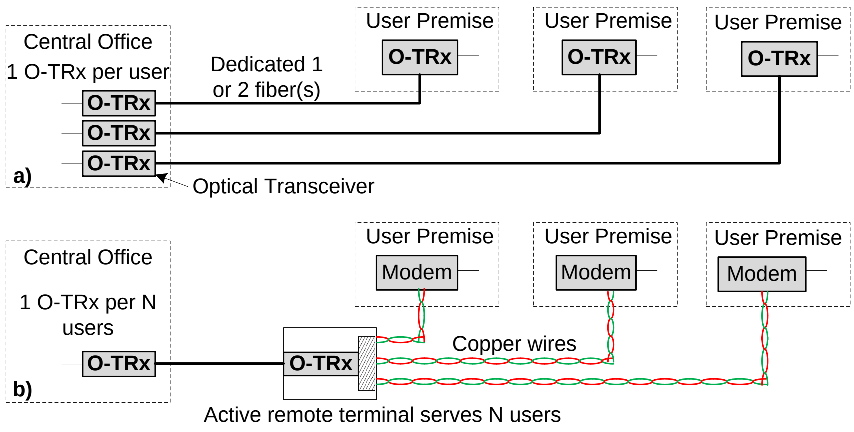

Fig. 1.6. Point to point optical access networks, a) FTTH with 1 or 2 dedicated fiber(s) for each user, b) FTTC with a sharing factor of N users.

Fiber-optic access has been envisioned as the "end game" for access networks for over 30 years because of potentially unlimited bandwidth, low attenuation of optical fibers, and low power consumption compared to copper-based solutions. Indeed, the first fiber to the home (FTTH) trial for 158 homes was conducted in Higashi-Ikoma District of Nara Prefecture, Japan in July 1978 [15]. There were also numerous early trials by the late 1980s including Elie Manatoba in Canada in 1981 [16], Milton-Keynes in England in 1982 [17], BIGFON in Germany in 1983 [18], and Biaritz in France in 1984 [19]. Although all trials were technically successful, optical access failed to be commercialized due to many unsolved problems such as high installation cost, electrical powering, uncertain service demands, competing technologies, and regulatory issues [20]. Among these factors, cost is the biggest problem since optical devices were in a very early stage of development. Therefore, optical access has only recently entered the mainstream when low-cost devices specifically designed for access networks became available.

There are many varieties of fiber-to-the-x (FTTx) referring to schemes used to provide broadband connections to end-users by fiber-optic technology which sometimes leads to confusion. In fact, there are two main schemes in which end-users (homes, offices) interface directly to optical networks or indirectly through other technologies such as DSL. The direct interface is called fiber-to-the-home (FTTH) or fiber-to-the-premises (FTTP). The indirect interface is referred as fiber-to-the-node (FTTN), fiber-to-the-curb/cabinet (FTTC), or fiber-to-the-building/basement (FTTB) depending on the distance and type of non-fiber link between the end-user and the optical interface. This section describes current optical access networks for all FTTx schemes.

Point to Point Architecture

A dedicated single mode optical fiber runs from the central office (CO) to the user premise shown in Fig. 1.6.a). The CO is the demarcation point between the metro network and the access network. The upstream and downstream channel use different wavelength windows in the same fiber, typically 1550 nm for downstream and 1310 nm for upstream. In some cases, two fibers are used instead of wavelength multiplexing. The common standards are point to point Ethernet over fiber such as 1000BASE-LX10 and 1000BASE-BX10 providing a 1G Ethernet connection over 10 km by a single fiber or a pair of fibers, respectively [21]. The future upgrade for individual users can be performed simply by replacing fiber terminals without affecting other users.

One of the disadvantages of this scheme is that each user requires one O/E transceiver at the CO and one dedicated fiber leading to high CAPEX and OPEX. The high cost comes from many factors, notably, the large space at the CO to host thousands of O/E transceivers, high power consumption, and unshared fibers in the outside plant. Therefore, point to point is suitable for short loop lengths (< 5km) but not for long loop lengths since the non-fiber-sharing results in a very high CAPEX [22]. Point to point is also more attractive for FTTC than for FTTH since the scheme can achieve a level of sharing factor and statistical multiplexing on the optical link as shown in Fig. 1.6.b).

Point to Multiple Point Active Ethernet

The point to multiple points active Ethernet is similar to the system shown in Fig. 1.6.b) in which the active remote terminal and twisted pairs are replaced by an Ethernet switch and optical fibers, respectively. This solution can leverage the economy of scale of Ethernet products to be low-cost. However, the active switch in the outside plant requires hosting space, reliable power supply (power backup must be provided), and regular maintenance that result in higher OPEX than other passive solutions in the long term.

Time Division Multiplexing Passive Optical Networks

The Full Service Access Network Industrial Consortium (FSAN) was founded in June 1995 by major telecom service providers and system vendors to study future access networks. The objective was to come up with a common broadband platform that could be used to deliver a wide range of voice, video and data services [23]. The common platform is the basis for cost reductions because of large production volumes and interoperability. Asynchronous transfer mode passive optical network (APON), the first PON standard, was drafted by the FSAN and subsequently ratified by ITU-T to be broadband PON (BPON) recommendation G.983.x in Oct. 1998.

The BPON physical architecture, shown in Fig. 1.7, is a point to multiple points architecture by employing passive power splitter(s) within the optical distribution network (ODN) to serve a number of users, typically 16 or 32. The fiber terminal at the service provider side is called optical line terminal (OLT). The terminal at the user side is referred to generally as optical network unit (ONU) but also referred to specifically as optical network terminal (ONT) when its actual location is within the user premise. The downstream data for different ONUs are time division multiplexed (TDM) and broadcasted to all ONUs in the window of 1480 to 1500 nm. The ONU then selects the data designated to it and discards the rest based on the address information in the header. In the upstream direction, BPON operates in a time division multiple access (TDMA) fashion in the window of 1290 to 1330 nm where each ONU transmits data within its assigned timeslot. To avoid collision, the OLT informs the start time and the stop time to each ONU, which are embedded in the downstream header. The downstream/upstream bit rates of 155/155 Mbps or 622/155 Mbps are shared among all ONUs. The typical split ratio is 16- or 32-way split restricted by path loss and ONU addressing limit. The maximum reach is defined to be 20 km. Three classes of power loss budgets for optical path loss are also defined, i.e., class A of 20 dB, class B of 25 dB, and class C of 30 dB. This allows cost optimization for different deployment scenarios such as class A can be used in a short reach and low split ratio deployment.

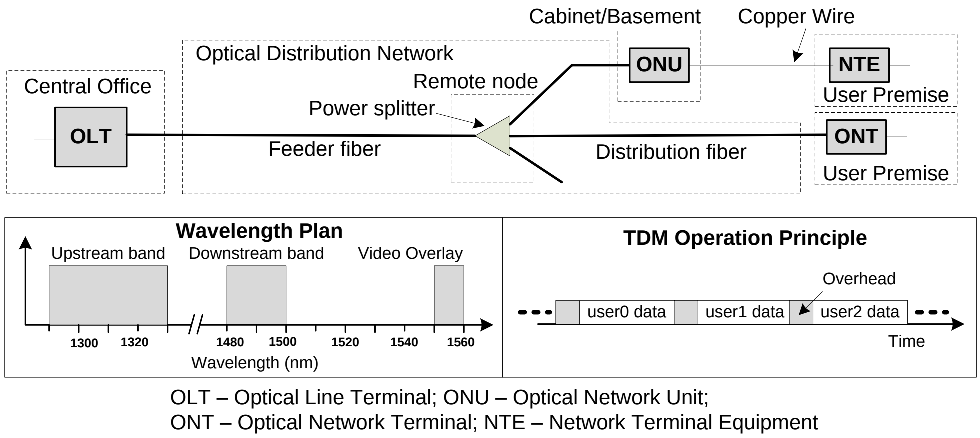

Fig. 1.7. Schematic of broadband passive optical access network (BPON) specified by the FSAN.

The point to multiple points topology requires extra protocols for the network control and management and the burst mode operation of upstream lasers (at the ONU) and receiver (at the OLT). The laser at the ONU has to be completely off during non-transmission period to avoid interference with the transmitting ONU. Moreover, the enable and disable time of the laser should be short to reduce overhead, e.g., lower than 12.86 ns in BPON. In the OLT, the burst-mode receiver is required since bursts transmitted by near ONUs are much stronger than bursts transmitted by far ONUs, e.g., 10 dB. The burst-mode receiver has to reset its gain quickly to adapt with power of the incoming burst. However, there are inherent advantages to this architecture:

- Cost sharing of the OLT transceiver and the feeder fiber (the fiber section before the power splitter as indicated in Fig. 1.7) is achieved. The number of transceivers and fibers terminated in the CO is reduced by a factor of 16 or 32 in comparison to the point-to-point solution.
- The passive ODN requires no power supply, minimum space, and low maintenance for devices located in a cabinet in the harsh outside environment resulting in a low OPEX.
- Electromagnetic interference (EMI) is avoided in comparison to copper solutions.
- ODN itself is transparent to any optical signal format allowing for future upgrades.
- Statistical multiplexing of traffic from all ONUs by dynamic bandwidth allocation (DBA) can be attained by using TDMA. Busy ONUs can be allocated long transmission timeslots while light-loaded ONUs can be allocated short timeslots according to their instantaneous needs. Service provisioning for different service requirements is separated from the infrastructure.
- Multiple splitting stages allow topological flexibility and future upgrades. A 4-way split, for example, can be placed right after the OLT to prepare for a future upgrade. Each branch later can be separated and served by a new OLT to increase total capacity by a factor of 4.

PONs have gone through several phases of evolution by mainly increasing line rates and split ratios. Gigabit-capable PON (GPON) G.984.x evolved from BPON G.983.x was standardized in March 2003 to increase the downstream/upstream speed to 2.5/1.25 or 2.5/2.5 Gbps, split ratios to 1:64 and 1:128 [24]. A GPON encapsulation method (GEM) was also defined to efficiently encapsulate a wide range of client signals including T1/E1 and Ethernet [25]. Most recently, 10G GPON (XG-PON) G.987.x was ratified in January 2010 to increase the downstream/upstream speed to 10/2.5 Gbps (XG-PON1) or 10/10 Gbps (XG-PON2, not yet standardized). XG-PON was designed to coexist on the same ODN with GPON by using different wavelength windows. XG-PON supports up to 1:256 split and advanced power saving modes by defining full service, dozing, and sleep mode [26].

In parallel to the FSAN from ITU-T, the Ethernet in the First Mile (EFM) study group was formed by IEEE in November 2000 aiming to bring Ethernet to the access area. Ethernet has been a very successful networking technology for local area networks (LANs). Ethernet interfaces are everywhere at homes, at offices, and at datacenters. Therefore, the idea about an access network that can natively support Ethernet is widely accepted. The EFM adopted many specifications from the FSAN for its EPON standard (IEEE 802.3ah-2004) including terminologies, the fiber type, fiber lengths, the wavelength plan, and split ratios [21].

Therefore, EPON has a similar fiber topology to GPON. The main difference is in the medium access control (MAC) layer where EPON MAC layer evolves from Ethernet technology (LANs) while GPON MAC layer evolves from SONET/SDH (synchronous optical network/synchronous digital hierarchy). EPON uses a line rate of 1.25 Gbps to support 1 Gbps Ethernet connection both downstream and upstream. In a similar trend, EPON capacity was extended by increasing the line rate, 10G-EPON (IEEE 802.3av) was ratified in 2009 with two flavors: 10 Gbps symmetric or 10/1 Gbps down/up asymmetric. 10G-EPON can coexist with EPON on the same ODN by using different wavelength windows [27].

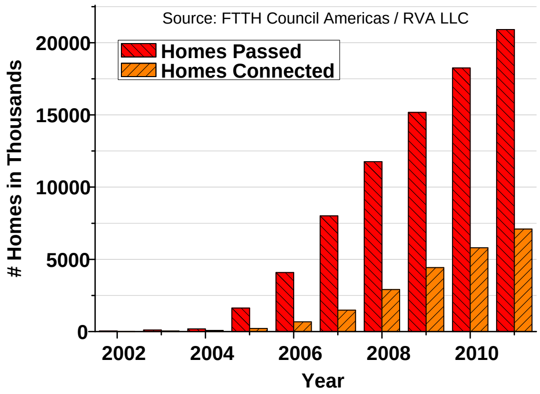

Fig. 1.8. North American FTTH homes cumulative including homes under coverage of FTTH (homes passed) and homes actually subscribed (homes connected).

Due to its advantages, mature state of standardization, and being drafted by the telecom industry, TDM PONs have been deployed at a remarkable rate and have become the most widely deployed optical access technology. The cumulative number of homes connected and homes under FTTH coverage in North America is shown in Fig. 1.8. The number of homes passed (homes under FTTH coverage) has multiplied more than 1000 times from 2001 to 2011 according to FTTH council Americas [28]. Most deployments are based on GPON, a technology of choice for Verizon, which by far is the largest FTTH provider in North America [29]. GPON is also the choice of Deutsche Telekom, France Telecom, and British Telecom, three major incumbents in Europe, for their FTTH rollouts [30][31].

Wavelength Division Multiplexing Passive Optical Networks

Wavelength division multiplexing (WDM) PON is another promising scheme to allow multiple users to share the same ODN. Each user is connected to the OLT through a dedicated wavelength channel, thus WDM PON can be seen as a stack of multiple point-to-point networks. In fact, WDM-PON is not yet standardized but it has been already successfully deployed in the first field trial in 2005 and subsequent commercial installations in South Korea [32][33][34]. The configuration for the field trial is shown in Fig. 1.9 in which 32 users share the same ODN by using dense WDM (DWDM) wavelengths with 100 GHz channel spacing.

Instead of using power splitters, WDM-PON employs a temperature-insensitive arrayed waveguide grating (AWG) for wavelength MUX and DEMUX in the remote node (RN). The channel speed is 100 Mbps resulting in aggregate network capacity of 3.2 Gbps.

Since the AWG has much lower insertion loss than the power splitter with the same port count, WDM-PONs require significantly lower power budget than TDM PONs allowing a higher reach or to use less sensitive photodiodes and/or less powerful transmitters. However, each ONU transceiver using a different wavelength poses a great challenge. If 32 types of ONUs are used for 32 wavelengths, inventory and maintenance cost will be high. Therefore, a single type ONU for all wavelengths is desirable which is regarded as the wavelength-agnostic or colorless solution. The Korean trial uses remote wavelength seeding for the Fabry-Perot laser at the ONU. A continuous-wave (CW) wavelength is injected to the laser, thus the laser lasing mode is locked to it. This use of Fabry-Perot lasers is called wavelength injection-locking [35]. To generate seed lights, amplified spontaneous emission (ASE) can be generated by a broadband light source (BLS) in the OLT and transmitted towards ONUs. This spectrum is then sliced by the AWG at the RN to be CW seed wavelengths. Transmitters in the OLT can also use injection-locking to avoid the use of wavelength-specific lasers by using a second BLS as depicted in Fig. 1.9.

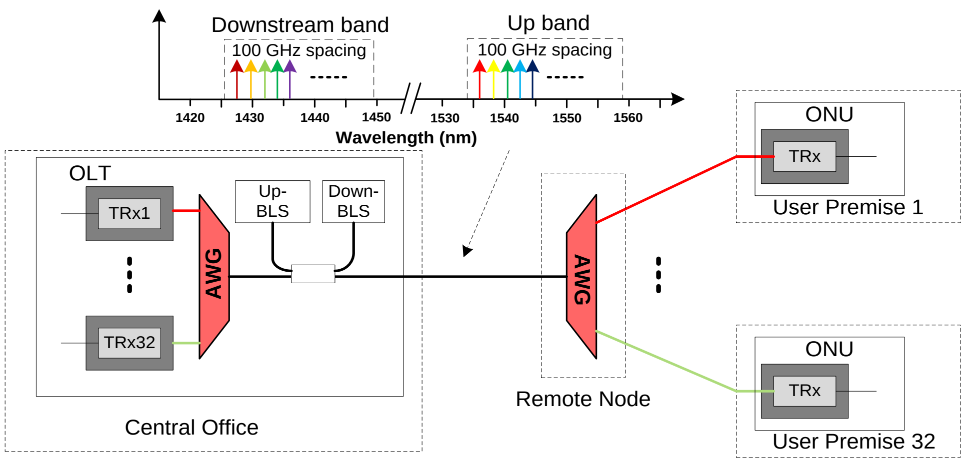

Fig. 1.9. WDM-PON architecture of Korea Telecom field trial in 2005 based on array waveguide grating and wavelength-locked Fabry-Perot lasers.

WDM-PONs provide each ONU with a dedicated wavelength channel, thus no statistical multiplexing. It is suitable for traffic scenarios on which statistical multiplexing can only produce a small gain. The 100 Mbps channel carrying mainly video streams in the Korean trial is argued to produce a insignificant statistical gain, thus no need of statistical multiplexing functionality [36]. When the diversity of services and the channel speed become larger, the lack of statistical multiplexing and of bandwidth provisioning flexibility are disadvantages of WDM-PONs over TDM-PONs.

1.3. Broadband Access Networks: the Future

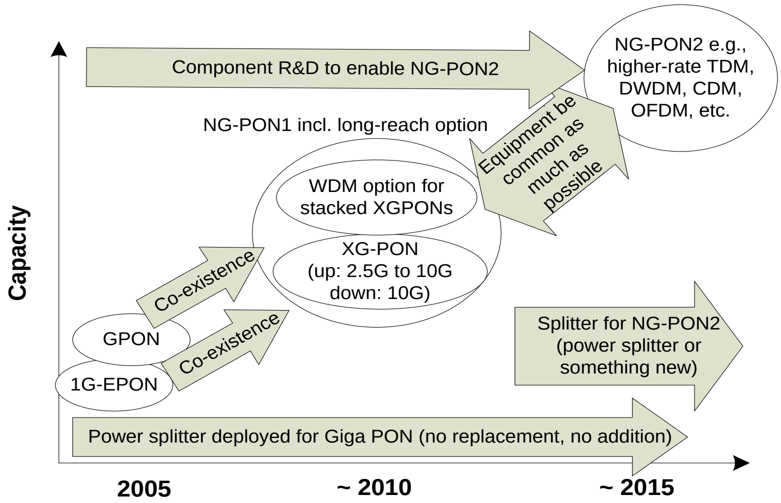

Fig. 1.10. NG-PON roadmap defined by the FSAN consortium in 2005.

TDM-PONs, as the mainstream technology for optical access networks, have gone through several evolution iterations from APON/BPON, GPON, to XG-PON. Hence, the discussion about the next iteration after XG-PON has been started. In fact, extensive discussions on the next generation PON (NG-PON) began after GPON was widely adopted. A wide range of technologies, from a small evolutionary growth to a complete revolutionary change, was placed on the table. To create a framework for NG-PON studies, the FSAN defined a roadmap in 2005, shown in Fig. 1.10, in which the NG-PON1 refers to evolutionary growth of GPON while NG-PON2 refers to a revolutionary or disruptive change [37]. The primary requirement for NG-PON1 is to be coexistent and seamlessly upgradable with/from GPON on the same ODN without service disruption.

XG-PON, after being finalized among competing candidates, was standardized for NG-PON1 in 2010 [38]. XG-PON has two flavours: XG-PON1 with 10G/2.5G down/up asymmetrical speed and XG-PON2 10G/10G down/up symmetrical speed. 1:64 split is the minimum requirement for XG-PON and split ratio up 256-way is possible.

Therefore, current research and development activities on optical access networks now aim towards NG-PON2 and beyond. This section will discuss high-level requirements and related technologies for future networks in this context.

1.3.1. Requirements for Next Generation Optical Access Networks

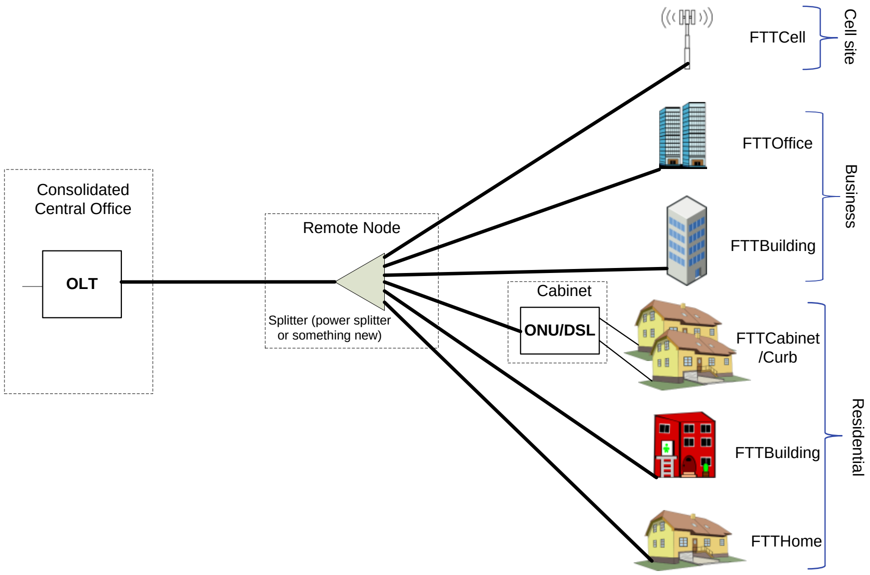

Fig. 1.11. Next generations of access networks as a single access platform.

Single access platform

The concept of full service access in 2012 is no longer restricted to voice, video, and data. NG-PONs are required to fully support various services for residential subscribers, business customers, and mobile backhauling applications through its high quality of service and high bit-rate capability as depicted in Fig. 1.11. NG-PONs, for example, should support legacy services of T1/E1 and precise timing for synchronization function of mobile backhauling. Operators require a single platform to deliver all services because the common platform substantially reduces maintenance and operational cost in comparison to the multiple platforms approach [39].

More users

More users or higher split ratios are desirable to improve overall economics of access networks. In addition, the high split ratio provides flexible splitter configurations and efficiently supports a variety of deployment scenarios. XG-PON can support up to 1:256 split both physically and logically. NG-PONs need to support more users exceeding, e.g., one thousand [40]. At that split level, simple power splitting might not be appropriate since the split loss will be very high.

Higher Capacity

The need to provide higher bandwidth is clear since the trend of traffic increase still continues in the foreseeable future. The exact figure has been under extensive discussions but 1 Gbps per home is widely accepted. 1 Gbps peak and 500 Mbps sustainable data rate per home is predicted according to OASE, a FP7 European ICT project, based on a projection of service bit-rates [41][42]. In fact, Google, an Internet service giant, announced in 2010 the deployment of an experimental fiber network to provide 1 Gbps to at least 50,000 and potentially up to 500,000 people [43]. After the construction period, the service was first launched in Sept. 2012 in Kansas City with a symmetric speed of 1 Gbps for $120 per month for Internet and TV and $70 per month for Internet only [44]. For mobile backhauling application, long term evolution (LTE) advanced, a 4G mobile technology, requires around 1 Gbps per sector. Thus, 3 Gbps per cell is needed for the typical configuration of 3 sectors per cell. In case of distributed eNodeB applications, which is the technique of centralized base band units and distributed remote radio units in cellular networks (fronthauling), NG-PONs have to support data transmission between the baseband unit and the remote radio unit. The interface between two units using CPRI/OBSAI (Common Public Radio Interface/Open Base Station Architecture Initiative) requires bit rates from 614.4 Mbps to 9830.4 Mbps through 7 options determined by the air capacity of the remote radio unit [45][46]. Therefore, the ONU for FTTCell requires up to 10 Gbps bit rate.

The need for higher aggregate network capacity is also driven by increasing the number of ONUs in the network as described in the previous requirement. Delivering 1 Gbps or even 10 Gbps to an ONU, which serves a home or a cell, is already possible for XG-PON as long as there are few ONUs (<10) sharing the network. However, to maintain split ratios of 1:32 or 1:64 and to increase the ratio further, the network capacity need to be improved at least to 40 Gbps [39].

The evolution in capacity of PONs, so far, has been achieved by the trajectory of increasing line rates of the downstream and upstream wavelength, i.e., 622/155 Mbps in BPON to 10/2.5 (or 10) Gbps in XG-PON. Increasing the line rate further to 40 Gbps poses a challenge for low-cost transceivers, especially in burst-mode [47]. Alternatively, the wavelength capacity can be scaled up by using polarization multiplexing (POL-MUX) [48][49], multi-level modulation formats with coherent detection [50], or orthogonal frequency division multiplexing [51][52][53]. These techniques are becoming commercially available for metro and long-haul applications but to be economically viable for the access application is still a challenge.

Alternatively, the network capacity can be increased by using more wavelengths. Techno-economical analyses by ALPHA, an FP7 European ICT project, show that stacking multiple TDM-PONs in the same ODN by WDM is more economical than deploying and operating multiple TDM-PON on separate ODN [54]. TDM-PONs can be stacked by using coarse WDM (CWDM) or Dense WDM (DWDM) [55][56]. Ultra dense WDM (UWDM) with support of coherent detection is another promising method [57][58]. In the latter, a large number of wavelengths are packed very close with a spectral distance in a range of several GHz.

Long Reach

Long reach was already considered as an option for GPON and XG-PON since long reach offers significant possibilities for consolidating central offices [59]. Long reach GPON and XG-PON can support up to 60 km reach. The consolidation can create net revenues for operators from sales of unused central offices and OPEX savings. Deutsche Telekom, the German telecom incumbent operator, aims to reduce the number of central offices from around 8000 to 900. A reach of 50 km is required to do this based on the survey of central office locations [60]. Therefore, a reach of 60 km (10 km is the margin for actual routes to reach the 50 km diameter) and probably 100 km is needed to cover more scenarios.

Reach and split ratio are closely related in TDM-PON since their limitation is posed mainly by the power loss budget. To compensate losses by a longer reach and/or a higher split ratio, optical amplifiers, also known as extender boxes, are employed within ODN [61]. The amplifying technology can be rare-earth doped fiber amplifiers (xDFA), e.g., Erbium-doped EDFA [62], semiconductor optical amplifiers (SOA) [63], Raman amplifiers [64], or OEO converters [65]. ODN is no longer fully passive but the low maintenance cost can be preserved by a proper amplifier design.

Green Access

As a part of the effort to reduce overall CO2 footprint of the telecom industry, future access networks should be more energy-efficient than today’s networks. The average energy per delivered bit should be reduced by several orders of magnitude to maintain today’s level of consumed energy. XG-PON, as NG-PON1, initiated several mechanisms to reduce power consumption based on load levels. The ONU can operate in three modes: full, dozing, and sleep to offer various levels of power saving. The ONU Tx is powered off when there no data to transmit in the dozing mode and both ONU Tx and Rx are powered off periodically in light-traffic conditions in the sleep mode. Future access networks need to increase energy-efficiency further by considering all possibilities ranging from network architectures and protocols, to optics and electronics devices [66].

Dynamic Bandwidth Allocation

As GPON and XG-PON, future access networks should support dynamic bandwidth allocation for the efficient sharing of network capacity among connected ONUs and traffic-bearing entities within a single ONU based on the dynamic indication of their activity. The bandwidth allocation for a traffic-bearing entity is dynamically increased or reduced in response to its instantaneous demand. In case of GPON and XG-PON, DBA only works in the dimension of timeslots since the network capacity is fully represented by timeslots in TDM-PONs. When other dimensions are added such as wavelengths or subcarriers, DBA of future access networks should be able to work on all possible dimensions to guarantee the efficient use of network resources [67][68].

Resiliency

Service resilience to ensure a small probability of service outage has been considered in standards for current PONs but has not been a strong requirement [69]. NG-PONs will have to support a diversity of high-value and high-bandwidth services for residential and business applications with more users are covered by a single NG-PON. Therefore, ensuring service availability is a key requirement for NG-PONs [70].

Partial Backward Compatibility

Coexistence with today's technologies is not a requirement for NG-PONs. That relaxation opens the door for new research breakthroughs, which may require a disruptive change to be implemented in future networks. However, as indicated in the FSAN roadmap shown in Fig. 1.10, reusing existing installed fibers, equipments, and devices at some extent is an advantage for a future access network candidate. The similarity between optics devices used in future networks and those of today's networks, for example, can help to reduce the cost.

1.3.2. Candidates for Next Generation Optical Access Networks

The FSAN industrial group is trying to narrow down technical options for NG-PON2. Technology candidates listed below are under discussion. One of them will be selected for NG-PON2 while others continue in the race for the technology beyond NG-PON2.

40 Gbps TDM PON

The 40G PON continues the current trajectory by increasing line rates without ODN modification, thus this technology is closest to standardized PONs [47]. The 40 Gbps line rate requires the development of low-cost high-speed transceivers. Furthermore, a 4-time increase in line rate requires an addition of 6 dB in power budget of combined transmitter power and receiver sensitivity relative to 10 Gbps. The 40 Gbps upstream is very costly because of burst-mode, which is already a challenge for 10 Gbps. Therefore, multiple upstream wavelengths can be used to achieve aggregate 40 Gbps by a lower line rate per wavelength, e.g., 4 wavelengths at a line rate of 10 Gbps. Chromatic dispersion compensation needs to be considered for 40 Gbps downstream. Techniques used for long-haul, such as fiber dispersion compensator, electronic compensation, complex modulation formats, may be adopted for the access application at a feasible cost.

OFDM PON

An orthogonal frequency division multiplexing (OFDM) PON utilizes a similar scheme which was developed for radio communication in which many narrow-band orthogonal subcarriers are used to transmit symbols in parallel [52][71]. Thus, OFDM allows high spectral efficiency and high resistance to linear dispersion, and efficient channel estimation/equalization.

Subcarriers can be modulated with different modulation orders and transmitted with different power levels to adapt to channel responses [53]. Bandwidth can be flexibly allocated to ONUs by assigning different numbers of subcarriers. However, OFDM has a number of drawbacks including high peak-to-average power ratio, sensitivity to frequency drift and to phase noise. The implementation cost is high since advanced digital signal processing (DSP) is required at both transmitter and receiver sides [72]. The powerful DSP also significantly increases overall power consumption.

WDM PON

The principle of WDM PONs was described in Section 1.2.2 with an example which employs AWG at the RN and remote seeding for wavelength-agnostic ONUs. There are also other wavelength-agnostic variants, i.e., mechanically locked tunable laser [73], self-seeded scheme [74], and color patch cord (interchangeable external wavelength filter) [75]. WDM-PONs have advantages in capacity and security in comparison to TDM-PONs. On the other hand, each type of use may require a different data rate and each user within a type also may have a different need. The virtual point-to-point principle of WDM PON do not give operators the flexibility in bandwidth provisioning that is not in line with the requirement of a single access platform.

Ultra-dense WDM PON

Ultra dense WDM PON is made possible by the use of coherent transceiver technology, which was developed for the long-haul application. Coherent detection can give up to 20 dB improvement in receiver sensitivity in comparison to intensity modulation and direct detection (IM/DD) based schemes [76][77]. In addition, coherent detection offers an inherent ultra-narrow optical filtering capability made possible by the electronic digital signal processing. This allows WDM channels to be placed close to each other. Ultra dense WDM PON is an attractive solution to increase reach and the number of users, e.g., it can offer 100 km reach and 1 Gbps symmetrical bit rate per channel with channel spacing of 6.25 GHz [58]. Despite these advantages, ultra-dense WDM is not yet ready for access networks since low-cost components such as IQ modulators and coherent receivers are not yet available. Furthermore, ultra dense WDM is not as close to current technologies as other candidates that make it lagging behind in the technology race for the future access network.

Hybrid WDM-TDM PON

Hybrid WDM-TDM PONs can be seen as a stack of TDM PONs on the same ODN, thus also known as wavelength-stacked PONs or TWDM PONs [78][22]. A configuration of stacking 4 XG-PONs on the same ODN is already considered for the expansion of NG-PON1. A higher number of wavelengths is also possible when DWDM is employed. A recent test-bed conducted by Huawei and China Telecom demonstrated that 4 stacked XG-PON1s using DWDM wavelengths (200 GHz spacing) in C band can fully coexist with GPON and standard

XG-GPON1 [79]. The test-bed used commercially available optics and reused software codes developed for XGPON1.

The similarity between TDM-PON and hybrid WDM-TDM PON reduces CAPEX since hardware and software developed for TDM PONs can be reused to a large extent. The similarity also allows a smoother mitigation path from current TDM PONs. Therefore, the hybrid WDM-TDM solution is regarded as the most outstanding candidate for NGPON2 since it can take advantages of both WDM and TDM worlds [80].

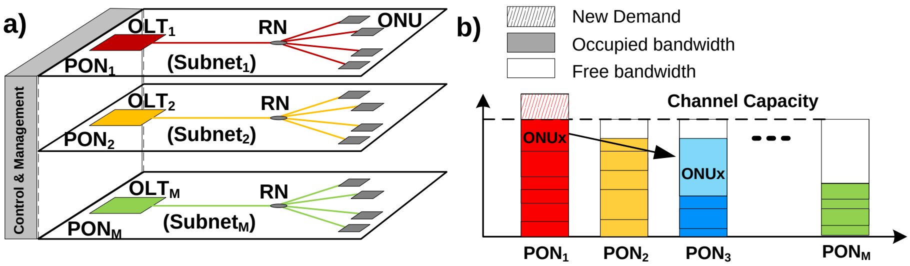

Fig. 1.12. a) A high logical level view of WDM-TDM PONs, b) Congestion mitigation by wavelength reconfigurability.

1.3.3. **WDM-TDM-based NG-PON2**

The FSAN consortium has made a major decision for NG-PON2 in April 2012. WDM-TDM was selected after narrowing down from a wide range of technologies, which were described in the previous Section. The wavelength dimension is added to further scale up the capacity of a single feeder fiber since increasing the line rate is no longer cost-effective beyond 10 Gbps [81][82]. WDM-TDM-based NG-PON2 stacks four XG-PON-like TDM PONs in a wavelength plan that allows coexistence with GPON and XG-PON. The ODN is still based on power splitters since there were strong requests from network operators to leave the current deployed outside plan untouched to protect their ODN infrastructure for GPON and XG-PON investments. The first roll-out of NG-PON2 is expected to take place by 2015 when GPONs are still in the middle of their life cycle.

Other technology candidates next to WDM-TDM have their own merits but they are exposed to higher risk for 2015 NG-PON2 time frame. Those technologies are not in the battle for NG-PON2 anymore but still candidates for future access networks beyond NG-PON2, especially OFDM and UDWDM.

1.3.4. Reconfigurable WDM-TDM Optical Access Networks

Although there are many physical implementation variants for the WDM-TDM PON family, they always can be seen as a set of TDM-PON sub-networks as shown in Fig. 1.12.a) from a high logical level view. A straightforward implementation is called the static WDM-TDM PON where these sub-networks are independent entities coexisting on the same ODN. A clear advantage of the static solution is its cost since neither wavelength tuning nor wavelength routing is required. However, the static solution does not exploit all possible dimensions for DBA as discussed in requirements for future access networks in Section 1.3.1. There are various benefits when exploiting the new wavelength dimension, e.g., decoupling physical connectivity with service provisioning, power saving and resources saving capacity by adjusting active capacity based on demand, and congestion mitigation.

An example of congestion resolution is shown in Fig. 1.12.b) in which the sub-network of *PON1* is congested and cannot accommodate an extra bandwidth request from *ONUx*. The request would be rejected when the network is static. However, if *ONUx* is able to change its working wavelength channel to *PON3*, the request could be accepted. Networks with such ONU reallocation capability is referred to as reconfigurable or flexible networks [78][22]. Local congestions are more likely to happen as higher temporal and spatial variations of traffic are expected. Local congestions can be avoided by wavelength reconfigurability since some ONUs can be moved out of a busy wavelength and allocated to a lightly-loaded one to reduce the wavelength sharing ratio. Thus, the sustainable bandwidth per ONU is improved in the busy wavelength. Besides congestion mitigation, wavelength reconfigurability can enable other advanced functions, which will be elaborated in Section 2.1.

In current architectures, wavelength reconfigurability requires a substantial increase in CAPEX per user, which is certainly prohibitive in access networks. The reconfigurable ONU typically needs to be equipped by a tunable filter (for downstream) and a tunable laser (for upstream). Those devices are popular for long-haul and metro applications but still expensive in order to be employed for customer premise equipments (CPEs). Therefore, introducing wavelength reconfigurability to access networks in an economically viable manner is very challenging. The research work reported in this thesis tries to overcome the cost barrier by designing reconfigurable architectures with limited tuning or without wavelength tuning. The cost-prohibitive challenge of wavelength reconfigurability will be further analyzed in Section 2.2.

1.4. Contributions and Scope of This Thesis

The research work reported in this thesis has been carried out at COBRA research institute, Eindhoven University of Technology within the framework of the PF7 European project ALPHA (Architectures for fLexible Photonic Home and Access networks). ALPHA is a large scale integrated project with a consortium of 17 partners from both industry and academia including Telefonica, Andrew Wireless/Comscope, France Telecom and Alcatel-Lucent. The project addresses the challenges of building the optimum future access and in-building networks for consumer and business environments. The project supports the evolution towards a cognitive network by dynamically utilizing resources of an optical network infrastructure to support a heterogeneous environment of wired and wireless technologies. The cognitive network is able to optimize its performance based on the real-time awareness of operational conditions.

In particular, the objective of the research reported in this thesis is to evaluate merits and investigate cost-effective implementations of reconfigurable optical access networks for both wired and wireless services. The research outcomes deepen the understanding and bring a new perspective to wavelength reconfigurability in optical access networks. The research is ranging from performance evaluations in the logical layer to proof-of-concept experiments in the physical layer with key contributions listed as follow:

1. Quantifying advantages of wavelength reconfigurability in terms of traffic performance and power consumption.
2. The finding that a limited flexibility already significantly improves the performance in comparison to the static case while the full flexibility can achieve further improvement but the difference with the limited flexibility is marginal.
3. The proposal of a novel architectural concept named the cyclically-linked flexibility that enables the network-wide bandwidth redistribution capability but only requires ONUs to be reallocated within a subset of two wavelength channels.
4. The development of a generalized simulation framework that allows evaluating the performance of various WDM-TDM PON architectures with different DBA algorithms.
5. The development of bandwidth rearrangement algorithms for the cyclically-linked flexibility.
6. The proposal of four access network architectures based on the cyclically-linked flexibility, each addressing a particular deployment scenario. These architectures are evaluated by proof-of-concept experiments, traffic performance, and cost comparison to highlight their unique merits.
7. The proposal of two application-specific reconfigurable architectures for dynamically delivering radio signals with proof-of-concept experiments.

These results were also contributed to another European project BONE (Building the Future of Optical Network in Europe) which is a FP7 Network of Excellence project.

After the introductory chapter, the thesis starts by analyzing existing reconfigurable networks with different levels of flexibility in Chapter 2. Reconfigurable architectures are positioned on the scale of flexibility level for a fair comparison. The result reveals that limited flexibility may offer a good cost-performance tradeoff. Chapter 3 extends the concept of limited flexibility to the concept of cyclically-linked flexibility, which is a variant of 2-wavelength limited flexibility. Performance of the cyclically-linked flexibility concept in terms of service blocking probability, packet delay, packet loss, and load balancing is compared to the static and full flexibility to demonstrate its merits. As an architectural concept, the cyclic flexibility needs to be realized by a physical architecture. Chapter 4 describes four realizations for different deployment scenarios. Chapter 5 is devoted to proof-of-concept demonstrations of two application-specific reconfigurable optical networks for dynamic radio signal delivery. Finally, Chapter 6 provides a summary of the research work and an outlook for further studies.

CHAPTER 2

LIMITED FLEXIBILITY: A COST-EFFECTIVE TRADE-OFF FOR WAVELENGTH RECONFIGURABILITY

The merits of wavelength reconfigurability along with its associated costs are elaborated to sharpen the motivation and challenges for wavelength reconfigurability in optical access networks. A parameter to indicate the level of flexibility is introduced in order to provide a fair comparison between the different reconfigurable architectures in terms of traffic capacity and power consumption. The comparison provides a guideline for flexibility level adjustment to optimize cost-performance tradeoffs. The contents of this chapter have been partly disseminated in [83] and [84].

2.1. Merits of Wavelength Reconfigurability

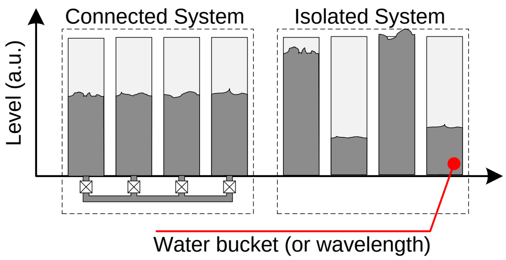

Fig. 2.1. Wavelength reconfigurability vs. wavelength static allocation as system of connected water buckets vs. system of isolated water buckets.

Wavelength reconfigurability is deployed in optical core and metro networks by employing all-optical routers such as reconfigurable optical add/drop multiplexers (ROADMs). The light path topology can be altered within a sub-second according to the real-time demand. It was a huge leap from the legacy method of manual light path provisioning, which takes the order of hours or days with human intervention. Reconfigurability has been proven to increase the efficient utilization of network resources since the network capacity can be diverted to where it is actually needed. Although requirements for the access network are different from those of metro and core networks, a similar idea has been proposed for access networks because wavelength reconfigurability enables advanced network functions that are required for future access networks [78]. This section elaborates those network functions, which were briefly mentioned in the previous chapter.

2.1.1. Congestion Mitigation and Load Balancing

Due to ever booming broadband services including mobile data services, traffic hotspots tend to occur more frequently as discussed in Section 1.1. The local congestion can be resolved by diverting more capacity to the hotspot using wavelength reconfigurability. The ONU serving the hotspot can be allocated more bandwidth when its working wavelength changes to an underutilized one. In an extreme case, the whole wavelength bandwidth can be allocated solely to an ONU while other ONUs in the system still can be served by other wavelengths albeit with reduced bandwidth.

Furthermore, the local congestion can be actively prevented before it actually occurs by load balancing among wavelengths in reconfigurable networks. This functionality can be represented as a system of connected water buckets as depicted in Fig. 2.1 in which the water level can be balanced among buckets. Water levels in a system of isolated buckets are completely independent from each other that are similar to load levels of wavelength channels in the wavelength-static system.

2.1.2. Power Saving by Active Capacity on Demand

Congestion mitigation and load balancing are clear advantages of wavelength reconfigurability during busy hours while in non-busy hours, wavelength reconfigurability can bring another advantage. A simple strategy to save power consumption in the CO may be to concentrate ONUs to one or more wavelength channels in order to allow the other wavelengths to be in standby mode during non-busy hours. In fact, wavelength channels can be activated and deactivated based on the real-time load to yield various levels of power saving in the CO. This saving method compliments to the ONU cyclic sleep methods, which saves power at the user side. The quantitative evaluation of this advantage is presented in this chapter.

2.1.3. Statistical Multiplexing Gain

Statistical multiplexing gain provided by wavelength reconfigurability is very important for future access networks, especially in long-reach scenarios supporting a high number of users. The importance is illustrated by an example of capacity planning, as shown in Fig. 2.2 in which three access schemes are used to provide the same planned capacity for subscribers C_{SUB} (the sum of guarantee bandwidth to subscribers). In the Current Scheme, multiple TDM-PONs with 20 km reach are used to serve C_{SUB}. The statistical multiplexing gain (G_{TDM}) of ONUs in a TDM PON allows the aggregate capacity of the 20 km access section to be reduced by a factor of 1:G_{TDM}. The traffic from these TDM-PONs is converted to the electrical domain and statistically multiplexed by the electronic switch, which allows another statistical multiplexing gain (G_{SW}). Therefore, the aggregate capacity of the 40 km metro section is reduced by a factor of 1:(G_{TDM} x G_{SW}) in comparison to C_{SUB}.

In the Future Scheme A, TDM-PONs are stacked to a static long-reach WDM-TDM network. As there is no electronic switch within 60 km of the merged metro/access section, the aggregate capacity of this section is only reduced by a factor of 1:G_{TDM}.

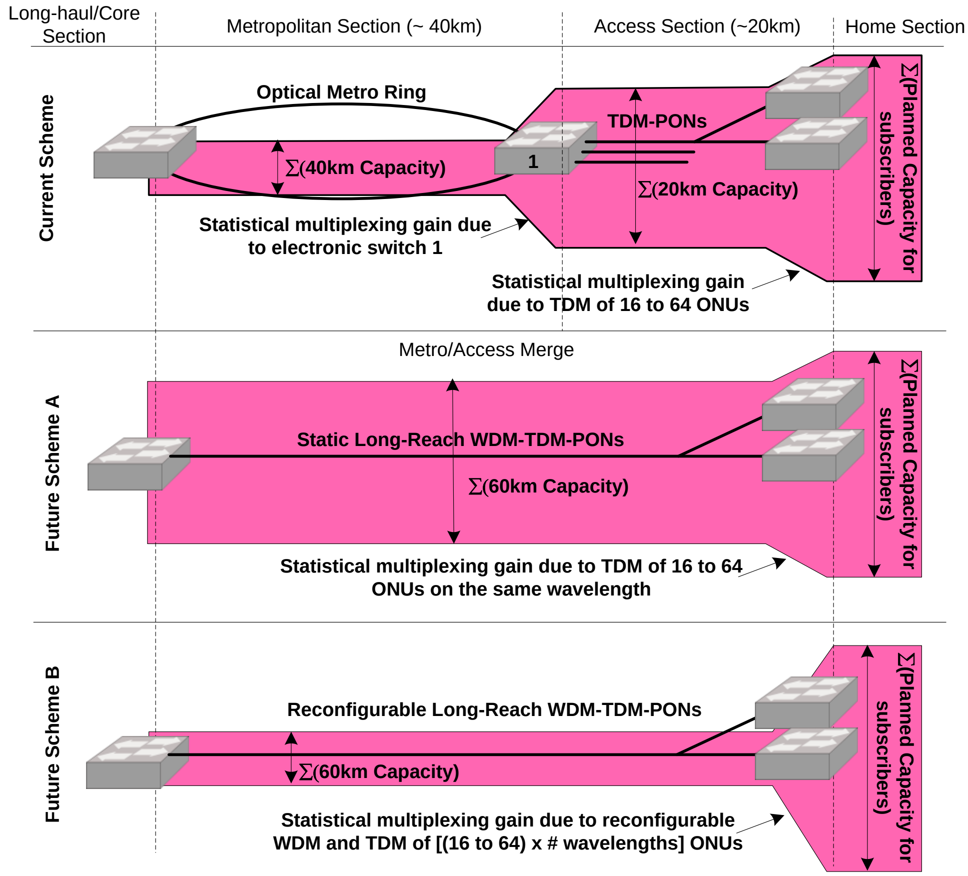

Fig. 2.2. Capacity planning of different access schemes for the same planned capacity for subscribers

In the Future Scheme B, TDM-PONs are stacked to a reconfigurable WDM-TDM network in which the aggregate capacity becomes a common bandwidth pool, which can be dynamically shared among all ONUs. This capability is similar to having an electronic switch within the all-optical metro/access section. Therefore, the total statistical multiplexing gain is similar to that of the Current Scheme $G_{RE} \approx G_{TDM} \times G_{SW}$.

Therefore, the example shows that wavelength reconfigurability is required to maintain the same deployed metro capacity to migrate from the Current Scheme to a future long reach stacked PONs with the same C_{SUB}. In other words, wavelength reconfigurability is needed to compensate for the statistical multiplexing gain previously provided by electronic switches handling multiple TDM-PONs when the geographical dimension of all-optical domain is expanded.

2.1.4. Network Virtualization

Virtualization of physical resources has become a major trend in the information technology world. The ultimate driver for this trend is to reduce the service cost and to improve the service quality. Virtual machines, for example, are used extensively in the online hosting service where customers use the virtual machine as a physical entity with specified processing power, memory, and storage capacity. This technique allows the hosting provider to use a single physical machine for multiple customers with service levels tailored to the requirements of individual customers. In communication networks, virtualization is very popular in Layer 2 and Layer 3 such as VLAN (virtual LAN) and L3VPN (Virtual Private Network) [85]. Layer 1 virtualization for optical core networks was also proposed to leverage the network flexibility enabled by all-optical wavelength routers [86]. In optical access networks, virtualization is beneficial because it allows:

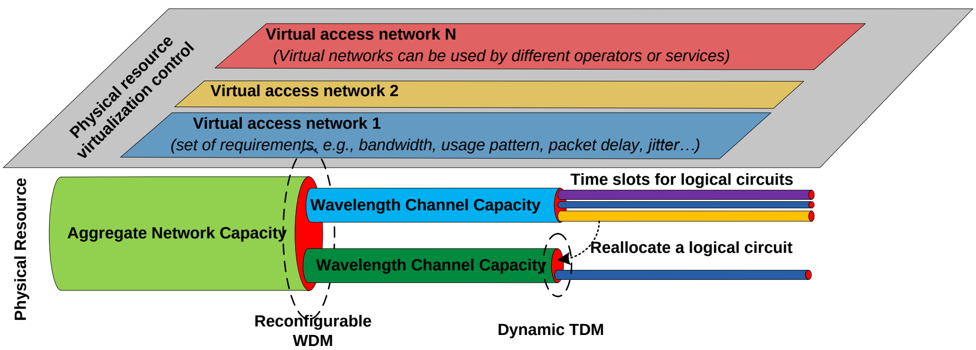

Fig. 2.3. Conceptual representation of optical access network virtualization with the support of wavelength reconfigurability

- To decouple the infrastructure provider role and the service provider role. Multiple service providers can share the same infrastructure under the open access business model [87].
- To decouple the service provisioning and the physical connectivity provisioning. Services can be added, removed, or modified without touching the physical connectivity. The service provider can offer services in a timely manner, for example, provisioning 2 Gbps connection during specified hours every day for the customer database backup.

In fact, network virtualization can be implemented on top of a static WDM-TDM PON but wavelength reconfigurability can further enhance network virtualization. In the static scheme, the ONU is restricted within the boundary of a wavelength channel with only dynamic sharing of timeslots implying that network virtualization is actually composed of multiple separate wavelength virtualization entities. Wavelength reconfigurability removes the wavelength boundary, thus separate wavelength virtualizations are now merged to a single virtual network entity as shown in Fig. 2.3. For example, the 2 Gbps connection provisioning for an ONU, which is mentioned earlier, could not be done in the static network when the working wavelength is congested by traffic from other ONUs sharing the same wavelength. In the reconfigurable network, the ONU can occupy the full wavelength capacity without blocking other ONUs traffic, which are reconfigured to be served by other wavelengths.

2.1.5. Conclusions

The functions discussed in this Subsection indicate that there is a clear motivation to have wavelength reconfigurability in WDM-TDM optical access networks. However, the lessons learnt from the 30-year history of FTTH indicate that in order to enter the access area, a technology needs to first overcome the cost barrier. The next section discusses existing reconfigurable architectures and their associated costs.

2.2. Existing Reconfigurable Architectures

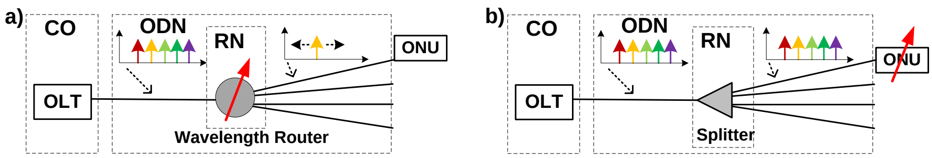

Fig. 2.4. Schematic representation for reconfigurable architecture categories, a) wavelength routing based, b) wavelength selection based [22].

In literature, there are extensive studies proposing reconfigurable architectures focusing on functionality [88][89][63][90][91], cost-effectiveness [92][93], migration [78], and enabling devices [94]. In principle, there are two geographical locations that are eligible to conduct wavelength reconfigurability: at the ONU by wavelength selection or at the RN by wavelength routing [22][88]. In special cases, the CO can also be used as a location for wavelength reconfigurability by wavelength steering. This section will go through each category to identify their pros and cons.

2.2.1. Wavelength Routing Category

In the wavelength-routing approach, the ONU working channel is decided by a wavelength router in the RN as depicted in Fig. 2.4.a). The wavelength routing function has been demonstrated using a range of technologies, e.g. thermo-optic Mach-Zehnder switches [88], wavelength selective switches (WSS) [91], an array of micro-ring resonators [95], an array of optical gates based on semiconductor optical amplifier (SOA) [90]. WSS based on liquid crystal on silicon (LCoS) is widely used for reconfigurable add/drop multiplexer (ROADM) in metro/core optical networks. Note that LCoS is considered as a mature technology for high port count of up to 23 for one stage and a maximum of 88 C-band channels at 50 GHz spacing. An integrated 2D array of thermally tunable micro-ring resonators is another promising method to construct the router. Any anchor wavelength and other related wavelengths, which are separated by a multiple of the free spectral range (FSR) of the micro-ring resonator, can be routed to a designated output port by changing the ring temperature. The FSR feature can be used to route simultaneously the downstream and upstream wavelengths when they are one or more FSR-s separated. A prototype of 4 micro-ring resonators was demonstrated in [95] to show the technical feasibility. The third method is to use an integrated array of SOAs since a SOA can provide a fast switching time (ns) and optical power gain. Although the switching time is not a strict requirement for wavelength reconfigurability, however, a switching time of the order of milliseconds is needed to avoid any interruption of on-going services.

Although the working wavelength can be changed, there is only one wavelength channel reaching the ONU at a time. The ONU can be designed to have a comparable cost to that of the static network but the ODN is no longer passive. Therefore, the wavelength routing category is considered to be not economically viable in the near future since wavelength routers are too expensive for the access. In addition, the router also increases the operational expenditure (OPEX) because more space, reliable power supply and environmental control are required at the RN.

2.2.2. **Wavelength Selection Category**

In this category, the ONU selects the working wavelength channel from several or all wavelength channels using tunable filters (for downstream) and tunable lasers (for upstream). The passive RN can broadcast [63] or multicast wavelength channels to ONUs [93]. The Broadcast-and-Select, as shown in Fig. 2.4.b), is a well-known architecture in this category. The ONU is exposed to all wavelengths among which the working channel is selected. This category allows the use of passive ODN, which maintains the passive merit of PONs, thus making this category more feasible than wavelength routing. However, the broadcasting nature induces excessive power loss, which must be compensated by one or more amplifying stages [78][22]. For example, the Broadcast-and-Select with 16 wavelength channels and an average of 32 ONUs per channel requires theoretically 27dB only for the split loss (1:512) while a practical split loss can be as high as 32dB due to imperfections such as splitter non-uniformities and splice losses [96].

Nevertheless, the excessive power loss is not the most problematic but the high cost of tunable ONUs. Tunable lasers and tunable filters have typically been developed and tailored for metro/core applications. Their cost is determined by the tuning range and the tuning speed, which were thought to be more relaxed in access applications. However, that is not the case for wavelength reconfigurability because the tuning range has to cover all possible wavelengths in order to guarantee the wavelength-agnostic property of the ONU. If wavelengths are scattered due to a coexisting wavelength plan, a very wide tuning range is required. Where if wavelengths are packed closely together, the tuning range is reduced but the tuning accuracy needs to be increased, which also has an impact on the component cost.

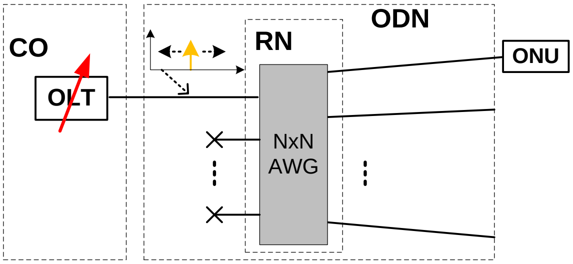

Fig. 2.5. An example of wavelength steering architecture in which the OLT serves each ONU a brief moment. Additional OLTs can connect to open ports of the NxN AWG to upgrade network capacity.

Regarding the tuning speed, wavelength reconfigurability requires the wavelength handover latency to be low enough to avoid any perceptible interruption of on-going services, especially ones associated with two-way speech such as telephony or tele-presence. The tolerable latency bound for such real-time services derived from the well-known E-model was specified to be 150 ms in ITU-T G.114 recommendation [97]. Users experience essentially transparent interactivity when the latency is kept within this bound. In fact, while it is a relatively new concept in optical networks, handover is a popular procedure in cellular mobile networks. In mobile networks, cell handover latency needs to be compliant with G.114, i.e., 150 ms to guarantee a seamless switching from one cell to another cell [98]. Therefore, the wavelength tuning time, as the largest component of wavelength handover latency, should be lower than 150 ms. It is even desirable to have a lower tuning time to avoid large buffer sizes given the high bit-rate in access networks. To switch an ONU, which is serving 1 Gbps on-going connections, 18.75 MB of data needs to be buffered for one direction during 150 ms.

2.2.3. **Wavelength Steering Category**

The wavelength sharing ratio in principle can only be changed by the RN or by the ONU. However, wavelength reconfigurability can be implemented in the CO for other purposes, which is classified as wavelength steering as shown in Fig. 2.5. Wavelength steering can be used for transmitter sharing among multiple ODNs as proposed in [99][100] in which a small bank of tunable transmitters at the CO are shared among multiple WDM-TDM PONs. These schemes argue to reduce the number of transmitters from the conventional method of using one DWDM transmitter for each wavelength in each PON. The actual aggregate capacity of all associated PONs is limited by the size of transmitter bank rather than the number of PONs and the number of wavelengths in each PON. Therefore, they are not true reconfigurable optical access networks as discussed so far. In the upstream direction, they can be classified as wavelength-selection as tunable lasers are employed in ONUs for reconfigurability.

2.2.4. Degree of Flexibility

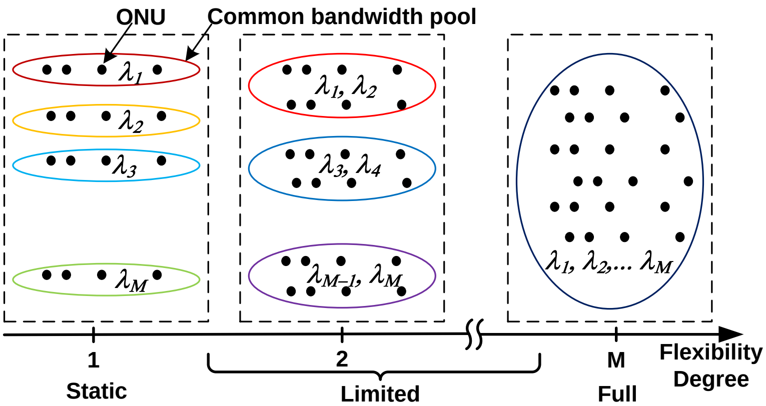

Fig. 2.6. Conceptual representation of networks on the scale of the degree of flexibility

Despite the differences amongst aforementioned WDM-TDM PON architectures, they always can be seen as a set of sub-networks, each equivalent to a conventional PON, as illustrated at a high logical level view of WDM-TDM PONs depicted in Fig. 1.12.a). From this perspective, the difference between reconfigurable networks and the static WDM-TDM PON is that ONUs in such networks are movable amongst sub-networks. However, some reconfigurable architectures allow ONUs to move to any sub-network, while others allow ONUs to move only within a limited and pre-defined number of sub-networks.

To differentiate these networks in terms of flexibility, a new parameter is proposed in this thesis and designated as the degree of flexibility F. It is defined as the number of possible sub-networks to which an ONU can be relocated. Although each ONU within a network in principle may hold different degrees of flexibility, only the uniform flexibility case is further analyzed where the degree of flexibility is the same for all ONUs. In this practical case, the degree of flexibility has the range from 1 to M where a static WDM-PON has $F = 1$ and a fully flexible one has $F = M$ (M is the total number of wavelength channels). The conceptual representation of the degree of flexibility is illustrated in Fig. 2.6 where a reconfigurable network with a given F is divided into distinct bandwidth pools. A bandwidth pool is shared amongst the member ONUs by dynamic wavelength and timeslot assignment. For example, the $F=2$ network is partitioned into $M/2$ bandwidth pools, each containing 2 wavelength channels. The ONU in this network can be reallocated between two particular wavelength channels.

The degree of flexibility allows a fair performance comparison to be conducted in terms of capacity to handle the traffic load. The traffic handling capacity is defined as the traffic load with which only 1 out of 100 bandwidth requests is rejected. 1% rejection is a widely-used level of quality of service for capacity planning while in the case of more stringent requirement, 1‰ can be used. Besides the traffic handling metric, the power consumption is another important metric since reconfigurable architectures are able to reduce the power consumption by allocating ONUs to a range of wavelength channels and powering down unused channels in non-busy hours. The power consumption for each degree of flexibility is also evaluated and compared in the following.

2.3. Traffic Handling Capacity Analysis

2.3.1. Chernoff's Bound for Connection Blocking Probability

In order to find the traffic capacity at 1% congestion probability, a model is derived to yield the congestion probability Pr_{block} for a given bandwidth request load. Since the aggregate capacity of a system with given F is divided into independent bandwidth pools as depicted in Fig. 2.6, the system Pr_{block} can be found from the congestion probability in individual bandwidth pools Pr_F.

Networks with different F are under consideration, each serving N ONUs, which are uniformly distributed over all bandwidth pools. These networks have the same aggregate capacity which consists of M wavelength channels, each with a data transport capacity B Mbps. Assume that an ONU, when active, requests a capacity of R Mbps. Therefore, a network with given F is divided to M/F bandwidth pools, each containing F channels and $N_F = F\times(N/M)$ ONUs.

The congestion occurs in a bandwidth pool when the sum of requested bandwidths is larger than the capacity of bandwidth pool. Since each active ONU requests R bandwidth, the congestion occurs when the number of active ONUs is larger than the threshold of $D_F = (F\times B)/R$. The traffic model of an ONU is modeled as an ON/OFF process with probability p in ON state. Assume that ONUs behave independently, the probability that k out of N ONUs are active is given by the binomial distribution [101].

$$\Pr_F[k] = \binom{N_F}{k} p^k (1-p)^{N_F-k} \qquad \text{(Eq. 2.1)}$$

Using Chernoff's upper bound, with the moment generating function $M_k(s)$ of $Pr_F[k]$ and parameter s>0, we find

$$\Pr_F\left[k > D_F\right] \leq e^{-sD_F}\, M_k(s) \qquad \text{(Eq. 2.2)}$$

Where

$$M_k(s) = E\left[e^{sk}\right] = \sum_{k=0}^{N_F} e^{sk}\,\Pr[k] = \left\{p\left(e^s - 1\right) + 1\right\}^{N_F} \qquad \text{(Eq. 2.3)}$$

The tightest bound is

$$\min_{s>0}\; e^{-sD_F} M_k(k) \qquad \text{(Eq. 2.4)}$$

We can find s by solving

$$\frac{d\left(e^{-sD_F} M_k(k)\right)}{ds} = 0 \qquad \text{(Eq. 2.5)}$$

Solving above equation, we obtain

$$e^s = \frac{(1-p)\,D_F}{p\,(N_F - D_F)} \qquad \text{(Eq. 2.6)}$$

Hence Eq. 2.2 becomes

$$\Pr_F(k > D_F) \leq \left(\frac{p}{D_F}\right)^{D_F} {N_F}^{N_F} \left(\frac{1-p}{N_F - D_F}\right)^{N_F - D_F} \qquad \text{(Eq. 2.7)}$$

Since bandwidth pools can be considered as independent stochastic systems, the upper bound of the system congestion probability experienced by an incoming request *Pr* is the average of Pr_F from individual bandwidth pools. In a particular case, if all bandwidth pools are identical in terms of ONUs, capacity, and offered load, Pr_{block} is directly given by Eq. 2.7.

2.3.2. Numerical Results

The numerical results are computed for networks with 16 wavelengths (*M*), each with a net capacity of 10 Gbps. In addition to the static network (*F*=1 network) and the fully flexible network (*F*=16 network), networks with limited flexibility *F* = 2, 4, and 8 are also investigated. The total number of ONUs in each network is 512, thus 32 ONUs per wavelength channel in average. The bandwidth request of each ONU *R* is 500 Mbps.

Since the analytical result gives the upper bound of congestion probability, which can be considered as the worst-case performance, a simulation model is developed in OPNET using the same specifications to obtain most-likely congestion probability. In the simulation model, the resource reservation map shown in Fig. 2.7 is the central entity for the book keeping of occupied and free bandwidth. The scheduling algorithm uses the map as the reference for guaranteed bandwidths, which should be provided to the ONUs. Basically, the map is a 2D array in which rows represent wavelengths and each element represents a bandwidth block of 1 byte in a 125 μs scheduling round. Based on the flexibility constraint, the reservation algorithm finds a wavelength with enough free blocks in the bandwidth pool for reservation otherwise the incoming request is rejected if no available wavelength is found. When more

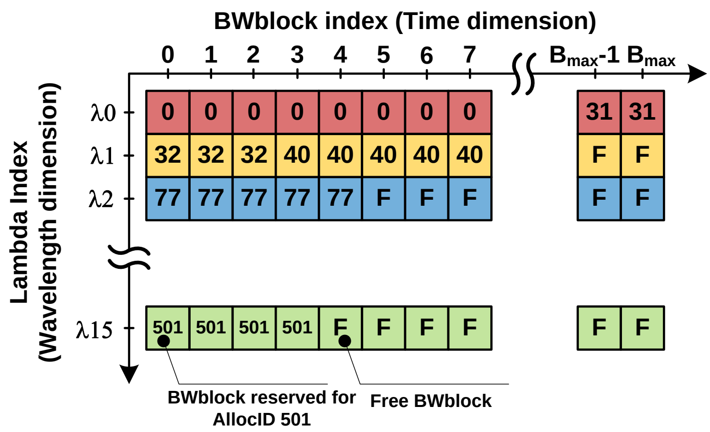

Fig. 2.7. Bandwidth reservation map for 125μs scheduling round in Resource Reservation Control in OPNET. Each BWblock is equivalent to 1 byte and B_{max} is 156250 for 10 Gbps.

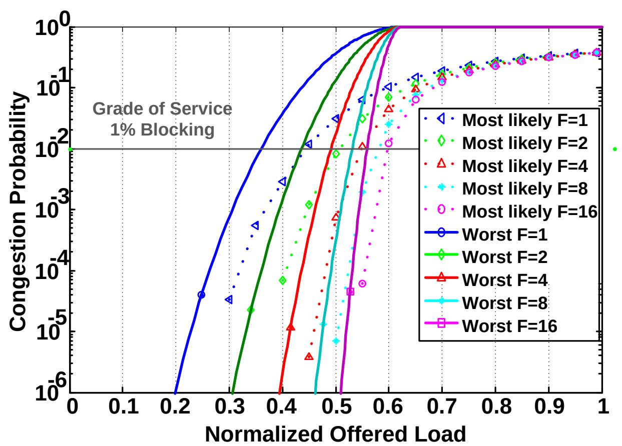

Fig. 2.8. Congestion probability for 500 Mbps connections in networks of 16 wavelength channels, 10 Gbps per channel networks with different degrees of flexibility.

than one available wavelength is found, the least-occupied wavelength is selected. For example, a request of 500 Mbps connection in a fully flexible network is equivalent to finding the least-occupied channel and reserving 7813 free blocks if there are enough of them. The reserved blocks for a connection are changed to the free state when the teardown signal is received. In an ONU, the inter-arrival time and the hold time of the connection requests follows exponential distributions.

Both the worst-case performance and the most-likely performance are shown in Fig. 2.8 in solid lines and dash lines, respectively. The performance is shown in the form of congestion probability versus offered load (normalized to the maximum offered load when all ONUs are active full time). The simulation results converge with the analytical bounds in low congestion probabilities because Chernoff's bound is tighter for the lower tail of the binomial distribution. The bounds become looser when the congestion probability is higher. However, simulation results reveal a similar trend as the analytical results: the traffic capacity (the normalized offered load at 1% blocking) of flexible networks does not linearly increase with the degree of flexibility. The *F*=2 network has the worst-case traffic capacity of 0.436 which is 21.1% higher than that of *F*=1 network. When upgrading from *F*=8 network to *F*=16 network, the additional improvement drops with only 5.3%. In a more stringent blocking level, e.g. 1‰, the nonlinear improvement trend is clearer.

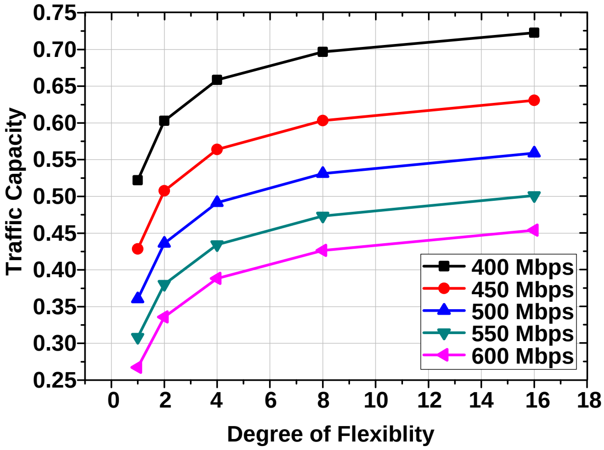

Fig. 2.9. Traffic handling capacity at 1% blocking vs. degree of flexibility for different connection bandwidths.

This trend is clearly shown in Fig. 2.9 for various values of bandwidth request. The absolute values of traffic capacity for each bandwidth request are different but they all express the same trend: the network with very limited flexibility (*F*=2 or *F*=4) can significantly improve the traffic capacity while highly flexible networks can further improve the capacity but with much lower margins.

In fact, the demand from each ONU can be different and change over time. The model cannot directly give the traffic capacity in that case. However, the traffic capacity still falls in a region defined by two curves in Fig. 2.9. For example, if the bandwidth request is somewhere between 400 Mbps and 600 Mbps, the region is defined by the highest and the lowest curve in Fig. 2.9. In the model, the ONU reallocation time is neglected. The reallocation time should take into account the transceiver wavelength switching time and the re-ranging time. When the ONU switches to a new wavelength, the propagation delay is lightly different to the previous one, re-ranging may be needed to obtain the roundtrip time between the OLT and the ONU (using a look-up table to expedite the process also possible). Ranging is required to adjust the ONU transmission time because of the differences in distance, thus in propagation delay between ONUs to the OLT. Therefore, the ONU reallocation time is not zero and not the same for different architectures, and it depends on the protocol employed. For instance, the ONU reallocation time can be almost zero if a make-before-break reallocation can be realized with a dual transceiver. In other architectures, the reallocation time cannot be zero as the transceiver wavelength switching time should be considered. The model also does not consider the logical limitations. It assumes that a wavelength channel can be shared by any number of ONUs. However, it might be not true in practice since GPON-like protocols only allow up to 128 ONUs per PON but EPON-like protocols allow up to 32767 ONUs (virtually unlimited). Therefore, the exact performance is different from case to case but I believe that the non-linear trend still holds true.

2.4. Power Consumption Analysis

2.4.1. Energy Consumption Model

By leveraging the network reconfigurability, a simple strategy to save the power consumption can be used in which ONUs can be allocated to a range of wavelength channels to allow the other channels to be in standby mode during non-busy hours as discussed in Section 2.1.2. Let e_C (kW) and t_P denote the power consumption by a channel in the OLT (the channel line card and related parts) and number of busy hours per day, respectively. Assuming that all M channels need to be enabled to accommodate the peak load, we can derive the energy consumption (kWh) per day during busy-hours.

$$E_P = t_P M e_C \qquad \text{(Eq. 2.8)}$$

Hence, the energy consumption (kWh) in non-busy hours in one day

$$E_O = (24 - t_P) m_O e_C \qquad \text{(Eq. 2.9)}$$

where m_O is the number of active channels in non-busy hours.

Since a network with given F contains M/F independent bandwidth pools, we can derive the number of active channels in non-busy hours.

$$m_O = (number\ of\ active\ channels\ in\ a\ bandwidth\ pool) \times (number\ of\ pools)$$

$$= ceil(F \times L_O / C_F) \times (M/F) \qquad \text{(Eq. 2.10)}$$

where L_O (Mbps) is the actual traffic load in a bandwidth pool in non-busy hours, C_F (Mbps) is the capacity of a bandwidth pool, and the *ceil* function returns the nearest integer that is larger than the argument.

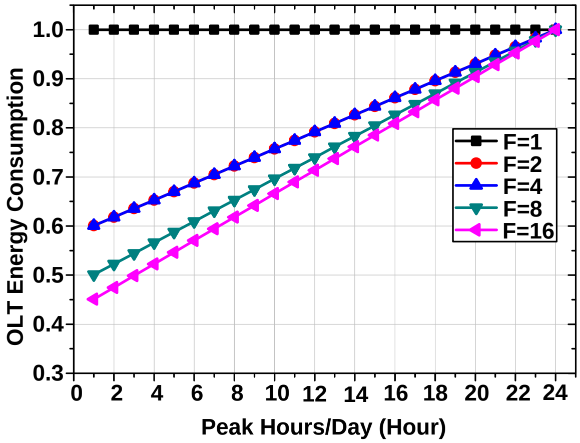

Fig. 2.10. Energy consumption (relative to the maximum consumption) of the OLT as a function of peak hours per day in networks with different degrees of flexibility (F).

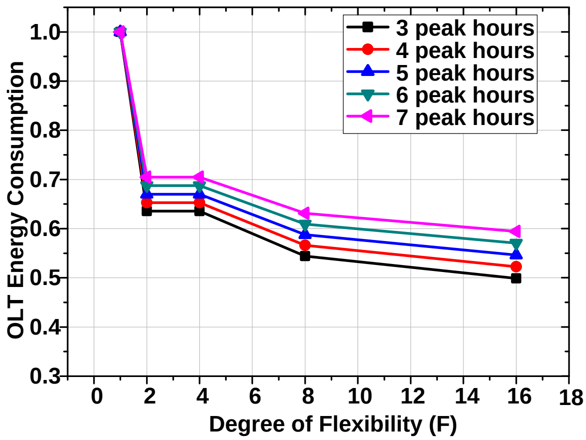

Fig. 2.11. OLT energy consumption versus degree of flexibility for different numbers of peak hours per day.

Apart from the energy consumption by channels, I consider a baseline consumption E_B which accounts for 20% of the maximum line card consumption E_{MAX} (20% of $24Me_c$). Finally, we can derive the daily energy consumption at the OLT normalized to the maximum consumption.

$$E_{OLT} = \frac{E_O + E_P + E_B}{E_{MAX} + E_B} = \frac{t_P M + (24 - t_P) m_O + 4.8M}{28.8M} \qquad \text{(Eq. 2.11)}$$

2.4.2. Numerical Results

The OLT daily energy consumption depicted in Fig. 2.10 is obtained by evaluating Eq. 2.11 for networks with F = 1, 2, 4, 8, and 16. I assume that in busy-hours all of 16 channels are active to accommodate 100% of the traffic and in non-busy hours the average traffic is 30% of the peak-traffic. Regardless of the number of busy hours per day, the F=1 network (static) consumes the same power during the day because in any case, it is not able to move ONUs out of a channel in order to power down the transceiver. Another intuitive observation is that there is no power saving in flexible networks when the number of busy hours is 24. However, at a typical value of 5 or even 10 busy hours per day, the figure reveals a trend analogous to the traffic capacity analysis. The networks with a limited flexibility can thus significantly reduce the power consumption while highly flexible networks can further reduce the consumption but in a small amount.

The trend is clearly shown in Fig. 2.11 in which there is a sharp decrease in the consumption when the degree of flexibility changes from 1 to 2. The F=2 network indicates a saving of 33% in the OLT daily energy consumption in case of 5 busy hours per day while F=16 network can only save 13% more. Even then there is no difference between the consumption of F=2 and F=4 because they have to enable the same number of channels in non-busy hours. The non-busy traffic assumption (30 % of the network capacity) leads to this phenomenon.

To investigate how the level of non-busy traffic affects the power saving, different load levels are examined as shown in Fig. 2.12. In this figure, the number of busy hours is fixed to be a typical value of 5 hours per day [102]. The plot confirms an intuitive prediction that there is no saving when non-busy traffic load is almost equal to network capacity. The network with F=2 is able to save the power when the non-busy traffic load is lower than 50 % of the capacity. Since in non-busy hours, networks are usually under 50% utilization, the F=2 network is potentially saving considerable power although ONUs in this network can be only reallocated between two wavelength channels. A lower level of non-busy traffic is more favorable for highly flexible networks. However, F=2 can still provide more than half of the saving achieved by the fully flexible network at the level of 10 % as shown in Fig. 2.12.

The power consumption analysis uses a basic model of real traffic that varies smoothly from the peak to the bottom during 24 hours as seen in a typical access traffic traces [102]. To compute the daily energy consumption for a real traffic profile, the model is still applicable since we can break down the 24 hour trace to segments, each of which covers a small period, e.g., 5 minutes. Since the segment is relatively short, the traffic in the middle timestamp or the average traffic volume can approximate the representative traffic volume of each segment in that period. Then, we can yield the energy consumption of each segment by applying the model. Finally, the daily energy consumption is obtained by the sum of all segments.

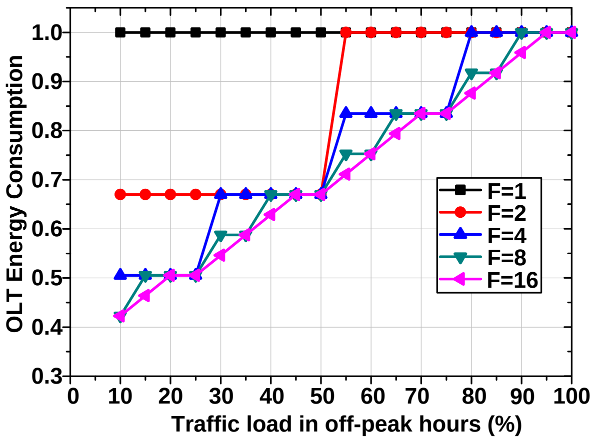

Fig. 2.12. Energy consumptions of the OLT (relative to the maximum consumption) as a function of traffic load in off-peak hours (relative to the peak traffic) in networks with different degrees of flexibility (F).

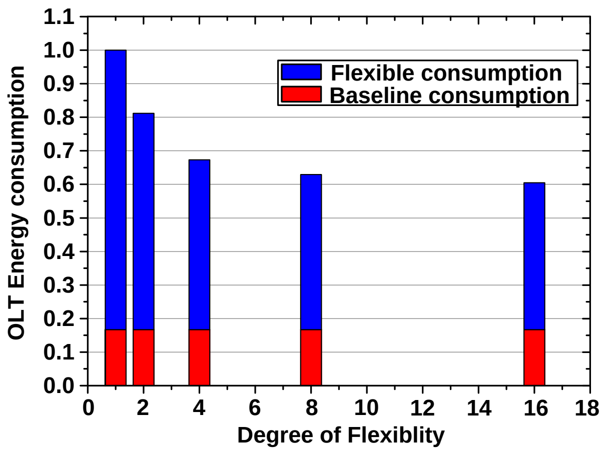

Fig. 2.13. Energy Consumption of the OLT computed based on the actual traffic trace at a KPN CO.

This method is applied to an actual traffic trace captured at a KPN central office in Amsterdam which is shown in Fig. 1.3.a). The profile is the aggregate Internet traffic from mixed consumers and businesses in a high take-rate access network. In this profile, the load reaches the lowest level from 4 to 8am since both consumer and business tend to be inactive in this period. From the start of office hours, the load increases gradually and reaches the highest level around 9pm in the evening. The energy consumption based on this profile for each degree of flexibility is shown in Fig. 2.13 where the nonlinear trend is confirmed. The $F=2$ and $F=4$ networks indicate a saving of 18.8% and 32.7% while the $F=8$ and $F=16$ networks save 37.0% and 39.5%, respectively. Assuming the OLT consumes 100 W power when fully active, the $F=2$ and $F=4$ networks potentially save 164.7 and 286.5 kWh/OLT/year, respectively.

In fact, this traffic pattern provides a conservative saving figure because a typical take rate of FTTH deployments is lower than 50% leading to a lower load level and the mix of user types also makes busy hours longer. For example, an average take rate is 40% in United States according to FTTH Council Americas and 17.5% in Europe as of Dec. 2011 according to FTTH Council Europe [28] [103].

Furthermore, if the equipment power consumption reduces, we can simultaneously save power in the cooling system (rack and building cooling). Therefore, the energy bill for the central office, where the OLTs are located, is lowered considerably yielding a reduction in the operating expenditure (OPEX) and in the CO_2 footprint of access networks.

2.5. Limited Flexibility

In this section, the Broadcast-and-Select architecture shown in Fig. 2.14.a) is considered to be modified to $F=2$ limited flexibility. The modified architectures are then compared with the original one and the static architecture in terms of power budget to evaluate how $F=2$ can help to reduce the network cost.

The Broadcast-and-Select architecture is a prominent candidate for wavelength reconfigurability because the ODN is passive and compatible with current TDM PONs. All the wavelength channels are broadcasted to ONUs by one or more power splitting stages and ONUs select the working channel by a tunable or switchable transceiver. This architecture is fully flexible since an ONU is exposed to all the wavelengths but requires large power budget because of its broadcasting nature.

Limiting the degree of flexibility to 2 whilst the network performance is still largely preserved as proven in previous sections can reduce the large power loss budget requirement. Accordingly, the power splitter can be replaced by a combination of AWG, combiners, and splitters, which can be realized by discrete components or an integrated device, as shown in Fig. 2.14.b). If the wavelength planning allows the cyclic property of the AWG to be exploited, we can further reduce the insertion loss by the architecture shown in Fig. 2.14.c). In fact, an architecture with *F=3* has been proposed in [93]. In the same fashion, the *F=4* network can be achieved by using the fourth order of AWG free spectral range (FSR). This method provides a smooth path to upgrade the network capacity and degree of flexibility without any change in the ODN.

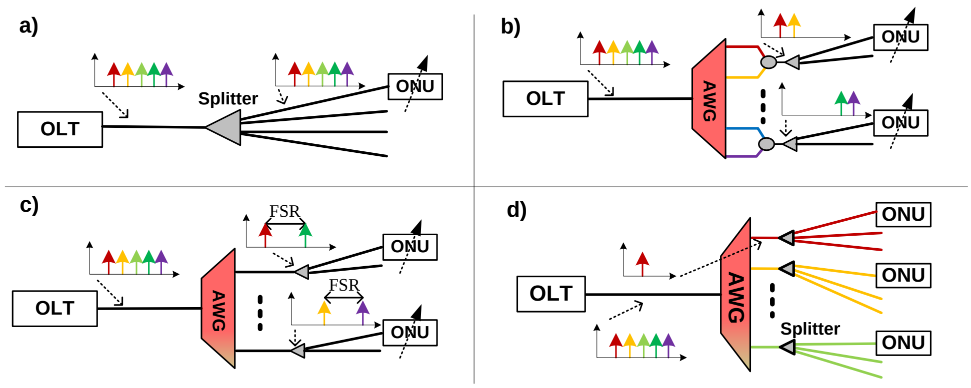

Fig. 2.14. a) Schematic representation of Broadcast-and-Select architecture, b) Schematic representation of F=2 architecture, the ONUs are uniformly distributed to each branch, c) Schematic representation of F=2 architecture exploiting the cyclic property of AWG, only downstream wavelengths are shown, d) Schematic representation of static WDM-TDM PON.

The accumulated worst-case insertion loss in the RN of various networks, each with 16 wavelength channels and 512 ONUs is estimated and shown in Fig. 2.15. The worst-case 1:2 split loss of 3.55 dB is used as the base for split ratio scaling [96]. By limiting the flexibility, the architecture in Fig. 2.14.c) saves 8.65 dB compared to the Broadcast-and-Select and requires 3.55 dB more power when compared to the static network shown in Fig. 2.14.d). The power saving allows more users to be supported, longer reach, and/or lower cost transceivers whilst avoiding the use of optical amplifiers in the field.

Furthermore, the limited flexibility also makes the network scalable in terms of wavelength and ONU dimensioning. The RN worst-case insertion loss is shown in Fig. 2.16 when the number of wavelength channels is scaled. As the number of ONUs per wavelength is kept at 32, it is clear to see that the insertion loss for the Broadcast-and-Select increases with the number of wavelengths (actually with the number of ONUs). On the other hand, *F=2* and static networks can maintain almost the same insertion losses because the split ratio for each wavelength is the same (1:64 for *F=2* and 1:32 for static). A slight increase in the insertion losses is due to the AWG insertion loss, which is a component of RN insertion loss, increasing slightly with port count. However, a commercially available 88-channel 50 GHz spaced AWG induces only 5.5 dB insertion loss at most [104]. As observed, the Broadcast-and-Select is a suitable architecture for low channel count since there is no significant difference in the insertion loss when the number of wavelength is less than 8. This observation supports the

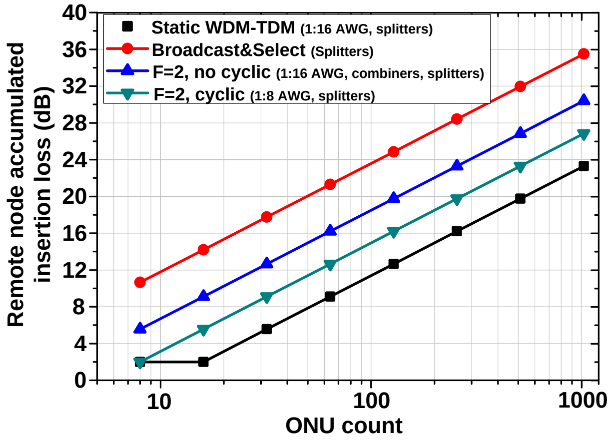

Fig. 2.15. Remote node accumulated insertion loss when increasing number of ONUs in different network architectures.

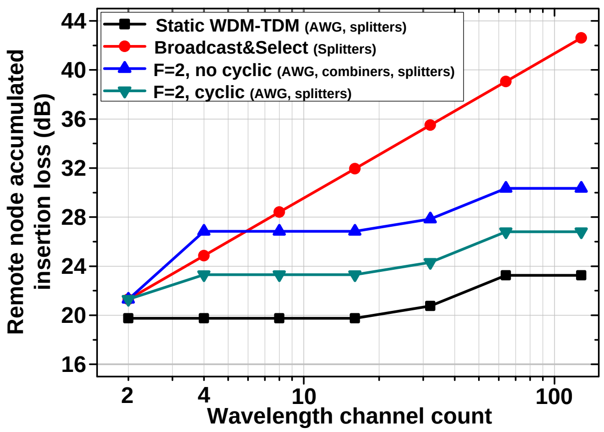

Fig. 2.16. Remote node accumulated insertion loss in different network architectures when increasing wavelength dimension (average number of ONUs per wavelength channel is 32).

configuration of NG-PON2 in which 4 wavelengths are used on the power-splitter-based ODN. Beyond NG-PON2, when more wavelengths are used, the power-splitter-based ODN should be changed.

2.6. Conclusions

In this chapter, I have shown that wavelength reconfigurability can reduce network congestion in busy hours and reduce the power consumption in non-busy hours. Furthermore, the analysis shows that it is not necessary to have a high or full flexibility since an architecture with limited flexibility can largely achieve the merits of reconfigurability. The most limited flexibility network, when *F=2*, can improve the traffic capacity by 21.1% and reduce the OLT daily energy consumption by 18.8% in comparison to the static network. Based on some specific assumptions, the OLT of F=2 network with 16 wavelengths and 512 ONUs can potentially save 164.7 kWh/OLT/year. A highly or fully flexible network can further reduce the congestion and the power consumption but the difference is marginal. Therefore, I conclude that the flexible WDM-TDM access networks improve the network efficiency considerably and it is not necessary to have a fully flexible network with its increased costs. However, the optimal value for the degree of flexibility is not specified since the optimal value is not the same for different traffic scenarios, deployment scenarios, user types, number of wavelengths, and business policy amongst the plethora of considerations. For example, if the traffic in off-peak hours is not lower than 50% of the network capacity, the limited degree of 2 should not be selected since no power saving can be achieved. In that case, the limited degree of 4 may be more appropriate.

Furthermore, I have presented the impact of limited flexibility for the wavelength-selection based architectures. The limited flexibility requires a lower power budget and is more scalable than the fully flexible Broadcast-and-Select. One can also apply this method to wavelength-routed architectures [90][94] to reduce the number of switching elements in the RN.

CHAPTER 3

CYCLICALLY-LINKED FLEXIBILITY: A QUASI-FULL FLEXIBILITY WITHOUT WAVELENGTH TUNING

This chapter further extends the concept of limited flexibility to the concept of cyclically-linked flexibility. The proposed architectural concept limits the ONU degree of flexibility to two but still maintains the network-wide bandwidth redistribution capability. The logical performance of the cyclically-limited flexibility is evaluated by a computer model to demonstrate its merits. The contents of this chapter have been partly disseminated in [92] and [105].

3.1. Concept of Cyclically-linked Flexibility

3.1.1. Dual Fixed-Wavelength Transceiver

The two main challenges for wavelength-selection-based wavelength reconfigurability are the requirement of high power loss budget and the cost of tunable transceivers at the ONU. The first challenge can be addressed by using a limited flexibility degree as demonstrated in Chapter 2. The use of optical amplifiers in the field can also address the loss challenge and it is economically viable in many cases [106]. Therefore, the high cost of a tunable transceiver is more problematic since user premise equipments account for the largest share of total equipment cost, e.g., 32% in Belgacom's deployments (the Belgium incumbent) [107]. The requirement for tuning range and tuning speed cannot be relaxed as discussed in Section 2.2.2.

In fact, the cost of a tunable laser module includes many items such as testing, packaging, and controlling. The cost of the laser chip itself is a minor contributor to the final module cost [108]. One of main cost drivers is the wavelength control that includes the wavelength stability and the wavelength tuning control. Wavelength stability requires temperature control of the laser chip. The cooler method by using the thermoelectric material (Peltier effect) commonly used in core network applications is expensive for access network applications. Therefore, uncooled methods were studied in order to remove expensive cooler but still maintain wavelength stability [109][110][111][112]. In uncooled methods, the laser chip is always heated to a temperature above the ambient environment temperature. These uncooled components remain under development and are not yet widely available commercially.

Wavelength tuning needs to be addressed not only within the ONU but also in the network itself. The OLT has to assist the ONU to fine tune the wavelength in relation to the center of filter profiles which are cascaded along the light path to maximize the received power and to avoid interference [113]. Furthermore, bias currents to the laser electrodes (~10 electrodes) need to be set by a microcontroller and can also contribute significantly to the cost. The micro controller is needed to process control commands and to map input parameters, e.g., a look-up table of the wavelength index to the corresponding current values which vary from one laser chip to another.

Besides the tunable laser, a tunable receiver is required for downstream wavelength selection. The tunable receiver is usually composed of a photodiode and a tunable filter as depicted in Fig. 3.1.a). The tunable filter technology has been developed for wavelength reconfigurability in core networks. However, recent efforts on tunable filters targeting the access network were reported, which promise to produce inexpensive tunable filters [114][115].

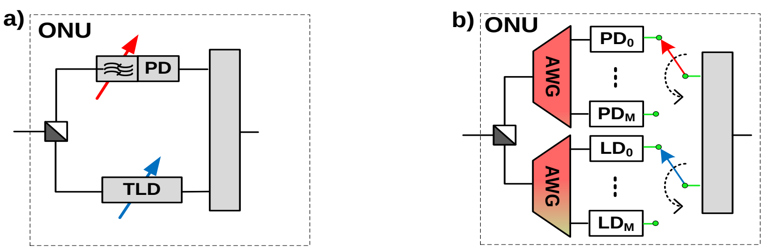

Fig. 3.1. a) Schematic representation of tunable transceiver b) Schematic representation of an array of fixed transceivers.

Another potential solution to avoid the cumbersome process of wavelength tuning and its associated regular calibration procedures is to use an array of fixed transceivers, each dedicated to one wavelength channel as shown in Fig. 3.1.b). The working transceiver can be selected electrically. The athermal characteristic of the fixed wavelength filter based on AWG, TFF (Thin Film Filter), or FBG (Fiber Bragg Grating) allows a stable operation without any wavelength and temperature control. In addition, the break-before-make mechanism when switching the working wavelength can be realized, which eliminates any concern about the interruption of on-going services [78]. The array including wavelength MUX/DEMUX can be monolithically integrated in a single chip, as demonstrated in [116]. However, a large size array, which is required for a large wavelength count, is also expensive and even technologically immature. Therefore, it is desirable to have a network architecture that requires a small transceiver array but still guarantees high bandwidth redistribution capability. The next section further describes a concept that requires an array of only two fixed transceivers, which is the smallest array size.

3.1.2. Cyclically-linked Wavelength Configuration

Partitioning wavelengths to several sub-groups can reduce the size of the transceiver array. Chapter 2 has shown that the statistical multiplexing gain is only slightly affected by the partitioning. However, these sub-groups are still disjoint resulting in the bandwidth redistribution capability to be limited within each sub-group and cannot be done on a network-wide scale. For example, the network can be partitioned to the degree of flexibility of 2, as shown by the 2-wavelength limited inset in Fig. 3.2. The 6-wavelength network has three separate bandwidth pools. Therefore, it is clear to see that the network-wide bandwidth redistribution capacity cannot be done. To overcome the disjoint problem, the linking of 2-wavelength bandwidth pools in a cyclic configuration to form a single cyclically-linked bandwidth pool (CLBP) is proposed in this thesis. Two adjacent wavelengths are linked by a group of ONUs in a cyclic manner. Hence, there are two different ONU groups associated with a wavelength, where one is shared with the previous-index wavelength and the other is shared with the next-index wavelength. Without loss of generality, the inset in Fig. 3.2 shows the construction for 6-wavelength CLBP at the conceptual level.

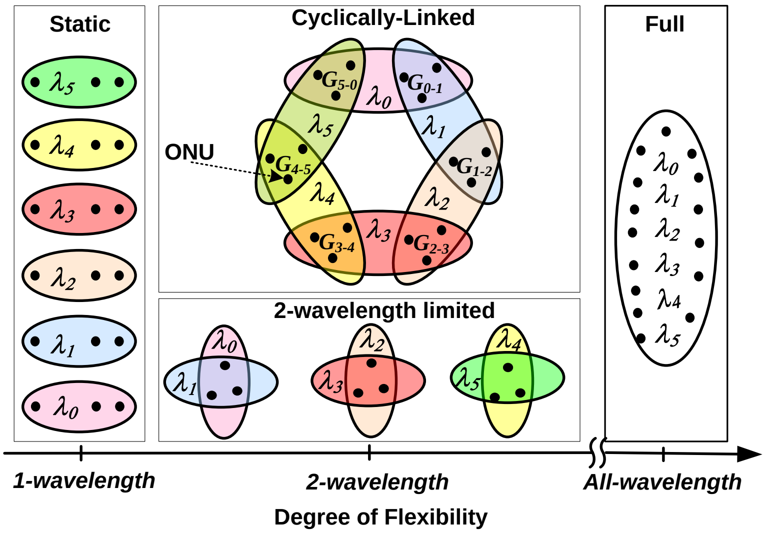

Fig. 3.2. Conceptual representation of wavelength reconfigurability schemes for 6-wavelength networks, the cyclically-linked flexibility is a variant of 2-wavelength limited.

From the ONU's perspective, CLBP or the cyclically-linked flexibility is the same to 2-wavelength limited flexibility where the ONU can operate only within two wavelengths but from the network's perspective, all wavelengths are joined to be a single bandwidth pool which enables network-wide bandwidth redistribution capability. The bandwidth rearrangement process can shift available bandwidth from a light-load wavelength to an overloaded wavelength by several steps. As an example depicted in Fig. 3.3, there is a bandwidth request in $\lambda 1$, which is already congested while $\lambda 3$ remains largely available. Unlike the full flexibility (Broadcast-and-Select), the requesting ONU in CLBP cannot be reallocated to $\lambda 3$ to enjoy the free bandwidth directly. However, the free bandwidth itself can be reallocated or shifted to $\lambda 1$ by rearranging occupied bandwidth blocks. To shift a part of the free bandwidth space from $\lambda 3$ to $\lambda 1$, we can first reallocate one or more ONUs in the group $G_{2\text{-}3}$ from $\lambda 2$ to $\lambda 3$. Virtually, we swap the occupied space and the free space between two wavelengths by reallocating ONUs. After the first swap, we now have enough capacity in $\lambda 2$ to perform the second swap between $\lambda 1$ and $\lambda 2$. Finally, the rearrangement process with two bandwidth swaps shifts the free bandwidth to $\lambda 1$. The network now can accept the bandwidth request that would have been rejected if the network is static or originally 2-wavelength limited.

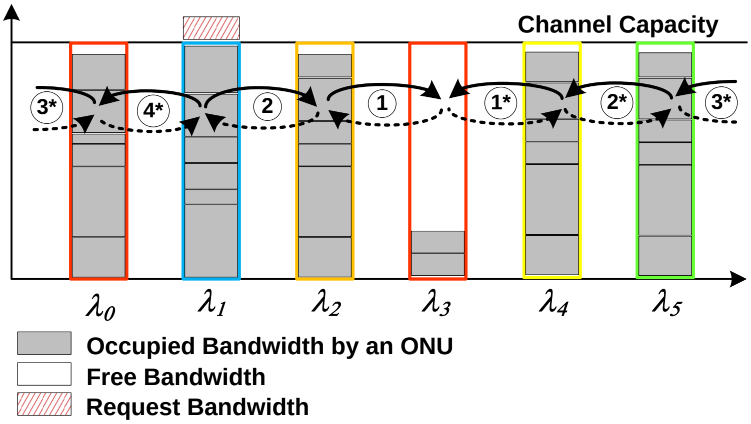

Fig. 3.3. Example of bandwidth rearrangement steps of the cyclically-linked flexibility for the 6-wavelength network.

However, the bandwidth swap may be unsuccessful when there is no possible combination of ONUs in the busy wavelength that is larger than the requested bandwidth but fits to the free bandwidth space in the light-loaded wavelength. The unsuccessful swap attempt is referred as a swap blocking. The fundamental reason for swap blockings is the block-wise allocations, meaning that the occupied bandwidth blocks cannot be split arbitrarily to multiple wavelengths. In the example, if there is a swap blocking in the counter clockwise direction, we also can swap in the clockwise direction because of the cyclic property. Nevertheless, bandwidth redistribution in CLBP may not be always possible and may involve many other ONU reallocations. Hence, this potential for disruptions to in-service ONUs needs to be minimized. If the make-before-break mechanism can be realized, the ONU can establish the connection in the new wavelength before tearing the old connection that can remove the concern about service disruptions. However, the signaling overhead generated by ONU reallocations still need to be minimized by reducing the number of reallocations. Chapter 3 continues with the dynamic wavelength and timeslot assignment on cyclically-linked networks while Chapter 4 describes cyclically-linked physical architectures.

3.2. Network-Wide Bandwidth Rearrangement

3.2.1. Wavelength and Timeslot Management

This section describes a general framework designed for wavelength and timeslot management in WDM-TDM access networks. This framework is extended from XG-PON TDM operations by adding the wavelength dimension.

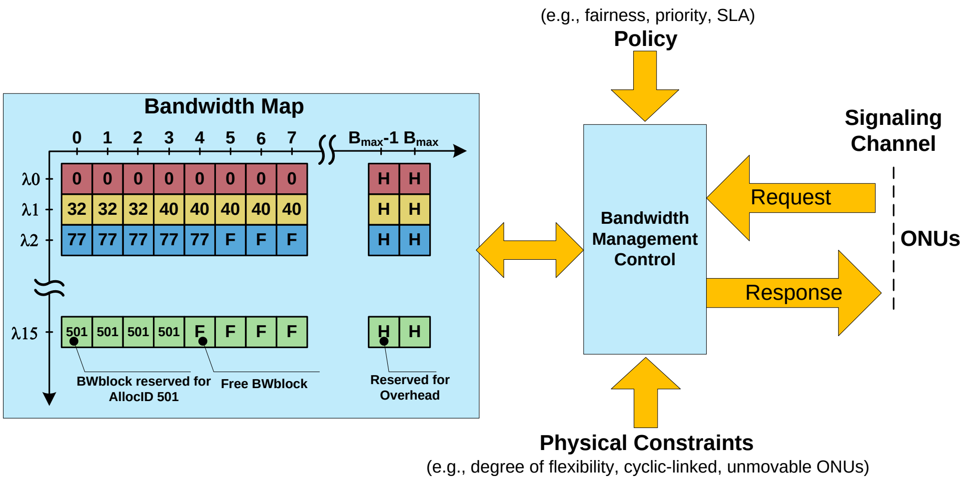

Fig. 3.4. Bandwidth management structure, the bandwidth map represents wavelengths and timeslots in 125 μs scheduling round with each block is corresponding to 4 bytes. Bmax is determined by the wavelength line rate.

The bandwidth management control and its interfaces are shown in Fig. 3.4 in which the control messages are exchanged with ONUs through a logical channel dedicated for signaling. ONUs inform the control (in the OLT) about their real-time demand, e.g., queue lengths and the control responses with the assignment of wavelength and timeslot. The control also receives a set of policies from the administrator to distribute bandwidth accordingly. Service level agreements (SLAs) between the network operator and subscribers, for example, are enforced through this interface. Besides, physical constraints must be visible since the control needs to know which wavelengths are possible for a particular ONU. The physical architecture and the actual deployment will determine these constraints. The cyclically-linked architecture, for example, restricts ONUs to have only two possible wavelengths but each ONU group has different sets of two wavelength indexes. In an actual deployment, there can be the case that some ONUs are not capable of wavelength switching. It is because they are not equipped with proper transceivers or simply a partial malfunction of transceivers. The control also needs to be informed with such kinds of constraints.

All inputs are processed by a particular dynamic wavelength and timeslot assignment algorithm, also known as dynamic bandwidth allocation algorithm (DBA) or dynamic wavelength and bandwidth allocation algorithm (DWBA). The algorithm interacts with the bandwidth map (*rvsp_map*) that is the central entity for the book keeping of entire network bandwidth. Basically, *rsvp_map* is a 2D array shown as the inset in Fig. 3.4 in which rows represent wavelengths and each element represents a bandwidth block of 4 bytes in a 125 μs scheduling round. When the element is reserved for a logical connection identity (*allocID*), its content is assigned to the corresponding *allocID*, otherwise, the content has a special value indicating a free block. The block size of one 4-byte word was selected for the OPNET implementation to compromise between the bandwidth granularity and the computational cost.

3.2.2. **Overview of Computer Simulation Model**

The cyclically-linked bandwidth rearrangement algorithm and its counterpart algorithms for static, limited flexibility, and full flexibility are implemented in OPNET discrete event simulation platform by the C/C++ programming language. Models of the OLT, the ONU, the WDM optical fiber, the power splitter, and bursty traffic sources are also implemented in order to have a complete operational setup of the network.

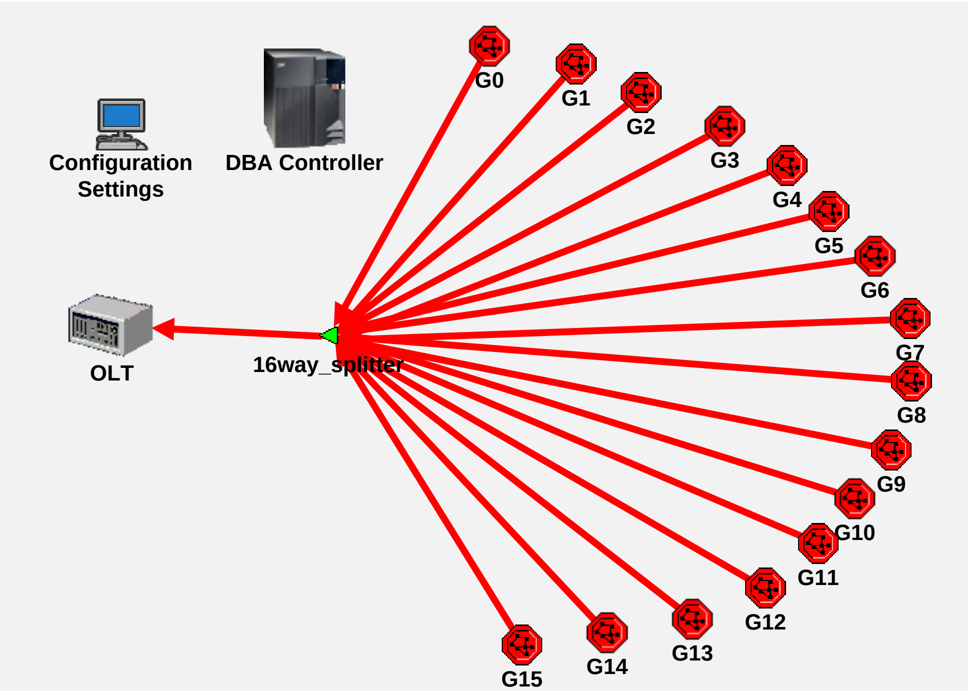

Fig. 3.5. WDM-TDM optical access network setup with 16 ONU groups and the configuration settings to set common simulation parameters. The DBA function is decoupled from OLT for easy upgrades.

The setup of 512 ONUs with *ONU_ID* from 0 to 511 connecting with the OLT through two splitting stages of 16-way and 32-way is shown in Fig. 3.5 and Fig. 3.6. ONUs are divided to 16 groups numbered from *G0* to *G15*, each has 32 members. There are 16 wavelength channels, each can be set to operate at 2.5 Gbps or 10 Gbps. The data plane and the control plane are implemented separately to create a flexible model. Data packets and overheads are transferred through fibers in the data plane. The control plane is implemented by "air" communication channel, i.e., the remote interrupt mechanism of OPNET to emulate the logical signaling channels. Signaling messages between ONUs and the DBA controller, e.g., REQUEST and GRANT signal, are exchanged through this channel. The signaling interface is closely referred to XG-PON G.984.7 recommendation [117]. The DBA controller is decoupled from the OLT for the purpose of upgradability. The configuration settings module is created for packet source parameter assignments such as mean packet rate and Hurst-parameter (represent to the burtiness of generated packets) for multiple sources in a batch. Hurst parameter is also known as Hurst exponent is ranging from 0 to 1 indicating the long-range dependence of a time series. The empirical studies have shown that access traffic is bursty exhibiting long-range dependence in nature with a Hurst parameter around 0.8 [118][119][120]. The configuration settings module helps to remove the time-consuming manual parameter assignments for 512 sources for each traffic scenario. The capability of setting directly at the source is still preserved but only will be used for special sources in order

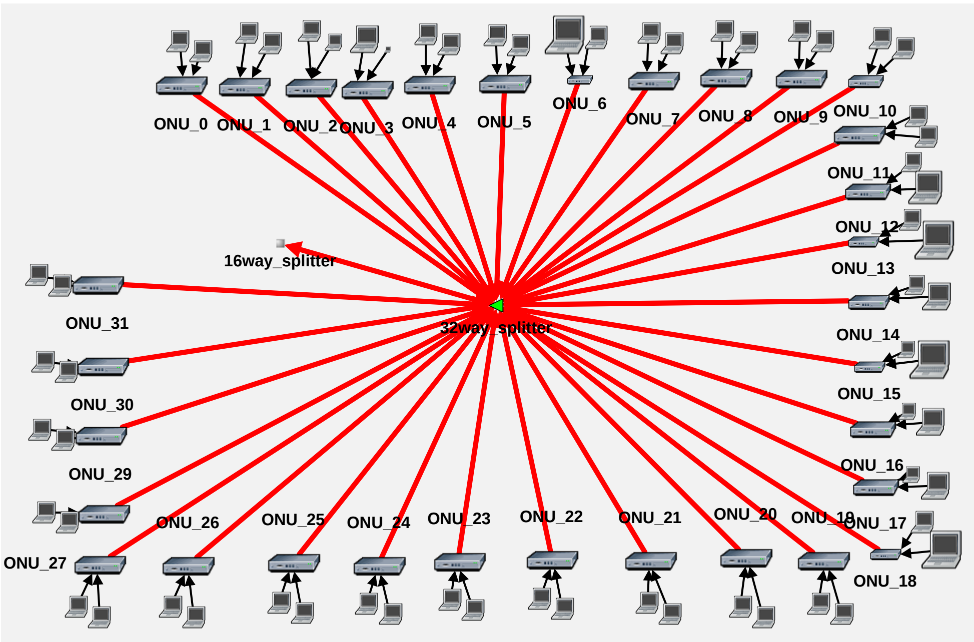

Fig. 3.6. The topology of *G0* subnet of ONUs, each ONU is attached with two bursty traffic sources. The traffic generation parameters can be set directly at the source or set in batch via the Configuration Settings module.

to have different behaviors from the rest.

Each ONU is attached to two bursty packet sources as shown in Fig. 3.6, however, the second one is only intended for future use. Packets are generated by the source and sent to the ONU via a patch cord. The ONU accepts packets into its queue before sending them to the OLT. An ONU reports its queue status to the DBA controller to ask for the bandwidth for the next transmission cycle right after finishing the data transfer in the current cycle. Upon receiving a GRANT message with assigned wavelength and timeslot, the ONU will forward packets according to wavelength and time values in the message. Right before sending, the ONU perform the framing and writes appropriate header information such as *ONU_ID*, *Alloc_ID*.

A lightweight mode was developed to reduce the number of operations on each packet since each packet goes through hundreds of operations during its life cycle. In this mode, the computation is reduced by simulating the network at the flow level when information about individual packets is not needed (each Alloc-ID creates a flow of packets when active). On the other hand, the lightweight mode is unable to provide detail about individual packets such as delay or jitter. Therefore, the lightweight mode is used to investigate the performance at the connection (flow) level while the full mode is used to investigate the performance at the packet level.

In fact, the setup physically allows the ONU to send packets to any of the 16 channels. It enables a maximum flexibility to simulate any physical constraint by enforcing it onto the DBA algorithm. Therefore, the model provides a facility to simulate any scheme with different physical constraints including static, full, limited-flexibility and cyclically-linked flexibility. In other words, the model framework provides application programming interfaces (APIs) to implement any DBA algorithm with different physical-induced and policy-induced constraints.

3.2.3. Swap-Based Bandwidth Rearrangement Algorithm

The unique and core feature of CLBP is the network-wide bandwidth redistribution based on a rearrangement process. Appropriate ONUs are reallocated step by step to shift a certain free bandwidth space from the source wavelength to the destination wavelength. There are many possible reallocation plans to get the work done. To select a plan, there can be several criteria, however, the most obvious one is the total number of in-service ONU reallocations since we want to minimize disruption for in-service ONUs. In the following, a heuristic rearrangement algorithm is developed bearing in mind that criterion. The algorithm is implemented in the bandwidth management control to facilitate the operation of cyclically-linked networks

The flowchart of the algorithm, as depicted in Fig. 3.7, from the point that the OLT receives a bandwidth request with a given *allocID* from an ONU to the point that the decision over the request is made. The logical connection size in Mbps is converted to the corresponding number of 4-byte blocks (*RqBW*). If the number of free blocks in the current lambda (*Rq_λ_freeBW*) is enough to accommodate *RqBW*, the request is accepted. Otherwise, the other λ (since the ONU can move between two given λs) is inspected for the possibility to accommodate the ONU. The free space (*other_λ_freeBW*) should be large enough to host not only the request bandwidth (*RqBW*) but also in-service AllocIDs of the ONU

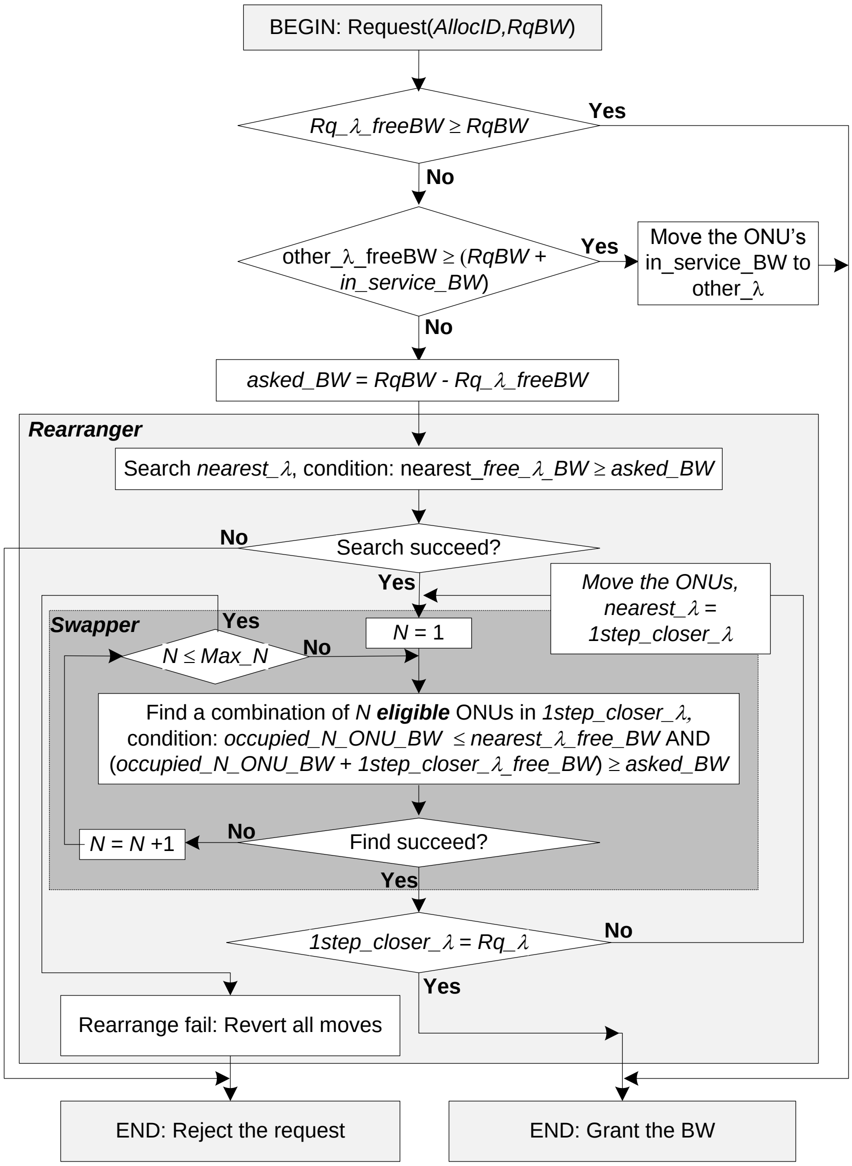

Fig. 3.7. Simplified flowchart of swap-based bandwidth allocation rearrangement algorithm by moving step-by-step free BWblocks from a free wavelength to the congested wavelength.

(*in_service_BW*). The reason is that the ONU may be allowed to have more than one logical connection and this algorithm supposes that the ONU can only enable one transceiver out of two available transceivers.

If the space in the other lambda is not enough, we have no other choice but to shift free blocks to the request lambda (*Rq_λ*). The source lambda is the nearest lambda (*nearest_λ*) which has enough free blocks. Note that we can look for *nearest_λ* on both sides of *Rq_λ* because of the cyclic property. The algorithm tries to move free blocks to *Rq_λ* step by step using the swapper. After one swap, free blocks are moved one lambda closer towards the destination, hence, the one-step closer lambda (*1step_closer_λ*) now becomes *nearest_λ*. The process repeats recursively until *1step_closer_λ* is equal to *Rq_λ*.

Within the swapper, the algorithm tries to find appropriate ONUs in *1step_closer_λ* to move to *nearest_λ*. Eligible ONUs are members of the ONU group which links *1step_closer_λ* and *nearest_λ*. To minimize the number of reallocated ONUs, the swapper starts to search for a single ONU that makes the free space in *1step_closer_λ* (*occupied_N_ONU_BW* + *1step_closer_λ_free_BW*) larger than *asked_BW* when it is reallocated to *nearest_λ*. The ONU also needs, of course, to fit within the free space of *nearest_λ* (*occupied_N_ONU_BW* ≤ *nearest_λ_free_BW*). If no single ONU meets the condition, the swapper searches for combination of two ONUs, and so on. I limit the size of ONU combination ($N \leq Max\_N$) to avoid too many reallocations in one swap. When the combination reaches the size limit and no combination meets the condition, the swap is blocked meaning that the rearrangement is declared to be unsuccessful. The bandwidth reservation map remains in the original stage and the request is rejected.

3.3. Logical Connection Level Analysis

3.3.1. Blocking Probability Analysis

The performance in the logical connection level is first investigated. The statistic of interest is the logical connection blocking probability. Different schemes are compared using various traffic scenarios. The result for a simple scenario is shown in Fig. 3.8 in which each ONU can request only one logical connection with a fixed size of 500 Mbps and the bandwidth request is coming in a Poisson process. The wavelength capacity is 10 Gbps. Thus, the scenario allows us to verify the simulation model by the widely-used Erlang-B formula. The simulated static and full blocking probabilities (in dots) are in agreement with probabilities calculated using Erlang-B formula.

The cyclically-linked flexibility cannot be directly verified by Erlang-B since it involves complex rearrangement processes that are out of the scope of Erlang-B model. However, Fig. 3.8 shows that the full and cyclically-linked flexibility yield exactly the same performance. In fact, the result is expectable for this traffic scenario since the rearrangement process is always successful if there is enough free bandwidth elsewhere in the network. The underlying reason is the uniformity of the connection size and each ONU can have only one connection. The swapper can always successfully find an ONU with occupied bandwidth of 500 Mbps (1954 blocks) in *1step_close_*λ to fit in the free space in *nearest_*λ. In case of not enough free space being available in the network, both full and cyclically-linked schemes have no other choice but to reject the request. Therefore, the cyclically-linked flexibility has the same performance to the full scheme when the bandwidth rearrangement is always successful. Therefore, the cyclically-linked flexibility is indirectly verified by the Erlang-B model.

In practical scenarios, the ONU can have several logical connections, each for a different service. Table 3.1 summarizes three scenarios numbered from 0 to 2. Scenario 0 is an extension from the basic scenario in which the connection size is uniformly distributed from

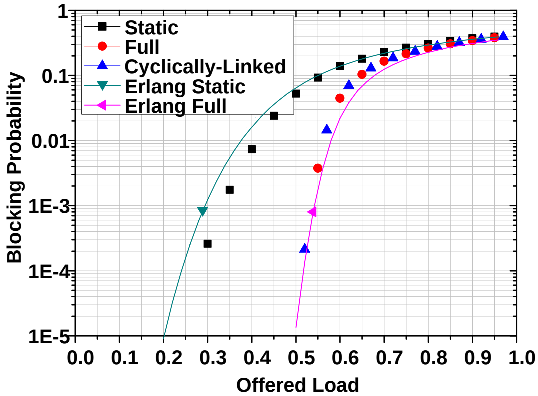

Fig. 3.8. Logical connection blocking probability as a function of offered load for request bandwidth of 500 Mbps, one AllocID per ONU.

TABLE 3.1. TRAFFIC SCENARIOS IN THE CONNECTION LEVEL

Scen.	Connect./ONU	Connect. Size	Comment
0	1	Uniform distributed, 100 ÷ 900 Mbps	Extension from the basic Scen.
1	10	Uniform distributed, 10 ÷ 90 Mbps	Generic scenario
2	4	2 8kTV Connect. (160Mbps), 1 Data+Cloud Connect. (170Mbps), 1 video telephony Connect. (10Mbps)	Typical future home

100 to 900 Mbps. Hence, the expectation or mean connection size for each ONU is 500 Mbps. Scenario 1 further splits a single connection per ONU to 10 smaller connections. The expectation load for each ONU is still 500 Mbps. Scenario 2 represents a future home with triple-play services in which 2 connections for 8kTV, 1 connection for Internet access including cloud computing, and 1 connection for high quality video telephony [41]. Note that the expectation load for each home is still 500 Mbps.

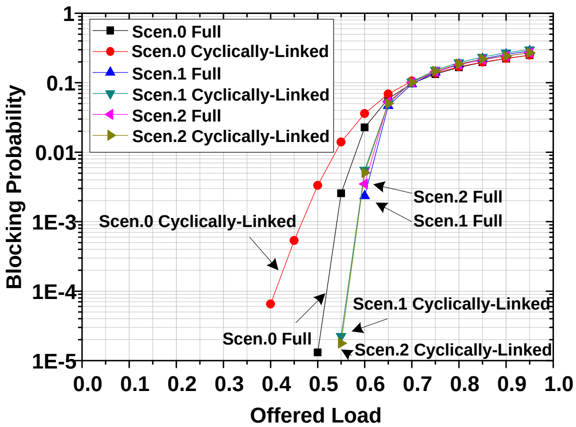

Fig. 3.9. Logical connection blocking probability as a function of offered load for various traffic scenarios.

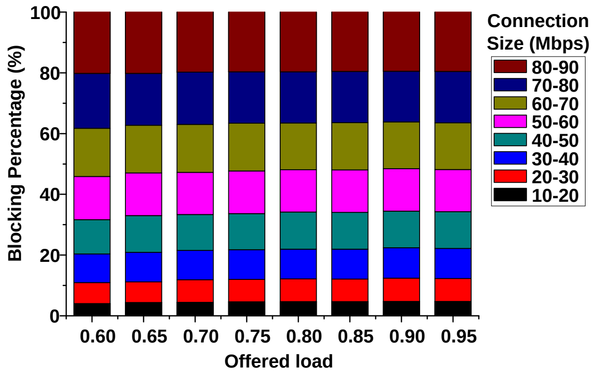

Fig. 3.10. Breakdown of blocked connections by the connection size.

The connection blocking probabilities for these scenarios are shown in Fig. 3.9 in which the full flexibility yields better performance in all cases. The cyclically-linked flexibility cannot achieve the same blocking probability to the full flexibility because the rearrangement is not always successful. However, differences in scenario 1 and 2 are small while scenario 0 shows a sizable difference. The connection size in scenario 0 is as high as 900 Mbps, which is much larger than that of scenario 1 and 2. The larger connection size results in more difficulty for finding a reallocation plan, leading to higher blocking probability. The breakdown in terms of sizes of blocked connections shown in Fig. 3.10 reveals that largest connection sizes in Scenario 1 account for 20% of total blocks while only 12.5% of generated requests fall to this range. The cyclically-linked flexibility, or more precisely the swap-based rearrangement algorithm, yields better performance for small connection sizes. For a deployment scenario with large connection sizes, a specially optimized algorithm can be designed to further reduce the performance gap.

3.3.2. Rearrangement Algorithm Performance

The performance proximity of the cyclically-linked flexibility to the full flexibility is achieved at the expense of other in-service ONU reallocations. Therefore, the performance indicator in question is the impact of the rearrangement process to an in-service ONU. Equation 3.1 estimates the probability for an ONU being reallocated in a rearrangement process. The ratio between moved ONUs and total number of ONUs is computed for each rearrangement operation (successful rearrangement attempt). The impact probability is estimated by averaging all value of the ratio.

$$\Pr_{im} = \frac{1}{\#rearrangement\ operations} \sum^{All} \frac{\#Moved\ ONU}{\#Total\ ONU} \qquad \text{(Eq. 3.1)}$$

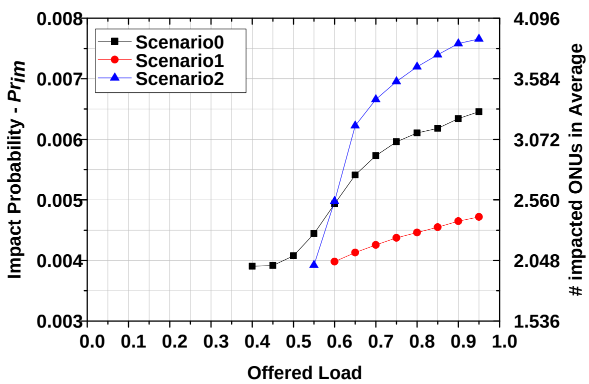

Fig. 3.11. Rearrangement impact probability for different traffic scenarios.

The rearrangement impact is shown in Fig. 3.11 for three traffic scenarios in which probabilities are ranging from 0.004 to 0.008, equivalent to 2 to 4 ONU reallocations. Hence, it shows that the cyclically-linked flexibility has a minimal impact to in-service ONUs. In the collected statistics, there are many operations requiring only one ONU reallocation when *nearest_λ* is right next to *Rq_λ* while there are few operations that require at most 11 reallocations. The rearrangement occurs only after the load of 0.4 in scenario 0. Before reaching that level, there is no impact at all because the requesting ONU can find free bandwidth in its current wavelength *Rq_λ* or in the other wavelength *other_λ*. Scenario 0 shows earlier impacts than other scenarios since requests with a large connection size have

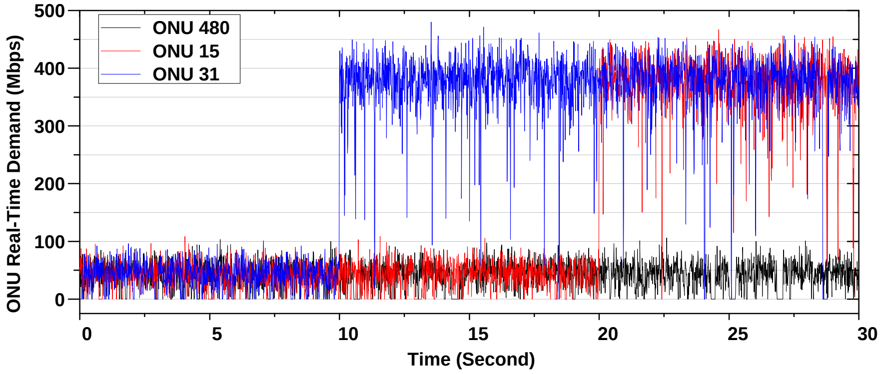

Fig. 3.12. Time trace of generated traffic arriving at the ONU buffer at a resolution of 0.01s (3000 data points per 30s).

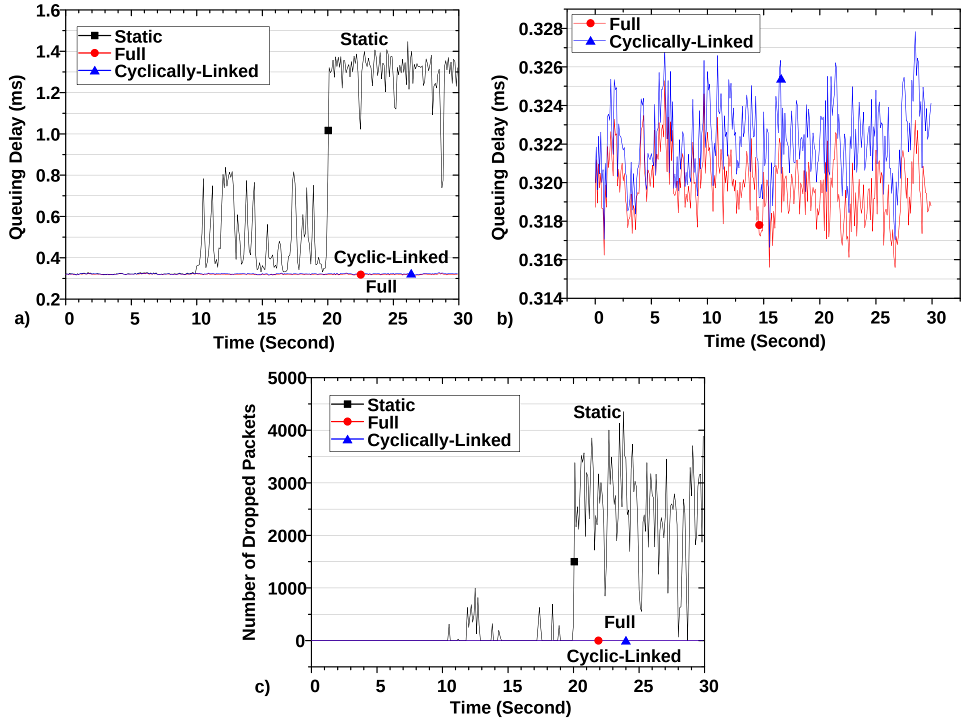

Fig. 3.13. Time trace of 20 seconds for various performance parameters, a) network-wide queuing delay for different schemes, b) network-wide queuing delay focus on the full and cyclically-linked flexibility, c) network-wide packet loss.

lower chance to find enough free bandwidth without rearrangement. The impact from Scenario 2 is higher than other scenarios when the load increases because there only three connection sizes exist on the bandwidth map. The swapper finds it more difficult to search for an appropriate combination of ONUs to move. When the connection size is more diverse, hence more choices can be made, the appropriate combination can contain less number of ONUs.

3.4. Packet Level Analysis

3.4.1. Queuing Delay, Packet Loss, and Load Balancing

The cyclically-linked flexibility performance was studied and compared with static and full flexibility at the logical connection level. To further investigate the performance, it is desirable to look at a finer time scale to see differences among schemes at the packet level. At this time scale, the most important moments are the transition to a new traffic stationary stage, which may trigger a rearrangement process. Three stationary stages of bursty traffic shown in Fig. 3.12 with Hurst parameter of 0.8 from three representative ONUs out of 512. In the first 10 seconds, all ONUs generate the same mean traffic of 40 Mbps (Internet access including IP-TV). From 10^{th} second, *ONU31* raises its mean demand to 370 Mbps and from 20^{th} second, *ONU15* also raises to 370 Mbps. The increase of 340 Mbps is equivalent to have one 8k TV, one cloud computing, and one video telephony connection as described in Table 3.1. Note that ONUs are indexed from 0 to 511 and *ONU0* to 31 are in $\lambda 0$ in the static network and also initially allocated in $\lambda 0$ in the full and cyclically-linked networks. This traffic condition represents scenarios in which the local high demand occurs on a wavelength while other wavelengths are under an average demand. The wavelength line rate in this analysis is scaled down to 2.48832 Gbps because the packet level requires very extensive computational power.

The network-wide queuing delay of packets is shown in Fig. 3.13.a) which includes results from the static, full and cyclically-linked flexibility. Queuing delay is used instead of ONU-to-OLT packet delay since the propagation delay is always a constant value for a given distance. Furthermore, the propagation delay component does not reflect the operation of DBAs. The static flexibility experiences occasionally high delay from 10^{th} second and constantly high delay from 20^{th} second. This excessive delay is contributed by *ONU15* and *ONU31* that receive not enough bandwidth (timeslots) in $\lambda 0$ to serve their queues. The full and cyclically-linked flexibility experience no significant change since the network load can be balanced among wavelengths. In fact, the full flexibility still yields better delay but the difference is barely around 0.005 ms as shown in Fig. 3.13.b). Similarly, the static flexibility experiences occasionally packet drops from 10^{th} second and frequent drops from 20^{th} second as shown in Fig. 3.13.c). Packet drops are caused by buffer overflow as the buffer size is limited to 1280 KB. Not all ONUs experience packet drops but only *ONU15* and *ONU31*, since the model applies the fairness scheduling algorithm with no priority policy in which ONUs receives a guaranteed bandwidth equal to total network capacity divided by the number of ONUs. If there is any surplus bandwidth, it is also split fairly among busy ONUs. In the full and cyclically-linked cases, the surplus bandwidth from other wavelengths can be utilized by *ONU15* and *ONU31* resulting in no packet drops.

In other words, the network load can be spread out more evenly among wavelengths in the full and cyclically-linked flexibility as observed in Fig. 3.14. Only the load from four representative channels is shown in which $\lambda 0$ and $\lambda 1$ are the eligible wavelengths of *ONU15* and *ONU31*, $\lambda 15$ is right next to $\lambda 0$, and $\lambda 7$ is the farthest lambda seen from $\lambda 0$ and $\lambda 1$. Hence, in the cyclically-linked flexibility, $\lambda 0$ and $\lambda 1$ have a higher load and $\lambda 15$ serves some ONUs from the busy $\lambda 0$ resulting in an increase in the load level. The load level in $\lambda 7$ is also slightly affected since ONUs are reallocated towards $\lambda 7$ from both directions due to the chain reaction triggered by the high load in $\lambda 0$ and $\lambda 1$. Although the load balancing in the cyclically-linked flexibility is not as good as in the full flexibility, the load difference between $\lambda 0$ (or $\lambda 1$) and $\lambda 7$ is 3.5 times smaller than that of the static case.

There are also many other possibilities of traffic scenarios to demonstrate the advanced performance of the cyclically-linked flexibility. However, there are also other possibilities in

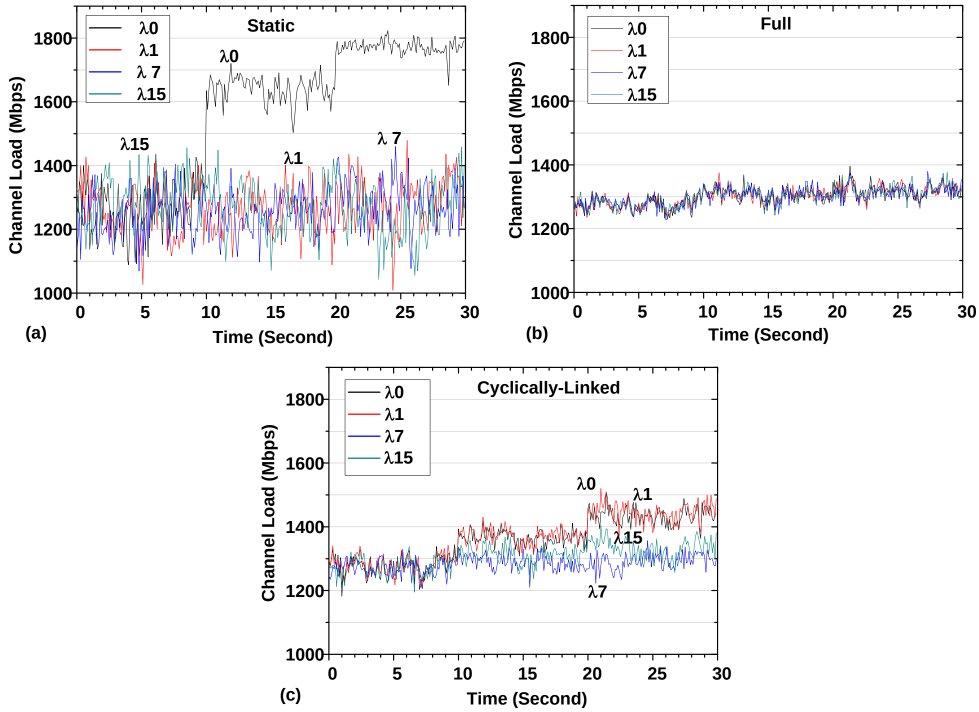

Fig. 3.14. Time trace of traffic load on representative channels, a) Static flexibility, b) Full flexibility, c) Cyclically-linked flexibility.

which the advanced performance cannot be observed, even in the full flexibility. For example, when all ONUs raise their demands at the same time, there is no free bandwidth in any lambda to perform the bandwidth rearrangement process. Practically, those possibilities are statistically unlikely, as previously mentioned, as access traffic patterns are subjected to high temporal and spatial variations.

3.5. Bandwidth Rearrangement Enhancements

3.5.1. Rearrangement Performance Indicators

The swap-based rearrangement algorithm was demonstrated to have a good performance in terms of blocking probability and impact probability. The current performance metrics are not sufficient to help further developing the algorithm. This section defines extra performance indicators in order to have more insight in the algorithm operations.

Possible outcomes for an incoming request have been observed by blockages or acceptances, which are indicated by the blocking probability. Blockages and acceptances can be further classified by underlying reasons as depicted in Fig. 3.15. Network-full blockages result from not enough free bandwidth in any lambda to accept the incoming request. The full blocking probability Pb_f is used to indicate this type of blockage. The other type of blockage results from unsuccessful rearrangement attempts and is represented by the rearrangement blocking probability Pb_{re}.

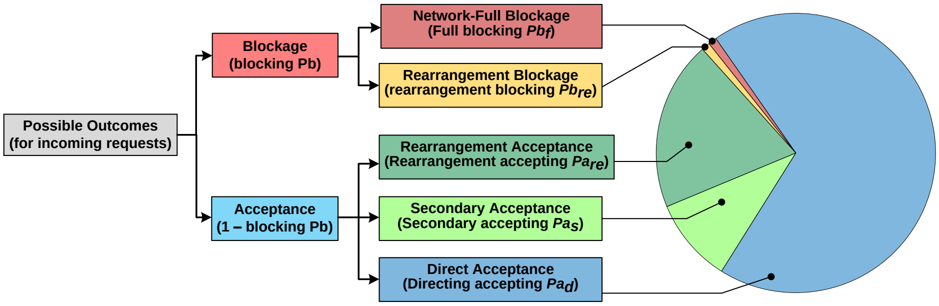

Fig. 3.15. Breakdown of possible outcomes for incoming bandwidth requests. The pie chart indicates a typical composition of probabilities (*Pr*) of outcomes.

Similarly, acceptances can be classified into direct, secondary and rearrangement acceptances. Direct acceptances, indicated by the direct acceptance probability Pa_d, result from direct acceptance of the incoming request to its current wavelength without any ONU wavelength reallocation. Secondary acceptances, indicated by the secondary acceptance probability Pa_s, result from reallocating the requesting ONU to the other possible wavelength (ONUs in the cyclically-linked flexibility can be reallocated between two possible wavelengths) in order to accept the bandwidth request without rearranging other ONUs.

Rearrangement acceptances, indicated by the rearrangement acceptance probability Pa_{re}, are acceptances after bandwidth rearrangement operations. As the sum of probabilities of all possible outcomes is equal to 1, we can derive Eq. 3.2 which is visualized as the pie chart in Fig. 3.15.

$$\left(Pb_f + Pb_{re}\right) + \left(Pa_d + Pa_s + Pa_{re}\right) = 1 \qquad \text{(Eq. 3.2)}$$

Numerical values of those probabilities are collected by extra statistical probes in the network simulation model to compare the performance between the swap-based rearrangement algorithm and a new algorithm.

In addition, a metric to indicate the successful probability of rearrangement attempts is desired to see the efficiency of rearrangement algorithms. The rearrangement efficiency η_{re} is defined as the number of successful attempts to the total number of attempts as shown in Eq. 3.3. After some permutations, the rearrangement efficiency η_{re} can be derived from rearrangement accepting probability Pa_{re} and rearrangement blocking probability Pb_{re} as shown in Eq. 3.4. Thus, the rearrangement efficiency η_{re} ranges from zero to one. The value of one means all rearrangement attempts are successful.

$$\eta_{re} = \frac{\#successful\ attempts}{\#attempts} \qquad \text{(Eq. 3.3)}$$

$$\eta_{re} = \frac{\dfrac{\#successful\ attempts}{\#bandwidth\ requests}}{\dfrac{\#successful\ attempts + \#unsuccessful\ attempts}{\#bandwidth\ requests}} = \frac{Pa_{re}}{Pa_{re} + Pb_{re}} \qquad \text{(Eq. 3.4)}$$

3.5.2. Fit-Based Bandwidth Rearrangement Algorithm

The algorithm described in Section 3.2.3 is based on swapping free bandwidth and occupied bandwidth between two adjacent wavelengths. The number of in-service ONU reallocations, indicated by impact probability Pr_{im}, is small because the free bandwidth is shifted from the nearest lambda, which has enough free bandwidth, and the swapper tries to find the smallest combination of ONUs. The rearrangement is declared to be unsuccessful when no suitable combination of ONUs can be found to swap. This strategy may declare an unsuccessful attempt when other possible reallocation plans are still available because:

- The sum of free bandwidth in several lambdas can be combined in order to accept a request. The swap-based algorithm does not consider those cases.
- The amount of bandwidth to swap is based on the size of incoming request leading to unnecessary blockages. Previous swaps may indirectly cause a blockage in the current swap. For example, the current swap can only find a

combination of ONUs which is slightly larger *nearest_λ_free_BW* resulting in a swap blockage. If previous swaps took into account this situation, they can shift a larger amount of bandwidth to avoid the later blockage.

Mentioned drawbacks can be resolved by an exhaustive search in the expense of computational cost and time or by a different approach for the algorithm. The current approach based on swapping is analogous to move furniture objects within a house with multiple rooms. The objects are moved between adjacent rooms in order to have space for a new object. Besides this heuristic approach, all objects can be removed from the house and refit back to the house room by room together with the new object.

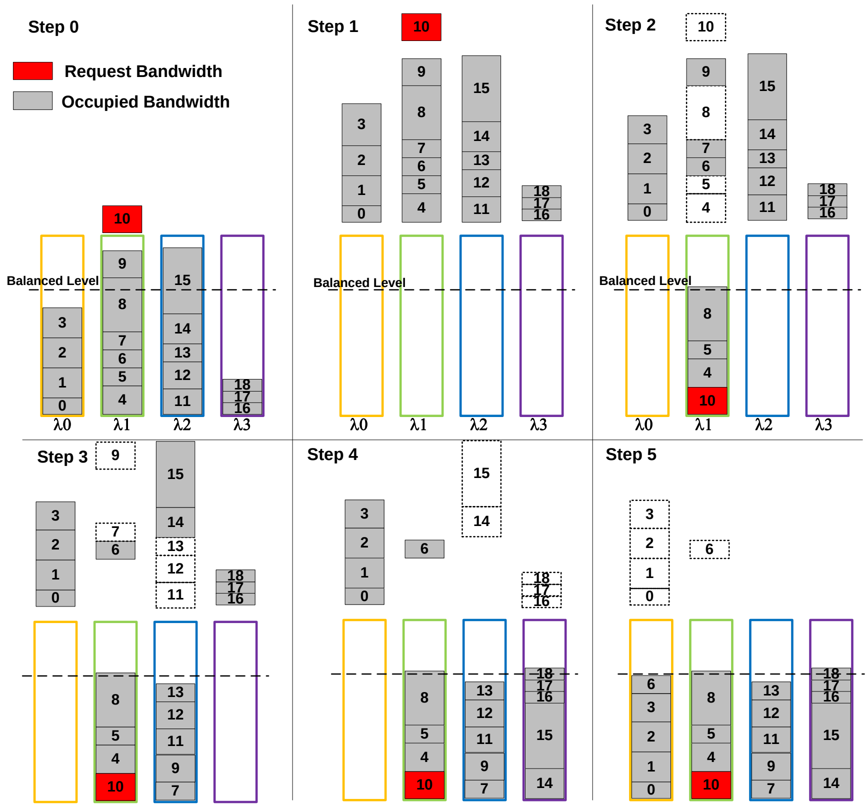

Fig. 3.16. Conceptual representation of fit-based algorithm to find a reallocation plan for the rearrangement process.

The new approach, called fit-based algorithm, is shown in Fig. 3.16 by presenting an example of fitting operations in 4-wavelength networks. A bandwidth request arrives at λ_1 while this lambda and the other eligible lambda (λ_2) for the request are full. In step 0, the balanced level of load across all wavelengths is computed. If occupied bandwidth can be divided into any arbitrary small units, the load level in all channels can be balanced exactly to the balanced level. In step 1, all occupied bandwidth blocks are removed from the bandwidth map to a temporary map. In step 2, the algorithm starts to fit the busiest channel, which is the lambda of the bandwidth request. The request bandwidth and then other occupied blocks are refitted in order to have the load level around the balanced level. A sub algorithm is used to find the best-fit ONUs among available ONUs. In step 3, the algorithm fits $\lambda 2$ first with occupied blocks in λ_1, which were not fitted in the previous step. Note that block 6 cannot be fitted in λ_2 since its eligible lambda is λ_0 and λ_1. The subsequent steps continue to fit other lambdas. In the last step, the algorithm scans for unallocated blocks (in this case only block 6) and assign them to the least-busy lambda between two eligible lambdas of the block. Finally, we yield a new bandwidth map with channel loads are around the balanced level.

The rearrangement can be unsuccessful when there is any unallocated block, which cannot fit back to the *rsvp_bw_map*. In the example, the unsuccessful attempt can result from block 6 if it is too large to fit into the free space in either λ_0 and λ_1. The next section will compare two

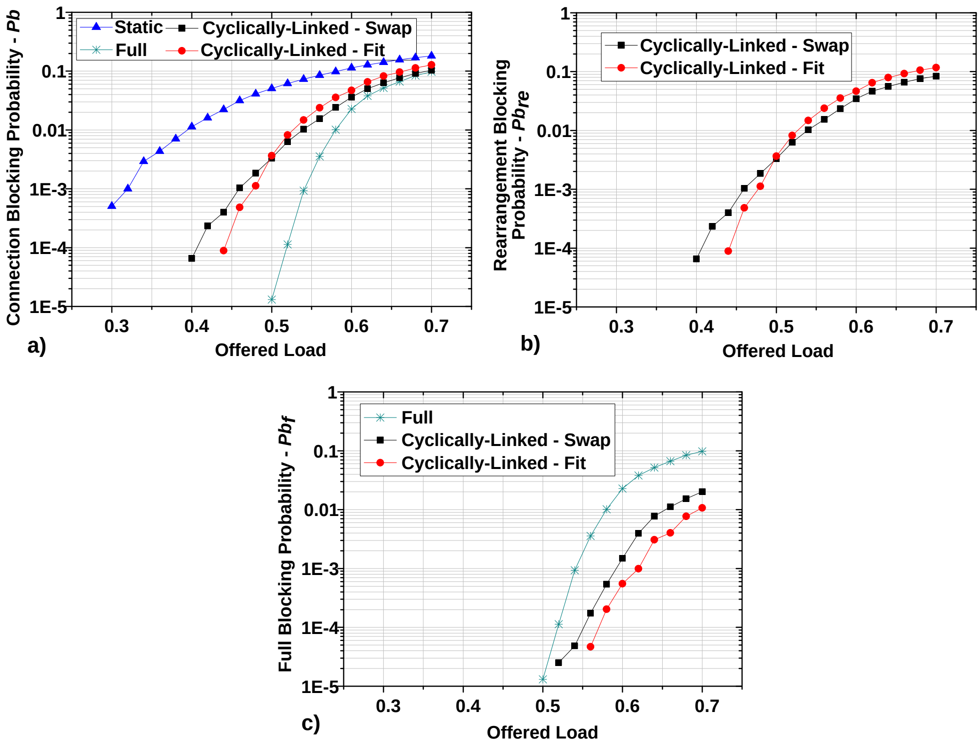

Fig. 3.17. Comparison of blocking probabilities between the swap-based and the fit-based approach, a) Connection blocking probability including the static and full flexibility as benchmarks, b) Rearrangement blocking probability, c) Full blocking probability.

rearrangement approaches by newly defined performance matrices.

3.5.3. Swap-Based and Fit-Based Performance Comparison

In this section, performances of two approaches, the swap-based and the fit-based, are analyzed and compared in terms of performance metrics defined in previous sections. The offered load is increased with a step of 0.02 in the range between 0.3 and 0.7, which is the interesting range of network operations. The network operates under the traffic scenario 0 defined in Table 3.1. Scenario 0 is selected because the difference between the full and the cyclically-linked flexibility is noticeable in this scenario.

The conventional performance metric, connection blocking probability *Pb*, is shown in Fig. 3.17.a) which also includes the static and the full flexibility as performance benchmarks. The fit-based approach yields better blocking probabilities than the swap-based approach for lower offered loads while the swap-based approach is better for higher offered loads. The blocking probability *Pb* is decomposed to the rearrangement blocking probability Pb_{re} and full blocking

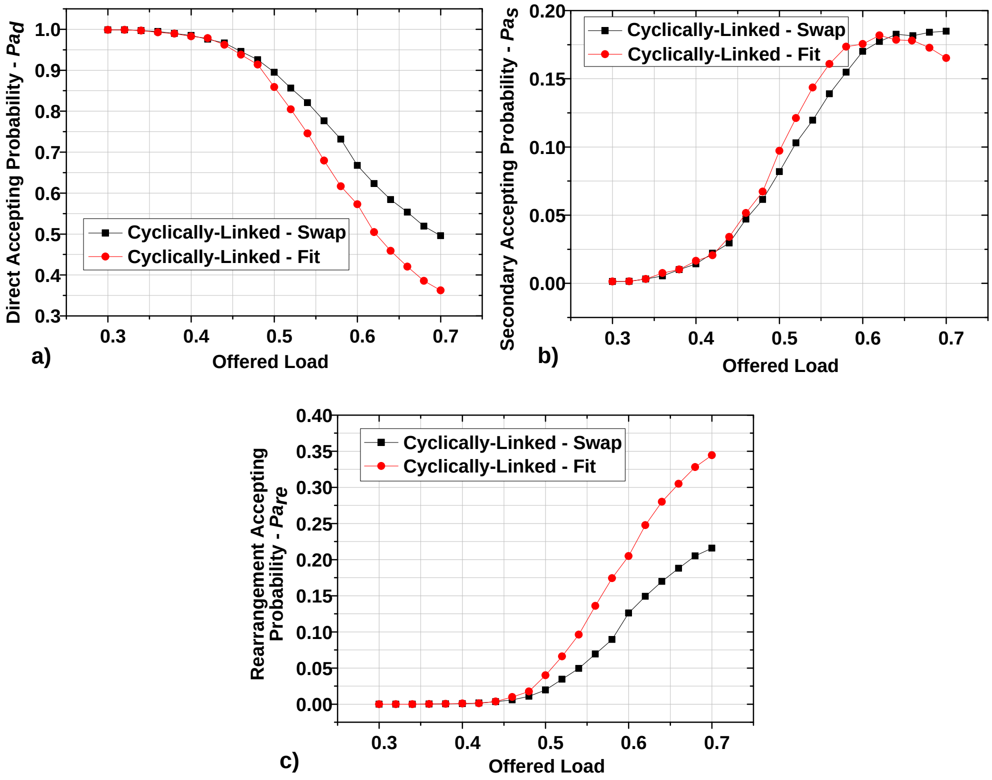

Fig. 3.18. Comparison of accepting probabilities between the swap-based and the fit-based approach, a) Direct accepting probability , b) Secondary blocking probability, c) Rearrangement accepting probability.

probability Pb_f, as shown in Fig. 3.17.b) and c), respectively. The performance trend of Pb_{re} is well reflected in that of Pb since Pb_{re} is the main contributor of Pb. Before the offered load of 0.5, Pb is fully determined by Pb_{re}. Although it is clear that the fit-based approach is better for lower loads and the swap-based approach is better for higher loads, we need to look at the acceptances to have a concrete explanation.

In the acceptance side, the swap-based approach has higher direct accepting probabilities compared to the fit-based approach, especially for high load as shown in Fig. 3.18.a). Channel loads are more balanced in the fit-based approach resulting in less direct acceptances, especially at large bandwidth requests. When the balanced level is close to the maximum capacity, there is a higher chance that the incoming bandwidth request cannot fit to the current and secondary wavelengths leading to a rearrangement attempt. In the case of swap-based, channel loads are less balanced resulting in some channels have less free space while other channels have more space. Direct acceptances still can happen in channels with more space in the swap-based approach. In return for less direct acceptances, the fit-based approach has more

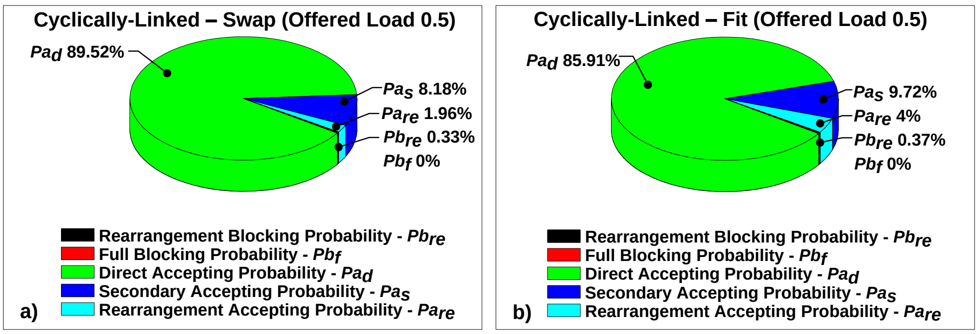

Fig. 3.19. Composition of outcomes for bandwidth requests at the offered load of 0.5, a) Swap-based approach, b) Fit-based approach.

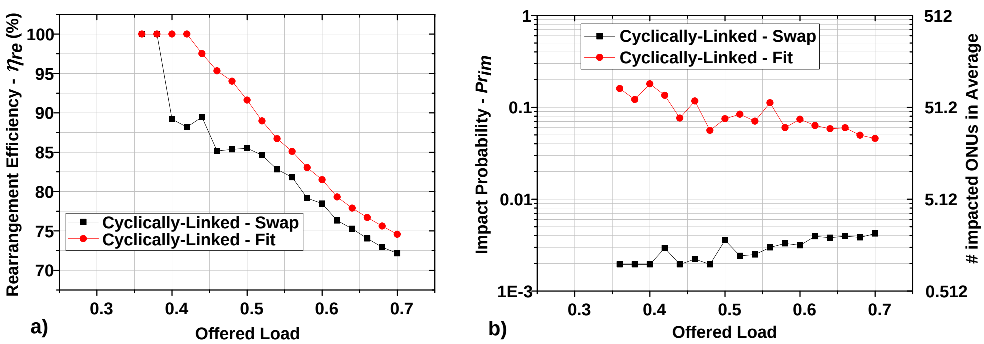

Fig. 3.20. Comparison between the swap-based and the fit-based approach, a) Rearrangement efficiency in percentage as a function of offered load, b) Rearrangement impact probability as a function of offered load.

rearrangement acceptances as revealed in Fig. 3.18.c) while the number of secondary acceptances is almost the same for both approaches. The secondary accepting probability Pa_s of the fit-based approach is going down at high load as shown in Fig. 3.18.b), which can be explained in a similar way to the behavior as the direct accepting probability Pa_d.

To observe differences in the operation of two approaches, the composition of outcomes at the offered load of 0.5 is shown in Fig. 3.19.a) and b) for the swap-based and the fit-based approach, respectively. In the load of 0.05, both approaches yield almost the same blocking probability Pb but by different compositions. The swap-based approach has a larger share of Pa_d while the share of Pa_{re} in the fit-based approach is more than double that of the swap-based approach. The differences suggest that there are more rearrangement attempts in the network employing the fit-based approach and the chance to be successful is higher than in the network employing the swap-based approach.

The rearrangement efficiencies η_{re} in terms of percentage, shown in Fig. 3.20.a), confirm this. The fit-based approach is consistently more efficient than the swap-based approach. However, this efficiency is achieved at the cost of more reallocated ONUs as revealed in Fig. 3.20.b). In average, around 10% of total ONUs is reallocated in a fit-based rearrangement while it is only 0.3% in a swap-based rearrangement. The operational principle behind these approaches leads to this result. The swap-based approach was designed with the priority of limiting the impact while the fit-based approach was designed with the priority of being more efficient. However, the impact probability of the fit-based approach reduces when the load increases while it increases in the swap-based approach. These opposite trends may suggest a direction to further develop rearrangement algorithms.

After having gained more insight in the operation of rearrangement approach, some remarks can be noted:

- Both approaches achieve good efficiency (>72 %). The efficiency by the fit-based approach was increased at the expense of more impact. A further development should increase the efficiency with less expense. For example, an extra step can be added in the end of the fit-based algorithm to revert unnecessary reallocations. *ONUa* after rearrangement is in $\lambda 1$ (previously in $\lambda 2$) and *ONUa* after rearrangement is in $\lambda 2$ (previously in $\lambda 1$). If we can swap back *ONUa* and *ONUb* to their original λ, two unnecessary reallocations can be prevented.
- There is still room to further optimize algorithms since there is still a gap between the full flexibility (as the fundamental limit), and the cyclically-linked flexibility and the rearrangement efficiency is below 100% for high offered loads.
- A higher efficiency does not necessarily result in better overall performance that includes other types of blockages and acceptances. The algorithm performance

should be seen in a wider view including direct and secondary accepting probabilities.

- The rearrangement can be optimized for a certain level of load. For example, for a load of 0.5 and lower, the network can use the fit-based algorithm and switch to the swap-based algorithm at higher loads.
- The fundamental reason for rearrangement blockages is the block-wise allocations. The occupied block of an *AllocID* has to be allocated within a single wavelength. If the constraint for an ONU to have only one working channel is lifted, the occupied bandwidth from the ONU can be arbitrarily divided between two working channels. Thus, fluid-wise allocations are possible resulting in no rearrangement blockages.
- The use of dual fixed transceiver makes it possible not only for fluid-wise allocations but also for the make-before-break mechanism. The handshaking procedure to the new wavelength including registering and re-ranging can be done before the ONU actually switches the data stream. The service interruption is avoided without extra buffering.

3.6. Conclusions

In this Chapter, I proposed a novel architectural approach that allows wavelength reconfigurability in WDM-TDM optical access networks avoiding the need for wavelength tuning and reducing the requirement of excessive power loss budget. Although the ONU only needs to switch between two pre-defined wavelength channels, the network-wide bandwidth redistribution capability is still preserved by the cyclically-linked configuration of wavelengths.

To demonstrate the operation of the cyclically-linked flexibility, a swap-based bandwidth rearrangement algorithm was designed with the objective of minimizing in-service ONUs reallocations. The algorithm demonstrates that the cyclically-linked flexibility has a performance close to the full flexibility. Furthermore, the average number of affected ONUs per rearrangement was shown to be only between 2 to 4. Algorithm enhancements were also presented that bring the cyclically-linked flexibility performance approaches closer to that of the full flexibility at the expense of more affected ONUs per rearrangement. Directions for further developments of the rearrangement algorithm were also discussed. Advanced algorithms could also take into account policy-induced constraints such as ONU prioritization or physical-induced constraints such as some ONUs with only one fixed wavelength transceiver. If advanced algorithms allow a small part of the ONU population with only one fixed wavelength transceiver, a reduced equipment cost can be archived or malfunctioning ONUs is tolerable.

As an architectural concept, the cyclically-linked flexibility needs to be implemented by a physical architecture. The next Chapter presents four proposed implementations, of which each is designed for a certain deployment scenario.

CHAPTER 4

RECONFIGURABLE ARCHITECTURES BASED ON CYCLICALLY-LINKED FLEXIBILITY

This chapter presents four reconfigurable architectures based on the concept of cyclically-linked flexibility. Each architecture is designed with different criteria towards different deployment scenarios. They are analyzed to highlight their merits in terms of the physical performance, cost, or the traffic performance. The contents of this chapter have been partly disseminated in [92] and [121].

4.1. Passive-Components-Based Architecture

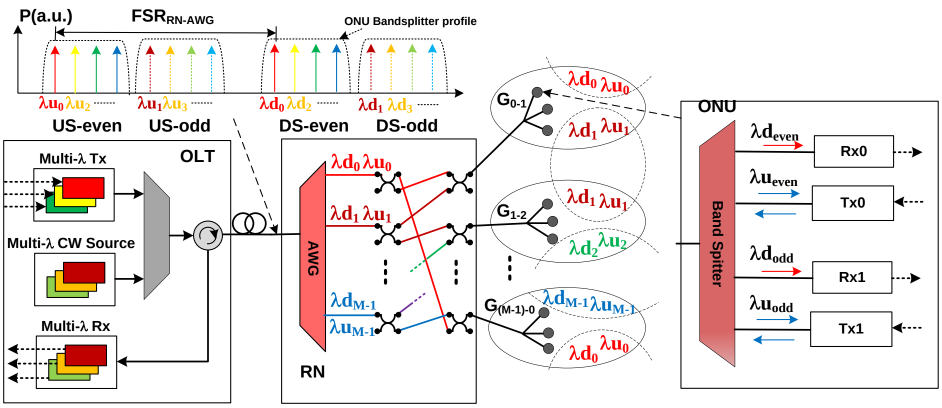

Fig. 4.1. Schematic representation of passive-components-based architecture in which downstream and upstream wavelength pairs are demultiplexed and then linked at the remote node in a cyclic manner.

In the conceptual level of cyclically-linked flexibility, each group of ONUs sees different pairs of wavelength channels and each channel has a downstream and an upstream wavelength. Therefore, the ONU wavelength-agnostic design is a challenge when implementing the cyclically-linked flexibility concept. The wavelength-agnostic or colorless property is certainly desired since it reduces the inventory problem that is caused by using different types of ONUs for different wavelengths. This section presents an implementation that realizes wavelength-agnostics by splitting the wavelength plan to four sub-bands and using reflective modulators.

4.1.1. PRO-Access Architecture

The proposed architecture, named Passive-component-based Reconfigurable Optical access architecture (PRO-Access), is shown in Fig. 4.1 in which the OLT transmits two wavelength bands. The lower band contains *M* continuous wave (CW) wavelengths for upstream (US) reflective modulation at the ONU side and the higher band contains *M* data-modulated wavelengths for downstream (DS) transmission. Each upstream wavelength has a corresponding downstream wavelength where the spectral distance is one (or more) free spectral range (FSR) of the AWG in the RN. As a result, both elements of the wavelength pair appear at the same port of the AWG. An output of the AWG is split into two branches, one branch combines with the previous-index wavelength pair and the other branch combines with next-index wavelength pair in a cyclic manner. For example, wavelength pair (λd_0, λu_0) is split and combined with wavelength pairs (λd_{M-1}, λu_{M-1}) and (λd_1, λu_1). The next pair (λd_1, λu_1) is split and combined with (λd_0, λu_0) and (λd_2, λu_2) as depicted in the RN architecture in Fig. 4.1. Thus, each RN output port can serve one group of ONUs with two wavelength pairs by employing a power splitter. Each group is served by two channels (4 wavelengths) and adjacent groups share a common channel forming the cyclically-linked flexibility configuration.

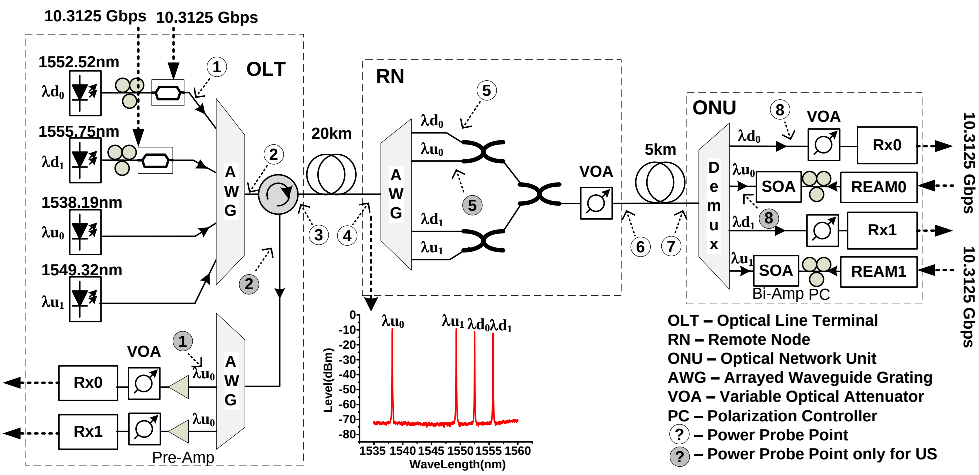

Fig. 4.2. Experimental setup for PRO-Access architecture as a subset of the described system, reflective electro-absorption modulators (REAM) are used as the transmitters at the ONU.

Since the upstream band is further divided into even-index and odd-index sub-bands and the same for the downstream band, the band splitter at the ONU can be designed to demultiplex four sub-bands to separate ports. Therefore, an ONU is able to demultiplex four received wavelengths to the appropriate ports because no wavelength falls into the same sub-band. The ONU electrically selects to operate on one wavelength pair or even both of them.

This configuration allows the ONU to be wavelength-agnostic while avoiding the use of tunable filters and tunable lasers.

PRO-Access fully implements the cyclically-linked flexibility concept in which both upstream and downstream are simultaneously considered. The dual-transceiver allows the ONU to be relocated in a make-before-break mechanism during the rearrangement process. Hence, interruption of on-going services can be largely avoided [78]. Consequently, network reconfiguration is transparent to upper layers.

4.1.2. Proof-of-Concept and Discussions

The proof-of-concept experimental setup shown in Fig. 4.2 consists of two wavelength pairs (λd_0, λu_0) and (λd_1, λu_2). The downstream wavelengths λd_0 (1552.52 nm) and λd_1 (1555.75 nm) are externally modulated by a 10.3125 Gbps non-return-to-zero (NRZ) 2^{31}-1 pseudorandom bit sequence (PRBS) and multiplexed together with CW US seeding wavelengths λu_0 (1538.19 nm) and λu_1 (1549.32 nm). These wavelengths are specified by the ITU-T 100GHz-spacing wavelength grid and selected from available DFB laser sources in the laboratory. The launched power towards the OLT-AWG is 0 and 3 dBm for DS wavelengths and US wavelengths, respectively.

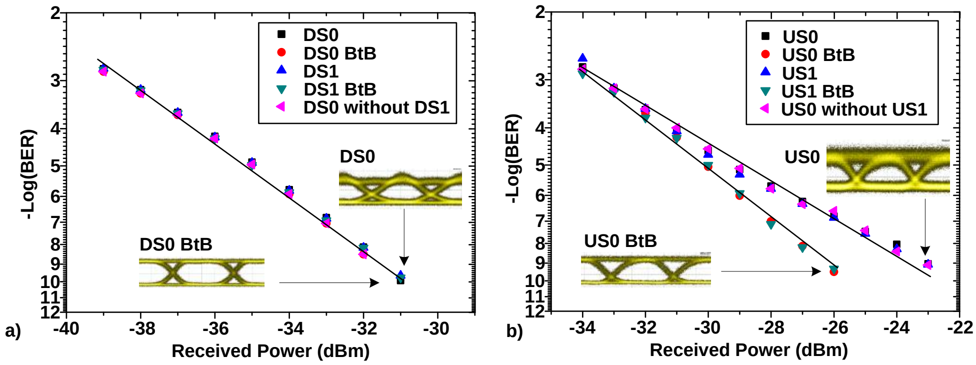

Fig. 4.3. Bit error rate performance, a) for downstream channels, b) for upstream channels.

After transmission over 20 km standard single mode fiber (SMF-28), they are demultiplexed at the RN by a commercial 32-port 100GHz-spaced C-band AWG with 2.5 dB insertion loss. Then λd_0 and λu_0 are combined using a 2x2 3dB coupler and the same for λd_1 and λu_1 to the emulate the cyclic property of the proposed AWG since the FSR of the experimental AWG is longer than the width of C-band (35 nm). The two pairs are then combined again to form an RN output port. The variable optical attenuator (VOA) in the RN emulates the losses associated with a split ratio of 1:8.

After transmission over 5km from the RN to the ONU, the wavelengths are demultiplexed by a 16-port 200GHz-spaced C-band AWG in which two downstream wavelengths are routed to the avalanche photodiode (APD) receivers and two upstream wavelengths are routed to the reflective electro-absorption modulators (REAM). The upstream wavelengths are modulated by 10.3125 Gbps NRZ 2^{23}-1 PRBS and propagate back to OLT. I used a SOA (semiconductor optical amplifier) which provided a gain of 20dB for each direction before the REAM to compensate for 8-dB REAM insertion loss and the transmission losses.

Results in Fig. 4.3 show four measurement cases in each direction including the case when only channel 0 (λd_0, λu_0) is working. In all downstream cases in Fig. 4.3.a), the error performance is identical to the baseline optical back-to-back (BtB) performance. The performance of *DS0* without *DS1* is also identical to the case with DS1 due to good isolation in the passive components. In the upstream performance shown in Fig. 4.3.b), all transmission cases have a power penalty of 2.5 dB to get error-free performance which is due to backscattering and reflections from the seeding wavelength transmission. Backscattering is mainly constributed by Rayleigh scattering and reflections occur at junctions within connectors and AWG structures. In fact, the reflection-induced penalty was already mitigated in the experiment by broadening the spectrum of upstream wavelengths. Phase modulation was applied on the DFB laser in the OLT to broaden the spectrum of CW signal [122].

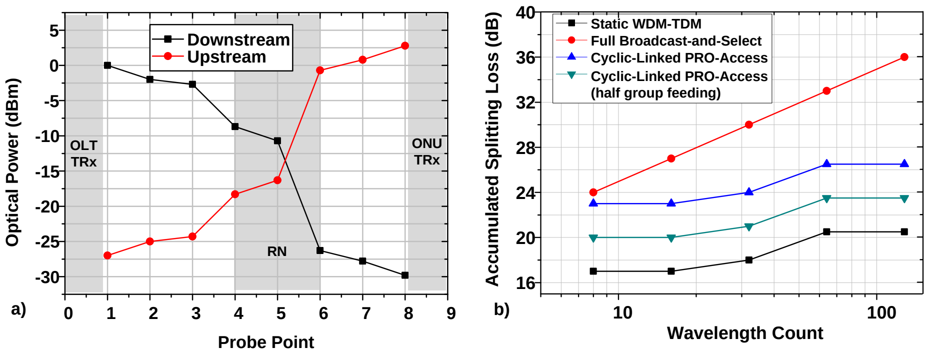

Fig. 4.4. a) Downstream and upstream optical power evolution of channel 0, b) Optical distribution network accumulated splitting loss as a function of wavelength count (in average 32 ONUs per wavelength).

In the schematic, a downstream wavelength should have an upstream wavelength spaced by one or more FSR to exploit the cyclic property of the AWG at the RN. This requirement is somewhat restrictive in terms of wavelength planning and AWG design. This requirement can be relaxed if the second input of 3dB couplers, used to split the wavelength pairs, is utilized. For example, λd_0 enters the first input while λu_0 enters the second input of the coupler in the top left of the RN in Fig. 4.1. Thus, the spacing between λd_0 and λu_0 can be arbitrary. The coupler acts as both combiner and splitter resulting in almost no additional power loss in comparison to the original configuration.

The proof-of-concept experiment used bulk components to implement the ONU optical functionality including REAM for upstream transmitters and APD for downstream receivers.

However, to simplify the technological process for optical integration, we can use four identical REAMs in which two function as modulators and the others function as receivers. We also can place a SOA in front of each REAM to boost the optical signal before modulating or receiving. The bandsplitter can be realized by an AWG, basically waveguides, situated in front of the SOAs. All of these devices can be monolithically integrated with the InP technology since they use an identical active layer [123][124]. The passive RN can also be integrated with the mature planar lightwave circuit (PLC) technology [125].

The primary constraint in passive optical access networks is the power budget which determines the reach and the maximum split ratio. The optical power evolution of channel 0 is shown in Fig. 4.4.a) where the probe points are indicated in Fig. 4.2. The total link loss for each direction is almost 30 dB while a total loss of 31 dB for downstream results in error-free transmission providing a margin of 1 dB. This margin could be improved by increasing the launch power, however, the launch power for DS wavelengths is maintained at a relatively-low level of 0 dBm to avoid nonlinear interchannel cross talk. In the upstream direction, the received power at the OLT is -27.1 dBm which results in 4.5E-7 error rate which is well below the forward error correction (FEC) limit of 1E-4. In the setup, I used a pre-amplifier (EDFA with 25 dB gain) in the OLT to achieve absolute error-free reception. The link loss in the setup indicates that with class C optics (30 dB power budget), the network with 16 wavelength channels can serve 256 ONUs with a reach of 25 km. To have larger number of ONUs, we can either reduce the reach or use an extender box in the field.

The ODN accumulated splitting loss, which includes the RN insertion loss and the power split loss after the RN, as a function of the number of wavelengths is shown in Fig. 4.4.b) for Broadcast-and-Select, static WDM-TDM, and PRO-Access. The static WDM-TDM shows only a slight increase in loss because the AWG insertion loss increases slightly with port count. However, a commercially available 88-channel 50GHz-spaced AWG induces only 5.5 dB insertion loss at most [104]. PRO-Access always has 6 dB higher loss than the static WDM-TDM PON (+1 dB to include imperfections of optical devices in practice). The 6 dB loss is attributed to two additional 3 dB couplers on the path of wavelengths. However, we can leverage the second output of combining couplers to feed half of the ONU group, thereby reducing the splitting loss by 3dB. For example, the first output of the coupler in the top right of the RN, shown in Fig. 4.1, feeds the first half of $G_{0\text{-}1}$ while the second output feeds the second half. This configuration results in more fibers to be deployed (additional cost) but in many cases it is desirable in multi-stage splitting plans. The ODN accumulated splitting loss for this case is also shown in Fig. 4.4.b) in which PRO-Access has 3 dB more insertion loss relative to static WDM-TDM PON. Therefore, static WDM-TDM PON as well as PRO-Access are more scalable in comparison to the Broadcast-and-Select (full flexibility) as observed from Fig. 4.4.b). The split loss is the limiting factor for scalability of the Broadcast-and-Select since it increases logarithmically with the number of wavelengths (32 ONUs per wavelength).

4.1.3. Conclusions

This section presented an implementation for the cyclically-linked flexibility architectural concept with the main properties of:

- Completely passive optical distribution network
- No wavelength tuning
- Wavelength-agnostic ONU design
- The use of similar components as designed for WDM PONs and TDM PONs

As the FSR requirement for wavelength sub-bands is relaxed, a wavelength plan can be designed to allow co-existence with deployed PONs for a smooth migration. However, the intrinsic limitation of the reflection-modulated method is the reach due to reflection noise which increase with the transmission distance. Therefore, PRO-Access is not suitable for a long-reach access solution.

4.2. Wavelength-Converted Long-Reach Architecture

As PRO-Access is not applicable for long-reach scenarios, there is a need to avoid the reflection-modulated method in order to increase the reach. This section presents an implementation of the cyclically-linked flexibility concept for long-reach scenarios with a cost-effective ONU design.

4.2.1. WCL-Access Architecture

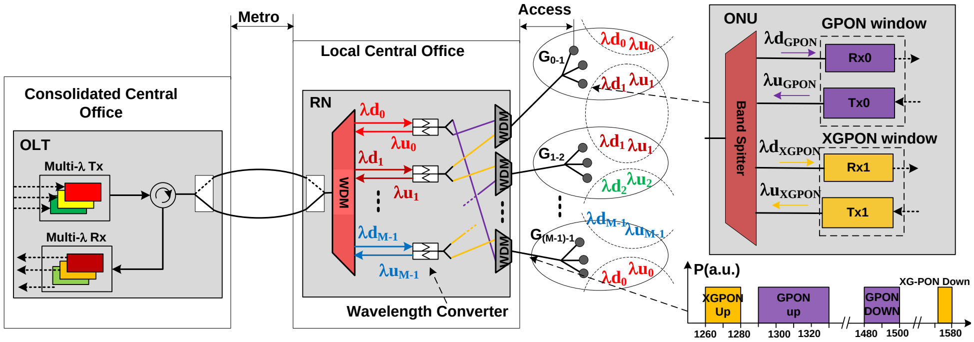

Fig. 4.5. Schematic representation of wavelength-converted long-reach architecture to support central office consolidation and direct migration from current PON deployments.

The proposed architecture, named wavelength-converted long-reach optical access network (WCL-Access), is shown in Fig. 4.5. The OLT is located in the consolidated central office while the remote is located in the distributed local central offices. The network between the two central offices is the metro section in which DWDM wavelengths are used to establish light-paths between the OLT and the RN. These wavelengths are then converted to either GPON-window wavelengths or XGPON-window wavelengths. These wavelengths are converted, split and combined to form the cyclically-linked configuration. For example, the wavelength λd_0 is converted to the GPON downstream wavelength and the corresponding GPON upstream wavelength is converted to the wavelength λu_0. The two GPON wavelengths are split and combined with other two XGPON wavelengths, which are obtained by converting λd_1 and λu_1 to feed group $G_{0\text{-}1}$ of ONUs. Thus, ONUs in $G_{0\text{-}1}$ interface with GPON and XGPON wavelengths, however, they are actually serviced by ($\lambda d0$, $\lambda u0$) and ($\lambda d1$, $\lambda u1$) in the metro section. Similarly, $G_{1\text{-}2}$ is serviced by (λd_1, λu_1) and (λd_2, λu_2), and so on to constitute the cyclically-linked flexibility structure.

The ONU transmits and receives only GPON and XGPON wavelengths that allows the use of transceivers similar to the ones designed for standardized PONs for cost-effectiveness. The same design for ONUs can be used in every branch guaranteeing the wavelength-agnostic property since only GPON and XGPON wavelengths are present in the access section. Note that although the GPON window is used, it not necessary to use GPON line rates. The access section is based on power splitting ,which is compliant with current PON deployments. The compliance allows network migration to the WCL-Access architecture without touching the outside plant.

This architecture uses low-cost ONUs but requires wavelength converters in the RN. The cost of wavelength converters is shared by ONUs. Therefore, the actual ONU cost should include this share. The following section will elaborate this issue and other practical issues.

4.2.2. **Practical Considerations**

Options for Wavelength Converter

The wavelength converter is the key component in this architecture, its design will affect the physical performance and cost of the WCL-Access architecture. Basically, the wavelength converter can be all-optical or O/E/O.

All-optical conversion methods based on cross gain modulation (XGM), cross phase modulation (XPM), or four wave mixing (FWM) have been extensively demonstrated [126]. However, all-optical conversion is not suitable for this application because of the burst nature of optical TDMA signal in the upstream direction. Signals coming from near ONUs (loud packets) are higher than the ones coming from far ONUs (soft packets) by several orders of magnitude. As XGM, XPM or FWM-based conversions are typically optimized for a certain level of the input signal, they fail to deal with a highly-fluctuating input signal. Moreover, the un-equalized power of signals may not be suitable for existing metro network deployments designed for the continuous mode. For example, EDFAs (erbium-doped fiber amplifier) designed for the continuous mode cannot be used for the burst mode because of the transient effect since a highly-fluctuated signal input into EDFA will be distorted by dynamic gain transience [127].

On the other hand, O/E/O-based wavelength converters or O/E/O transponders are able to offer a more suitable performance. The O/E/O-based converter can act as true 3R re-generator (reamplifying, reshaping, and retiming) leading to complete isolation between the access and the metro section in terms of signal impairments such as chromatic dispersion. In long-reach scenarios, chromatic dispersion becomes significant since the transmission distance is 60 km or more. In the metro section, the isolation allows us to use existing infrastructure designed for the continuous mode (SONET/SDH). In the access section, the isolation allows to use low-cost transceivers designed for 20-km reach in the ONU. Note that the wavelength converter used for the upstream direction needs to be equipped with the burst-mode receiver to properly receive upstream signals.

To reduce footprint and cost, OEO-based wavelength converters can be integrated as demonstrated in [128] and [129]. The integration of a burst-mode receiver with very small footprint for 10 Gbps was demonstrated in [130].

Cost per User

The wavelength converter is shared among users in the same branch, and thus eventually increases the cost per user. Therefore, it is important to justify this increment and to compare it with the conventional architecture. The conventional reconfigurable long-reach PONs employs optical amplifiers such as burst-mode EDFAs to compensate the power loss and tunable transceivers at the ONU for wavelength reconfigurability. Therefore, different devices used in the RN and the ONU can evaluate the cost difference between two architectures.

Let Co_F, and Co_C denote cost of the fixed transceiver and cost of the wavelength converter in the WCL-Access architecture, respectively. In this architecture, the ONU employs two fixed transceivers and the wavelength converter serves one ONU group and includes a converter for downstream and another for upstream. Let Co_T and Co_A denote cost of the tunable transceiver and cost of the optical amplifier module in the conventional Broadcast-and-Select architecture, respectively. In this architecture, ONUs employ tunable transceivers and one optical amplifier is used in the RN for each ONU group. Assume that the cost of other hardware is the same for both architectures; we can derive cost per user Cu_{WCL} and $Cu_{B\&S}$, which do not include common costs such as fibers and electronics, for the WCL-Access and Broadcast-and-Select architecture in Eq. 4.1 and Eq. 4.2, respectively

$$Cu_{WCL} = 2Co_F + \frac{Co_C}{N_B} \qquad \text{(Eq. 4.1)}$$

$$Cu_{B\&S} = Co_T + \frac{Co_A}{N_B} \qquad \text{(Eq. 4.2)}$$

where N_B is the number of ONUs per branch.

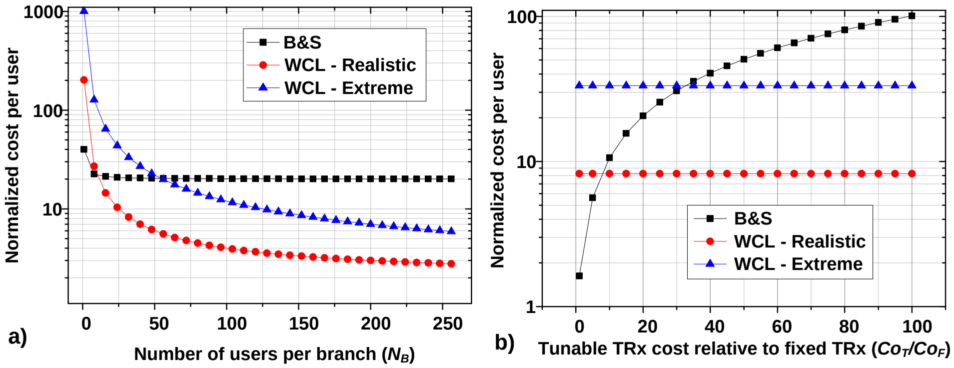

Fig. 4.6. Cost comparison between WCL-Access and conventional long-reach Broadcast-and-Select, cost is normalized to conventional PON TRx (Co_F), a) cost per user as a function of number of users per branch, b) cost per user as a function of tunable TRx cost relative to fixed TRx (Co_T/Co_F).

The cost per user as a function of number of users per branch N_B is shown in Fig. 4.6.a) in which the cost per user is normalized to the cost of the fixed transceiver Co_F. cost of the tunable transceiver Co_T is assumed to be 20 times higher than cost of the fixed transceiver Co_F, cost of the amplifier Co_A is assumed to be the same as cost of the tunable transceiver Co_T. There are two cases for cost of the wavelength converter in which Co_C is 200 times and 1000 times higher than Co_F. The first case represents a realistic estimation while the second case represents an extremely high estimation for the wavelength converter. The result shows that beyond 16 ONUs per branch the WCL-Access has a lower cost than the conventional Broadcast-and-Select in the realistic estimation while from the level of 56 ONUs per branch in the extreme estimation. Therefore, 64 ONUs per branch can guarantee the WCL-Access solution is cheaper than Broadcast-and-Select solution even in case that cost of the wavelength converter is extremely high. This achievement is due to the fact that the cost of the wavelength converter is shared among large number of users.

The assumption that Co_T is 20 times higher than Co_F is practical since the tunable TRx is not only wavelength tunable and long-reach operable but also much lower in the production volume than the conventional fixed TRx. In fact, tunable TRx is not yet available for access networks but those used in metro/core is ~$1000 per piece in high-volume orders while GPON TRx is ~$20. However, one still can question if cost of the tunable TRx can be reduced relatively to the fixed TRx. In order to address the question, cost per user as a function of Co_T to Co_F ratio is shown in Fig. 4.6.b). In this estimation, the number of users per branch is kept to 32 ONUs. In the realistic estimation, the Broadcast-and-Select solution is more costly than the WCL-Access solution when the ratio is 10 or higher. In the extreme estimation, the cost crossing between two solutions occurs when the ratio is around 35 times. Therefore, much reduction in cost of the tunable TRx needs to be made before the Broadcast-and-Select can be more cost-effective. This comparison highlights the advantage of using mass-produced optical transceivers, thus low-cost, in the design of WCL-Access architecture and shifting expensive devices from ONUs to the RN to be shared among users.

Wavelength Plan

In the architecture description, the wavelength plan of GPON and XGPON is used. However, it is not necessary to keep that plan. In the access section, only four wavelengths (two for downstream and two for upstream) are present resulting in many low-cost options for the wavelength plan. A plan of four CWDM wavelengths for each wavelength can be used in which each wavelength is allocated within a 20 nm window. The use of four identical CWDM windows eases the integration of two fixed transceivers and the wavelength demultiplexer in the same SFP module (small form factor pluggable).

The wavelength plan in the metro section, on the other hand, determines specifications for the wavelength converter. For a fully flexible wavelength plan, the OEO wavelength converter should be able to convert to any DWDM wavelength in the C band which may lead to a high module cost. In the other extreme, the OEO wavelength converter is able to convert to a specific DWDM wavelength, which requires a detail of available wavelengths (some wavelengths may be occupied by other services) in the metro section in the planning phase.

4.2.3. Conclusions

The WCL-Access architecture is the long-reach implementation of the cyclically-linked flexibility concept. The implementation requires wavelength converters in the distributed local CO. The use of wavelength converters enables several advantages:

- Completely decoupling of the metro and the access section in terms of wavelength plan and signal impairments.
- Conventional CWDM or PON transceivers can be used in the ONU.
- No wavelength tuning is required at the colorless ONU.
- Scalable in terms of number of wavelengths and ONUs.

4.3. Power-Splitter-Based Architecture

Although the outside plant of PRO-Access is passive, it is not fully compliant with the current PON deployments in which only power splitters are used in the outside plant. To apply the cyclically-linked flexibility in the current deployments without touching the outside plant, an implementation of the cyclically-linked flexibility is required so that the outside plant is based on only power-splitters. On the other hand, the power-splitter-based ODN is not scalable in terms of wavelength count and ONU count as demonstrated in Section 2.5. Therefore, this implementation aims primarily at wavelength reconfigurability in NG-PON2, which has four wavelength channels.

4.3.1. **PSB-Access Architecture**

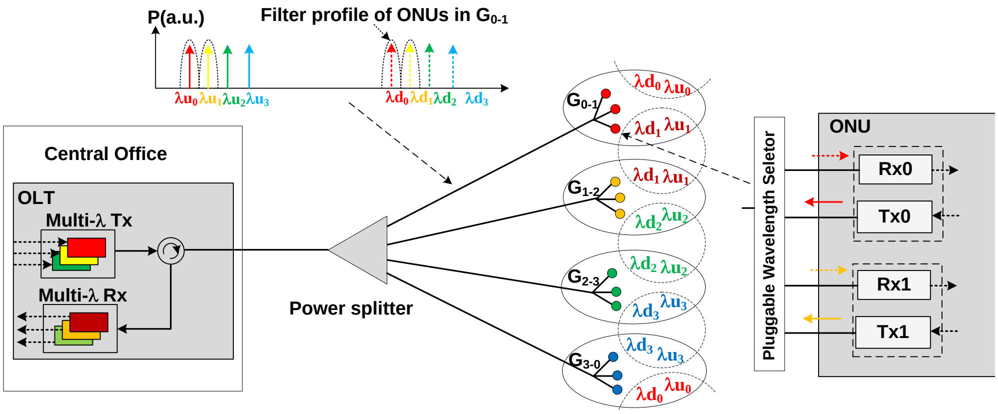

Fig. 4.7. Schematic representation of PSB-Access architecture for NG-PON2, wavelengths are selected on site by the pluggable wavelength selector.

The essential property of the cyclically-linked flexibility is that the ONU population is partitioned into groups of which each receives two pre-planned wavelength channels and adjacent groups share a common wavelength. Therefore, if wavelengths are broadcasted, the cyclically-linked configuration needs to be realized by appropriate wavelength filtering at the ONU.

The power-splitter-based implementation of the cyclically-linked concept, named as PSB-Access architecture, is shown in Fig. 4.7 in which each group of ONUs selects appropriate wavelengths to form the cyclically-linked divisions of ONU population. The ONU in $G_{0\text{-}1}$, for example, selects (λd_0, λu_0) and (λd_1, λu_1) and cancels unwanted wavelengths. ONUs in $G_{0\text{-}1}$ are not necessarily located in the same fiber branch. In fact, they can be located on any fiber end since wavelengths are broadcasted.

An ONU which is wavelength-specific adds extra inventory cost as different types of ONU need to be kept in stock. In this case, there are only four types of ONUs for four different groups. To minimize the inventory cost, a pluggable external wavelength selector can be used as shown in Fig. 4.7. The common ONU box is made wavelength-specific by plugging the wavelength selector on site. This practice has been applied for WDM PON commercial deployments in Korea [75].

The pluggable wavelength selector can be made from an optical coupler, circulators, and Fiber Bragg Gratings (FBG) as shown in Fig. 4.8.a). The schematic shows an example for the wavelength selector used in $G_{0\text{-}1}$ in which FBG_0 and FBG_3 are designed to reflect λd_0 and λd_1 and cancel unwanted downstream wavelengths. FBG_1 and FGB_2 are used to select the working wavelength for upstream transmitters. The upstream FBG partly reflects the selected wavelength back to the laser diode to set the lasing wavelength as shown in Fig. 4.8.b). FBGs can be fabricated directly on the patch core fiber to have a compact wavelength selector [131]. A scheme, which is similar to the upper arm of described wavelength selector, is commercially available as the wavelength selector for DWDM-PONs as shown in Fig. 4.8.c) [132]. Another option to select the wavelength is using a wavelength demultiplexer based on AWG or TFF (Thin Film Filter) as shown in Fig. 4.8.d). In the upstream, the mechanically-locked tunable laser, depicted in Fig. 4.8.e), is employed to get the appropriate wavelength by tuning the external cavity mechanically [75]. This is a type of set-and-forget tunable laser in which the thermally-stable wavelength is held without electrical energy once tuned.

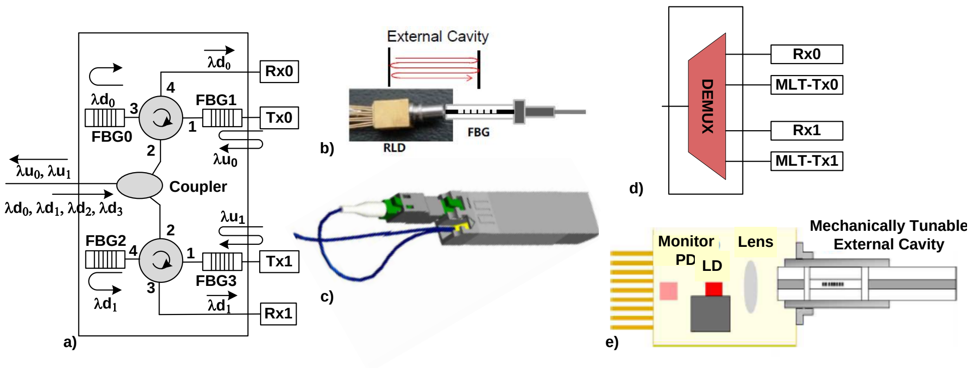

Fig. 4.8. a) wavelength selector based on optical circulators and fiber bragg gratings, b) wavelength setting for reflective laser diode by wavelength selection plug (courtesy MEL Telecom), c) wavelength selector for single transceiver (courtesy MEL Telecom), d) wavelength selector based on TFF or AWG wavelength demultiplexer, e) The schematic of mechanically locked tunable laser (MLT) (courtesy MEL Telecom).

4.3.2. Cyclically-linked NG-PON2 versus Wavelength-Tuned NG-PON2

As the cyclically-linked advantage of reducing excessive power budget is traded for the compliance to existing power-splitter-based outside plant, PSB-Access has the same limitation to the Broadcast-and-Select architecture in terms of scalability. Therefore, PSB-Access may be only practical in the scenario of NG-PON2 where only four TDM PONs are stacked. The straightforward solution for wavelength-reconfigurable NG-PON2 is to use tunable transceivers at the ONU side, referred as wavelength-tuned NG-PON2. This section will compare the cyclically-linked and wavelength-tuned scheme as two possible solutions for wavelength-reconfigurability for NG-PON2.

Computer models for the cyclically-linked NG-PON2 and the wavelength-tuned NG-PON2 were created with 128 ONUs and four 10 Gbps wavelength channels. Initially, 32 ONUs are distributed to each channel. The swap-based rearrangement algorithm is employed in the cyclically-linked NG-PON2. The performance is evaluated under three traffic scenarios as described in Section 3.3. In scenario 0, each ONU can request only one connection with the connection size between 100 Mbps and 900 Mbps while in scenario 1, each ONU can request up to 10 connections with connection size between 10 Mbps to 90 Mbps. Scenario 3 represents a future home scenario where a home can request two 8kTV channels of 160 Mbps, one cloud computing and data connection of 170 Mbps, and one video telephony call of 10 Mbps as summarized in Table 3.1.

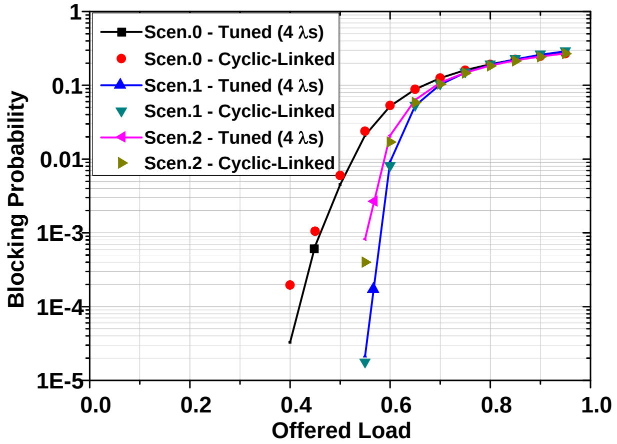

Fig. 4.9. Comparison of blocking probabilities between wavelength-tuned NGPON2 (the full flexibility of 4 wavelengths) and cyclically-linked NGPON2

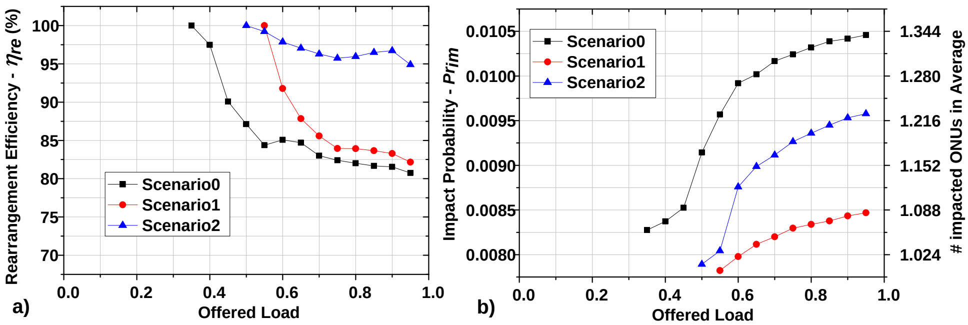

Fig. 4.10. a) Rearrangement efficiency of swap-based rearrangement algorithm, a) Rearrangement impact probability of cyclically-linked NGPON2.

The comparison of connection blocking probability between two schemes is shown in Fig. 4.10.a) in which wavelength-tuned cases are plotted by solid lines and cyclically-linked cases are plotted by dots. The cyclically-linked NG-PON2 yields blocking probabilities very close to the wavelength-tuned NG-PON2. Recall that there was a sizable difference between the cyclically-linked flexibility and the full flexibility in the traffic scenario 0 as shown in Fig. 3.9 in Section 3.3. In the case of NG-PON2, there is unnoticeable difference since the network has only 4 wavelengths instead of 16 wavelengths. The rearrangement algorithm experiences less unsuccessful attempts because it needs to swap maximum 2 steps instead of maximum 8 steps in the 16-wavelength network. The more swap steps the rearrangement needs, the higher probability is that the rearrangement gets blocked. This is clear by observing the rearrangement efficiency η_{re} shown in Fig. 4.10.a). The efficiency is always higher than 80% in which scenario 2 has the efficiency above 95%. Note that the rearrangement algorithm is less efficient in the 16-wavelength network as shown in Fig. 3.20.a) in Section 3.5. The less swap steps also result in a lower impact probability Pr_{im} as shown in Fig. 4.10.b). In average, the number of impacted ONUs is below the threshold of 1.4 meaning that most of rearrangement operations reallocate only one in-service ONU.

Performance in the logical layer is comparable between the cyclically-linked NG-PON2 and the wavelength-tuned NG-PON2 leaving the competition to the implementation cost. The cyclically-linked NG-PON2 has to use wavelength selectors to color ONUs while wavelength-tuned ONUs are colorless. However, the cyclically-linked NG-PON2 avoids the use of tunable transceivers as well as the cumbersome wavelength tuning. The tunable transceiver has to keep the wavelength stability and regularly recalibrate the wavelength with the assistance of the OLT. The wavelength selector is fully passive and athermal which ensures the stability of output wavelengths.

Furthermore, the use of a dual transceiver guarantees a seamless wavelength handover by the make-before-break mechanism. The connection at the new wavelength can be established before tearing down the former connection at the previous wavelength. The tuning time of tunable transceiver has to be fast enough to avoid the interruption of on-going services in the break-before-make mechanism as discussed in Section 2.2. In addition, the data have to be buffered during the handover process. For example, to switch an ONU with 1 Gbps on-going connections, 18.75 MB of data needs to be buffered for one direction when the handover time is 150 ms.

4.3.3. **Conclusions**

PSB-Access is an implementation for wavelength reconfigurability in NG-PON2 without wavelength tuning. The logical layer performance in terms of blocking probability is demonstrated to be similar to that of the wavelength-tuned NG-PON2 in which the ONU can be reallocated to any wavelength. Although ONUs need to be colored on site by the wavelength selector, avoiding wavelength-tuning is a clear advantage of the cyclically-linked

NG-PON2 when cost of wavelength-tuning does not yet meet the cost point for access networks.

4.4. Cyclically-linked Full Protection Architecture

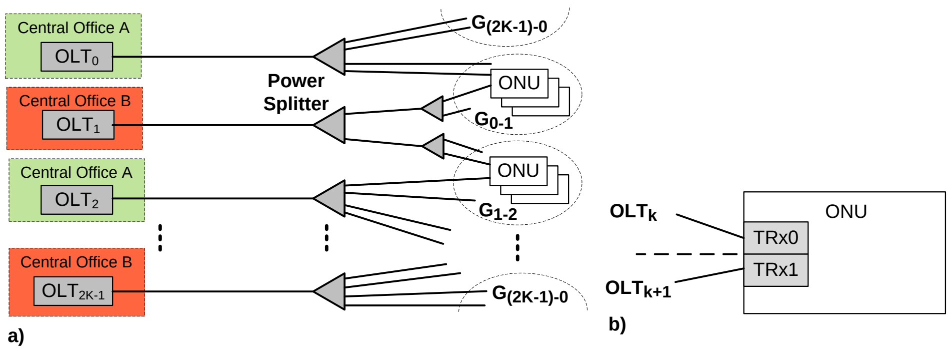

Fig. 4.11. a) Schematic representation of cyclically-linked protection of long reach PONs in dual-office configuration, b) ONU connectivility is protected by dual geographically-diverse physical links.

Optical access networks are evolving to include traffic from mobile backhaul/fronthaul. The number of end-users covered by a single network is also increasing requiring larger capacity and higher split ratios. Meanwhile, the central office consolidation has been proposed with long-reach access networks, which allow the maximum distance between the central office and end-users to be 60 km or more. As a result, optical access networks are running a higher risk of service interruption with a large number of customers being potentially affected. A failure in the consolidated central office, for example, may lead to service interruption in a wider area. Therefore, the requirement for access network reliability is more stringent than ever to guarantee service continuity in case of fiber cuts, device failures, long blackouts, or man-made/natural disasters.

Indeed, network protection was considered and specified for earlier generations of passive optical access networks. ITU-T G.983.5 recommendation for enhanced survivability for PONs specifies three protection schemes with different levels of redundancy [69]; Type A utilizes two feeder fibers to protect from the cut of either of the feeder fibers. Type B protection duplicates the shared part, i.e. the feeder fiber and the line card in the optical line terminal (OLT). Type C scheme provides the highest protection level with full duplication of the PON resources including the last drop to the user, which also allows the secondary path from the OLT to the optical network unit (ONU) to be utilized to carry extra traffic in the absence of failure [22]. To avoid the single point of failure of the consolidated office, the dual-office configuration was studied to provide a high-level service continuity [133].

Type C provides full protection but it is also the most costly scheme because of 1:1 OLT-to-ONU protection. In this section, a cost-effective modified type C protection, referred to as the cyclically-linked protection is proposed. This scheme engages multiple OLTs in the dual-office configuration to provide a cost-effective full protection as well as a congestion mitigation mechanism. In normal operation, traffic in a congested PON can be spread out to other PONs by the ONU rearrangement operation to avoid any local congestion.

4.4.1. Cyclically-linked Protection

The schematic representation of the cyclically-linked protection is shown in Fig. 4.11.a) in which 2*K-1* PON line cards or OLTs are involved. The even-indexed OLTs are located in the consolidated central office *A* while odd-indexed OLTs are located in the central office *B*. The ONU has two optical transceivers as shown in Fig. 4.11.b) in which one interfaces with an even-indexed OLT and the other interfaces with an odd-indexed OLT. The ONUs are divided in groups, each group is served by a pair of OLTs in a linked manner. For example, $G_{0\text{-}1}$ is serviced by OLT_0 and OLT_1 and $G_{1\text{-}2}$ is serviced by OLT_1 and OLT_2, and so on. $OLT_{(2K\text{-}1)}$, the last OLT, is paired with OLT_0, the first OLT, to service $G_{(2K\text{-}1)\text{-}0}$ forming the cyclic configuration. Therefore, each OLT associates with two ONU groups and adjacent OLTs are linked by an ONU group.

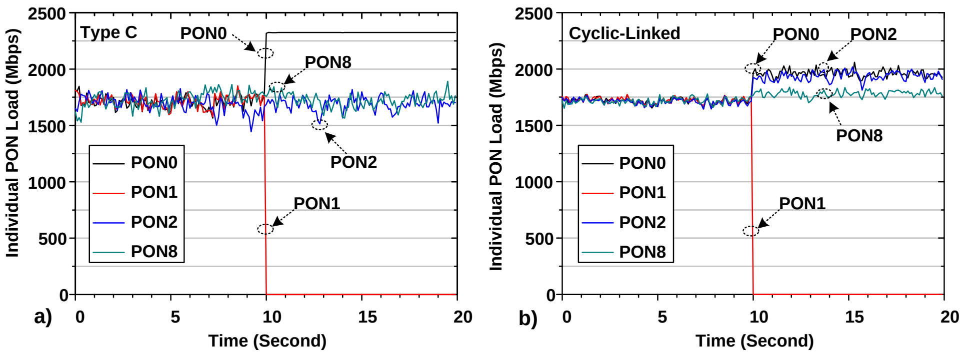

Fig. 4.12. Time traces of 20 seconds when *PON1* feeder fiber cut occurs at 10th second, a) Upstream channel loads of representative PONs in the conventional type C protection, b) in the cyclically-linked protection.

From the ONU's perspective, it is protected as in the conventional Type C protection as there are two possible access paths. However, from the network's perspective, the cyclically-linked protection enables the load balancing across all associated PONs through a bandwidth rearrangement process.

There are two options for network capacity planning. In the first option, half of the capacity is planned solely for the purpose of protection, i.e. a costly implementation of 1:1 end-to-end protection. In the second option, the full capacity is planned for normal traffic. When there is failure in a PON, affected ONUs are still online with reduced bandwidth. However, the magnitude of reduced bandwidth in the cyclically-linked is much lower than in the conventional Type C since the loss in capacity is not only covered by one remaining PON (as in the conventional Type C) but all associated PONs. For example, if a feeder fiber cut in PON_1 occurs, the burden is not only covered by PON_0 but also by other PONs by an appropriate bandwidth rearrangement. Therefore, the second option promises a high level of service continuity with a low impact on quality of service. This option also leads to a reasonable protection cost, which is the additional 3 dB loss budget, the double number of distribution fibers, and an additional transceiver in the ONU in comparison to the non-protected scheme. An OLT has to feed not only its own ONUs but also ONUs of the next-index OLT, resulting in an additional 3 dB loss. Therefore, the second option is more economical while still maintaining a high-level protection. The next section discusses the proposed scheme in the cost-effective option of capacity planning.

4.4.2. **Evaluation of Failure Resiliency**

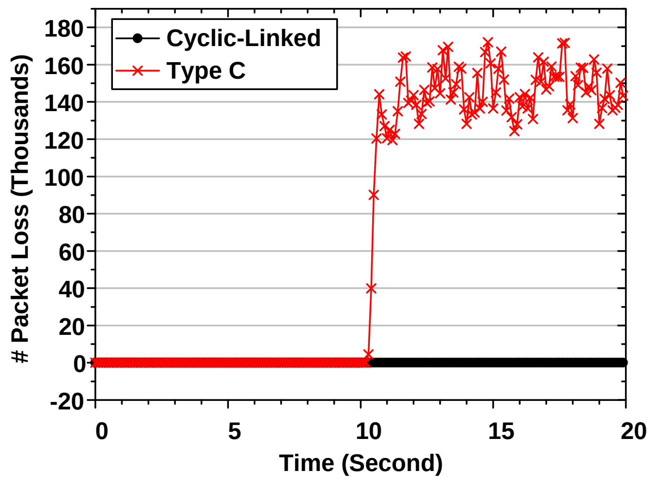

Fig. 4.13. Time trace of the number of packet loss by buffer overflow in ONUs when *PON1* feeder fiber cut occurs at 10th second

To understand the response of the cyclically-linked protection, the packet level performance was investigated. The conventional type C protection was also investigated in which PON_0 and PON_1 are paired for protecting each other, PON_2 and PON_3 are paired, and so on. There are 512 ONUs numbered from 0 to 511, each is attached with a bursty traffic source. In the cyclically-linked protection, ONU_0 to ONU_{31} are in $G_{0\text{-}1}$, ONU_{32} to ONU_{63} are in $G_{1\text{-}2}$, and so on. In the type C, ONU_0 to ONU_{63} are connected to PON_0 and PON_1, ONU_{64} to ONU_{127} are connected by PON_2 and PON_3, and so on.

In the case of failure, the response of the two schemes to a feeder fiber cut event during busy hours is investigated. Each PON operates at the average load of 70% of the full capacity, which is a high traffic load in practice. The feeder fiber of PON_1 is cut at the 10th second. Time traces of load on representative PONs are shown in Fig. 4.12.a) for the type C and Fig. 4.12.b) for the cyclically-linked protection. In the type C, traffic of PON_1 is transferred to PON_0 after the fiber cut that makes the load of PON_0 to reach the ceiling. In fact, the remaining capacity of PON_0 cannot accommodate the entire traffic from PON_1 resulting in high lost of packets as shown in Fig. 4.13. If the TCP protocol is used in the protocol stack, it will be forced to reduce the flow rate, resulting in service quality reduction or service drop. Packet loss is not found in the cyclically-linked protection as can be observed in Fig. 4.13. It is because the traffic from PON_1 generated by ONUs, which are members of G_{0-1} or G_{1-2}, is reallocated to PON_0 or PON_2 after the fiber cut. The increased load in PON_0 forces some ONUs in G_{15-0} to move to PON_{15} to balance the load and subsequently ONUs in other PONs are shifted outwards (seen from PON_1) to give space for newly arriving ONUs. In the other direction, the increased load in PON_2 creates the same wave of moves. The load of PON_8, which is the furthest PON seen from PON_1, is increased as shown in Fig. 4.12.b) because of these phenomena. Therefore, unlike in the type C, the burden is covered by all associated PONs in which PON_0 and PON_2 receive the direct impact while others experience the impact indirectly by accepting ONUs from the neighboring PON.

In the absence of failure, the cyclically-linked configuration can be used for load balancing to avoid any local congestion as demonstrated in Chapter 3. In non-busy hours when the traffic falls below 50% of the capacity, half of the associated PONs can be turned off to save power. It promises substantial energy savings, even in the case of only 5 non-busy hours per day as demonstrated in Chapter 2.

4.4.3. **Conclusions**

The proposed cyclically-linked protection has the same additional physical parts as the conventional type C in ITU-T G.985.3 but the performance evaluation clearly shows that the cyclically-linked protection is more advanced in the case of failure or local congestion. Multiple PONs are joined together to share the extra traffic burden which results in the better performance. In other words, this scheme uses a large pool of active capacity in the PONs to protect each other that avoids using standby capacity implying cost-effectiveness. More joined PONs can absorb a higher impact. However, 16 or even 8 PONs can absorb an entire PON failure during busy hours given that PON take-rates hardly exceed 70% level.

When an ONU is reallocated to the other PON, the fiber routes are different between the two PONs that require a re-ranging procedure, especially the new OLT is located in the other CO. The re-ranging procedure can be done before the ONU actually move the traffic to the new wavelength to avoid service interruption. In addition, the cyclically-linked protection requires an extra control over all associated PONs and a more careful design of fiber routes in the outside plant. However, I believe that these can be done with a minimal cost. The configuration is not restricted to long-reach scenarios but also can be applied to the single office and 20km reach deployment scenarios.

4.5. Conclusions

This chapter presents a family of architectures based on the cyclically-linked network flexibility. Three architectures were designed for wavelength reconfigurability in different deployment scenarios and a special architecture aims for the cost-effective full protection in current PON standards. Wavelength tuning is completely avoided in all architectures while the passive ODN is preserved in PRO-Access and PSB-Access and wavelength-agnostic ONU designs are achieved in PRO-Access and WCL-Access.

Table 4.1 summarizes the comparison of wavelength reconfigurable architectures including the conventional Broadcast-and-Select in which each architecture has its own merits that may fit with certain deployment scenarios. Green-field (new installations) and short-reach deployments are suitable for PRO-Access architecture while brown-field (upgrade) and short-reach deployments favor PSB-Access. Long-reach with central office consolidation deployments are the application area for WCL-Access. In all application areas, cyclically-linked architectures have to compete with Broadcast-and-Selection architectures with wavelength-tuning.

TABLE 4.1. SUMMARIZED COMPARISON OF WAVELENGTH RECONFIGURABLE ARCHITECTURES. THE CYCLICALLY-LINKED FULL PROTECTION IS NOT WAVELENGTH RECONFIGURABLE, IT IS COMPARED WITH THE TYPE C PROTECTION.

	Broadcast &Select	**PRO-Access**	**WCL-Access**	**PSB-Access**	**Full Protection**
Passive ODN	**Yes** / **No** for long reach	**Yes**	**No**	**Yes** / **No** for long reach	**Yes**
Current ODN compliance	**Yes**	**No**	**No** / **Yes** for access section	**Yes**	**Yes**
Long-Reach	**Yes** with amplifiers	**No**	**Yes**	**Yes** with amplifiers	**Yes** with amplifiers
Colorless ONU	**Yes**	**Yes**	**Yes**	**No**	**Yes**
System Cost	**High**	**Medium**	**Low**	**Medium** (incl. inventory cost)	**Low** (compared to Type C)
Scalability	**Poor**	**Good**	**Good**	**Poor**	**Good**
Possible Time Frame	**NG-PON2**	**After NG-PON2 for wavelength scaling**	**After NG-PON2 for Metro/Access Merge**	**NG-PON2**	**Adopted with CO consolidation**

CHAPTER 5

WAVELENGTH RECONFIGURABILITY FOR DYNAMIC RADIO SIGNAL DELIVERY

This chapter is dedicated to radio signal delivery over reconfigurable optical access networks. By wavelength reconfigurability, radio signals can be dynamically assigned to desired remote antenna units. Two application-specific architectures are described in which one is designed for dynamic cell capacity assignment and the other is a cost-effective implementation of the moving cell concept. The contents of this chapter have been partly disseminated in [90] and [134].

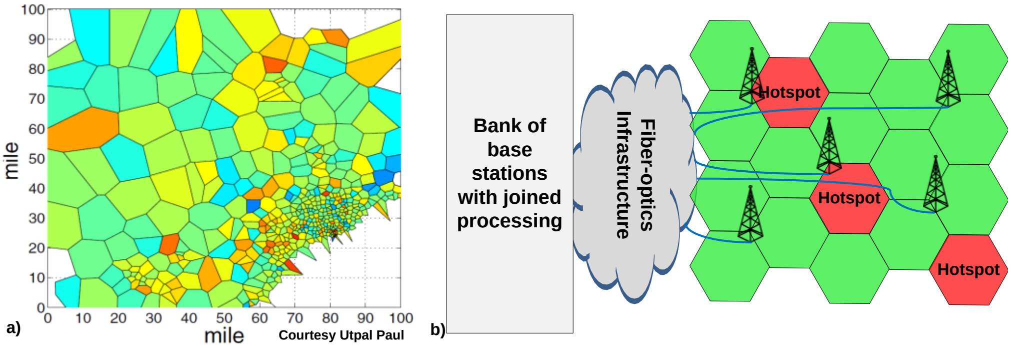

Fig. 5.1. a) Base stations and their Voronoi cells of a cellular network (courtesy Utpal Paul, INFOCOM 2011), b) Base station centralization with the support of a fiber-optical infrastructure.

5.1. Rationale

Smart handheld devices such as smartphones and tablets have been rapidly adopted in recent years. As a result, traffic generated by handheld devices has shown a steep rise at an annual rate of 78% as described in Section 1.1. The explosion creates valuable business opportunities as well as poses a great technical challenge for network operators. Radio frequency spectrum for mobile communication has become a scarce resource in which each operator owns a very limited allocation. A common technique to increase radio network capacity is to reuse frequencies. Radio cells, which are far apart, can use the same radio frequency without interference. In densely populated areas, the cell size may be reduced to tens of meters to increase the frequency reuse factor [135]. An example of cellular pattern is shown in Fig. 5.1.a) in which cell sizes in the urban area are smaller by several orders of magnitude than in the sub-urban areas [6]. When the frequency reuse method reaches its limit, the network capacity cannot be scaled up for a certain cellular technology. However, the dynamic nature of mobile traffic can be seen as an opportunity to meet the user demand without provisioning extra capacity. Instead of using a pre-planned allocation of cell capacities, the allocation can be dynamically changed in the course of operation to adapt to the real-time demand. A traffic jam in the city, for example, may pose congestion in the cell serving that area. If the cell capacity can be increased instantly in response to the high demand, the operator can maintain the quality of service as well as avoid losing revenue.

A reconfigurable fiber-optical infrastructure in conjunction with radio over fiber techniques can be used to realize dynamic allocation of cell capacities as depicted in Fig. 5.1.b). Base stations are centralized in a central office and radio signals are delivered to light-weight remote antenna units (RAU) by the fiber-optic infrastructure. The capacity allocation can be changed by altering the mapping between centralized base stations and distributed RAUs through wavelength reconfigurability [22][88][136].

The fiber-optic infrastructure can natively support the radio signal or its digitized form. A digitized radio signal is basically a binary bit stream, thus can be delivered by any of the reconfigurable architectures described in the previous chapter. This chapter focuses on architectures that can natively support analog radio signal delivery.

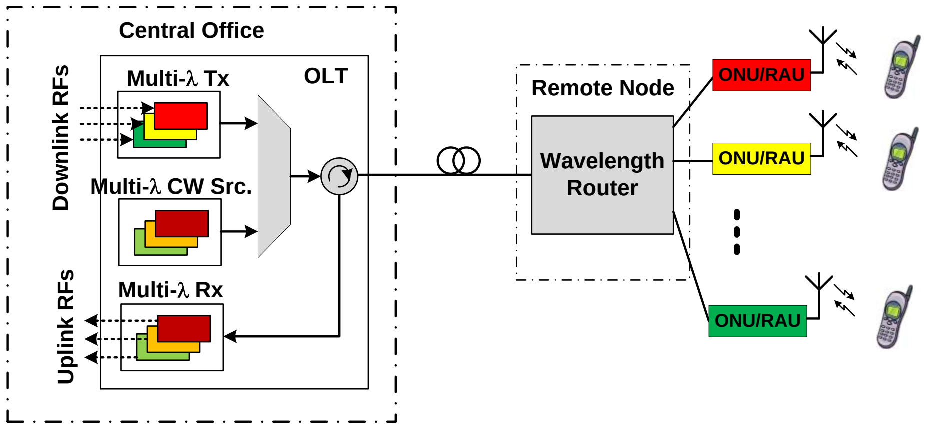

Fig. 5.2. Schematic representation of dynamic distributed antenna system based on active routing optical access network architecture.

5.2. Dynamic Cell Capacity Assignment

The distributed antenna system (DAS) was proposed to cost-effectively implement extremely small cells in urban area [22][137]. A bank of base stations is located in the central office (CO) and radio signals are delivered to remote antenna units (RAU) by means of optical channels. To have dynamic capacity allocation, radio frequency (RF) sub-carriers can be dynamically allocated to RAUs [138][139]. Congested cells are provided with additional RF sub-carriers, which are reallocated from lightly-loaded cells.

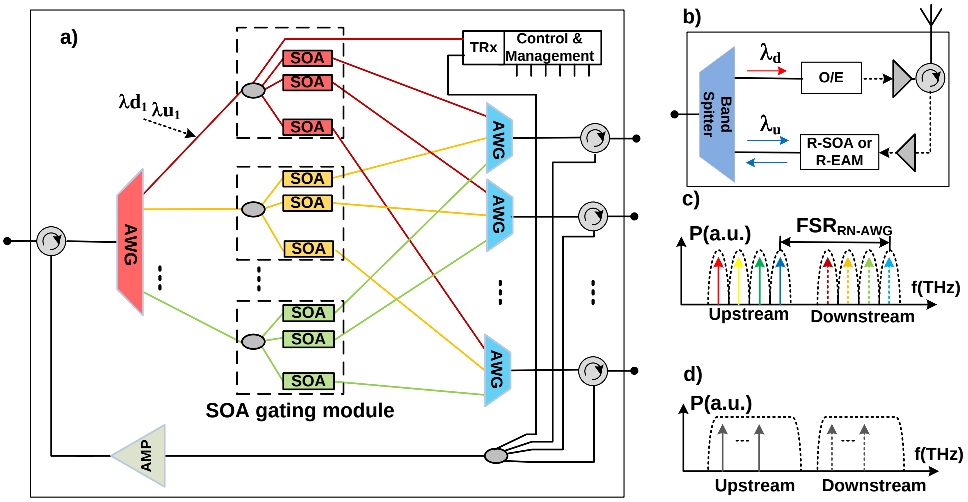

Fig. 5.3. Schematic representation of network elements, a) SOA array based remote node, b) Optical network unit / remote antenna unit, c) wavelength panel at the remote node input, d) wavelength panel at an ONU/RAU input.

To conventionally implement this scheme, a redundant capacity, e.g. hardware and backhaul resource, is added to every base station and activated or deactivated accordingly. Apart from the electronic implementation, an alternative is to use the dynamic DAS (DDAS) in which RF sub-carrier assignment is handled by wavelength reconfigurability in the optical domain. The electronic base stations are replaced by light-weight RAUs that dynamically share a common bank of base stations centralized in the CO. This approach decouples dynamic RF capacity allocation from the RF domain to allow transparency in terms of radio standards. Hence, it facilitates multi-standard operation and future upgrades.

The DDAS can be implemented either by RF switching or by optical switching. In the first option, the DDAS employs an RF switch matrix at the CO to dynamically map RF sub-carriers to statically routed wavelengths. However, the design of a large RF switch matrix is very challenging in terms of insertion loss, reflection, cross-talk, and linearity. Additionally, the RF switching matrix usually operates in a certain restricted frequency range, which reduces the transparency of DDAS.

In this section, the second option is studied to realize DDAS by the proposed active routing optical access network (ARON) in which an array of semiconductor optical amplifiers (SOAs) at the remote node (RN) performs downstream (DS) and upstream (US) wavelength routing. An optical wavelength couples with one or more pre-assigned RF carriers to allow RF reconfiguration to be carried out in the optical domain.

5.2.1. DDAS over ARON architecture

The ARON architecture is shown in Fig. 5.2 where the RN is able to route one or more wavelengths arriving from the optical line terminal (OLT) to an output port. Each RN output port connects to an optical network unit/remote antenna unit (ONU/RAU). The OLT located at the CO transmits two wavelength bands: modulated DS wavelengths and un-modulated continuous-wave (CW) US wavelengths as shown in Fig. 5.3.c). Each DS wavelength is modulated by a downlink RF signal. A DS wavelength couples with an US wavelength where the spectral distance is one or more free spectral ranges of the cyclic arrayed waveguide grating (AWG) in the RN as shown in Fig. 5.3.a). As a result, each pair of wavelengths is output from the same AWG port towards a SOA gating module. The state (ON/OFF) of SOAs in the gating module determines the RN output port the wavelength pair will be routed to.

At the ONU/RAU shown in Fig. 5.3.b), a DS-US waveband splitter directs the DS wavelength(s) to one port and the US wavelength(s) to the other. The US CW(s) is modulated by the uplink radio signal(s) using a reflective-type modulator such as a reflective semiconductor optical amplifier (RSOA) or a reflective electro-absorption modulator (REAM). The modulated US wavelength(s) is reflected back and propagates towards the OLT. The US wavelengths originating from an ONU/RAU carry the same RF signal(s) which allow the receiver module in the OLT to be simplified since a RF receiver can be coupled with an opto-electronic converter (O/E) by a bandpass filter in between to select the desired RF subcarrier. When a radio cell needs more capacity, the corresponding ONU/RAU will get an additional RF channel by routing one more DS/US wavelength pair to it.

Although the O/E receives multiple wavelengths at the same time, a negligible interference is expected because the carried RF channels are centered in different frequencies. The optical beat noise is also avoided since the beat noise spectrum is centered at a frequency that is equal to the difference of the optical wavelengths [140]. In the worst case, the difference of two dense WDM wavelengths is 50 GHz, which is very far from RF sub-carriers (well below 10 GHz). The ONU/RAU is wavelength-agnostic, and thus emits all the microwave signals carried by the received wavelength signals. Besides the electrical bandpass filter which has to select the desired microwave frequency, the ONU/RAU is also fairly frequency independent. Therefore, this approach has a radio-standard agnostic outside plant, which can ease future upgrades. In order to control and manage the RN, a common signaling channel is established between the RN and the OLT. By using this channel, the OLT and the RN can exchange control messages such as routing information, operational statuses. The signaling channel is physically embedded in the first wavelength pair by subcarrier multiplexing. Proof-of-concept experiment was devised to validate this concept, this will be further discussed in the subsequent sub-section.

5.2.2. Proof-of-Concept Experiment

The experimental setup shown in Fig. 5.4 focuses on investigating dynamic characteristics of DDAS over ARON. As a proof-of-concept, the OLT transmits four wavelengths, two for DS and two CWs for remote modulation at the ONU/RAU. The wavelengths are compliant to ITU-T 100-GHz spaced C-band wavelength grid and selected only because of their availability in the lab. Two DS wavelengths are modulated by *RF1* signal centered at 2 GHz and *RF2* signal centered at 2.04 GHz, respectively. The ONU/RAU uses an RSOA for modulating US CW by the *RF3* signal of 1.93 GHz and the *RF4* signal of 1.97 GHz. All RF signals are 20 MHz wide carrying 20 Msymbol/s in 16-QAM format, equivalent to 80 Mbps. To emulate the cyclic property of the proposed AWG in the RN, wavelengths in the same pair are combined again after the AWG. A similar configuration with the AWG in the ONU/RAU is used to emulate a waveband splitter. Using variable optical attenuators placed in front of each SOA, the loss for a splitting ratio of 1:64 is emulated.

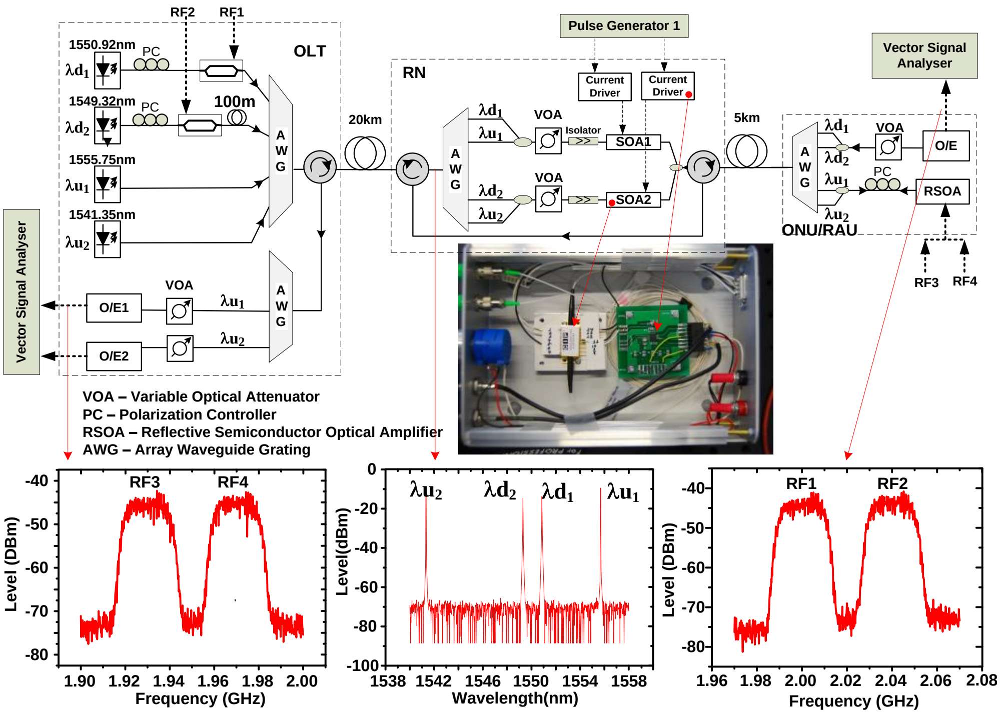

Fig. 5.4. Proof of concept experimental setup for dynamic cell capacity assignment, 2 downstream and 2 upstream wavelengths, each carries one radio frequency signal at 2 GHz band.

RF1 associates with *RF3* and *RF2* associates with *RF4* to form two pairs of downlink and uplink channels. The wavelength pair (λd_2, λu_2) carrying the RF pair (*RF2*, *RF4*) is constantly allocated to the ONU/RAU and the wavelength pair (λd_1, λu_1) carrying the RF pair (*RF1*, *RF3*) is allocated to the ONU/RAU for 150 μs and unallocated for 50 μs in a 200 μs cycle. With the symbol period of 50 ns, a single 200 μs cycle contains 4000 symbols. This experiment emulates the case where the radio cell served by the ONU/RAU requires more channels to increase the cell capacity.

To evaluate the quality of the received radio signals, the time traces of the error vector magnitude (EVM) of received symbol constellations are shown in Fig. 5.5. EVM is the

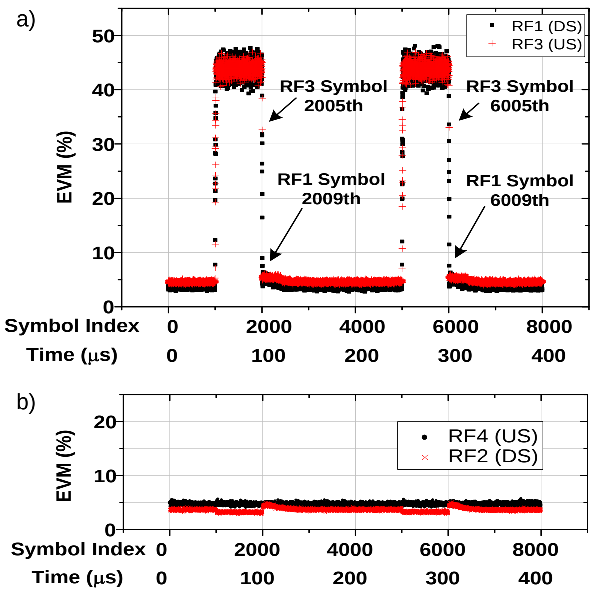

Fig. 5.5. Instantaneous EVM time traces for two cycles of ONU/RAU reallocation, a) The first RF pair , b) The second (existing) RF pair.

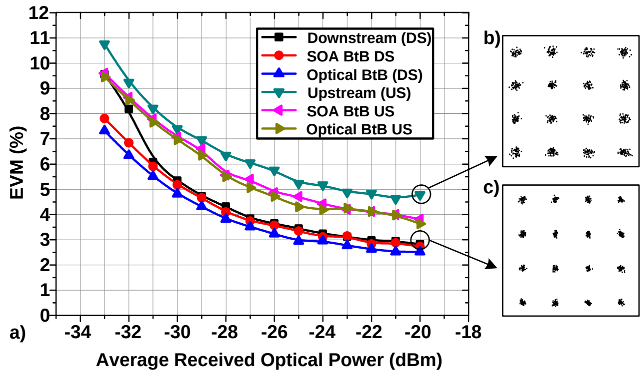

Fig. 5.6. a) Average EVM vs. received optical power test results, b) Received RF1 16QAM constellations, c) Received RF3 16QAM constellation.

indicator for the error between the received constellation points to the ideal constellation position [141]. The traces consist of two repeated 200 μs cycles, where *SOA1* is gated OFF for 50 μs from the 1001th to the 2000th symbol in the first cycle and from the 5001th to 6000th symbol in the second cycle. As observed in Fig. 5.5.a), after 9 symbols (450ns) from the moment that the ON signal is applied to *SOA1*, the *RF1* EVM falls below the acceptable threshold of 10 %. In principle, this turn-on period can be shorter because the control signal and SOA rise time is 1ns and 5ns, respectively. Due to the imperfect impedance matching between the control circuit and the SOA, the longer turn-on time is experienced. This matching may improve when the control circuit and SOAs are integrated on a single chip. The impedance mismatch effect still can be observed after EVM reducing below 10% as the EVM is higher than normal. This noise also impacts existing RF signals, which can be observed in the *RF2* EVM trace shown in Fig. 5.5.b). However, the EVM rises below 1% in only 250 symbols (12.5 μs).

The uplink *RF3*, on the other hand, needs only 6 symbols to get below 10 % because *RF3* bypasses the SOA in the US direction and only its seeding wavelength goes through the SOA. Therefore, downlink *RF1* determines the allocation time, which is 450 ns. The new allocation has no impact on uplink *RF4* performance as observed in Fig. 5.5.b).

Average EVMs of *RF1* and *RF3* as a function of received optical power are shown in Fig. 5.6. The average EVM is calculated for 50 cycles. In each cycle, the calculation excludes 50μs unallocated period from 1001th symbol to 2000th symbol and 450ns guard time from 2001th symbol to 2009th symbol. In each direction, there are three cases, including SOA back-to-back (BtB), in which 20km and 5km fibers before and after the RN are removed. The proximity between SOA BtB DS curve and DS curve reveals that the SOA is the dominant source for *RF1* signal impairment, not the transmission distance. In the upstream direction, the SOA BtB US almost coincides with the optical BtB plot, showing that the SOA is no longer the source for the *RF3* signal impairment but the transmission distance. The reason is that *RF3* bypasses the SOA in the upstream direction but is exposed to backscattering and reflections from the seeding CW wavelength. At the received optical power of -25 dBm, the EVM performances for both DS and US are 3.5% and 5.2% and the degradations to optical BtB cases are only 0.5% and 1% respectively. The optical upstream (RF uplink) performs worse than downstream because *RF3* centered at 1.93 GHz is almost close to the RSOA electrical bandwidth limit. Alternatively, the RF signal can be down-converted to remain within the RSOA bandwidth, which requires an extra local oscillator and may increase ONU/RAU complexity. To modulate higher frequencies, a REAM is recommended instead of the RSOA. REAMs can be used for frequencies up to 60 GHz [142], but exhibit high insertion loss, e.g., 8dB. Recent developments in devices combining REAM with SOA could mitigate these losses.

In the experiment, discrete optical components are used in the RN. However, integration of these components is expected to drive down costs and power consumption [143][144]. To address the heat generated by SOAs when active, which is an inherent issue of highly integrated photonic circuits, the RN configuration is designed to have a minimal number of SOAs that are simultaneously active. The proposed architecture can be cost-effectively implemented by photonic integration to reduce the RN cost.

5.2.3. Conclusions

In this section, a new concept of DDAS is presented based on a reconfigurable optical access network. DDAS is a promising solution for implementing dynamic frequency planning in cellular networks. As mapping between subcarriers and RAUs is done in the optical domain, the solution is relatively transparent in terms of radio frequencies, signal formats, and data rates.

A proof-of-concept demonstration was presented with bidirectional transmission. The physical performance was shown to have very low EVM penalty, i.e. 1% and 0.5% for both upstream and downstream transmissions. There is always only one SOA in the optical path between the OLT and the RAU which allows scalability with less concern on signal degradation. However, the broadcast-and-selection structure may pose a limit on scalability in terms of power budget. Amplifying stages can be used to compensate losses but their noises may become the limiting factor.

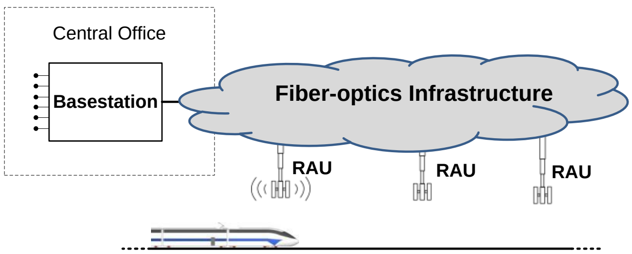

Fig. 5.7. The concept of moving cell in which a fiber-optic infrastructure is used to divert radio signals following the train.

5.3. High-Speed Network Connection of Train Passengers

5.3.1. Moving Cell Concept

People surfing websites or watching online clips on their handheld devices are becoming common in any public place, especially in trains. To facilitate such scenarios, the moving cell concept has been proposed to provide high-speed and reliable Internet connections for fast-moving passengers [145][146][147]. Instead of the train frequently crossing radio cells along the railroad, a radio cell is designed to follow the train. Hence, mobile users are able to stay in the same radio cell when traveling to avoid cumbersome handovers and packet loss. Mobile users can connect to the cell directly or through a radio head-end installed in the train.

A fiber-optic infrastructure together with radio over fiber techniques can be used to implement the moving cell concept as shown in Fig. 5.7. The radio base station is located in the CO and RF signals are transmitted through the infrastructure to reach a particular remote antenna unit (RAU) where the train is passing by. When the train enters the coverage area of the next RAU, RF signals must be redirected to the appropriate RAU. In earlier proposals, an optical switch is employed to route the wavelength, thus RF signals, to the desired RAU [145][147]. The optical switching fabric has to scale up with the number of RAUs leading to an increasing system cost. Furthermore, the use of a laser in RAUs requires a signaling channel between CO and RAUs to activate and deactivate RAUs with strict timing to avoid interference.

In this section, a new architecture is proposed that employs tunable lasers, fixed optical add/drop multiplexers (OADM), and remotely-fed RAUs. A tunable laser tunes the wavelength to address a particular RAU in order to avoid using an optical switch. Two relatively-slow tunable lasers are used in an alternating scheme instead of using an expensive fast tunable laser. Fixed OADMs coded by their add/drop lambda index add/drop the pre-assigned wavelengths to RAUs. For the uplink, the RAU uses an external modulator to modulate remotely-fed continuous wave signals to avoid using any laser source in the RAU.

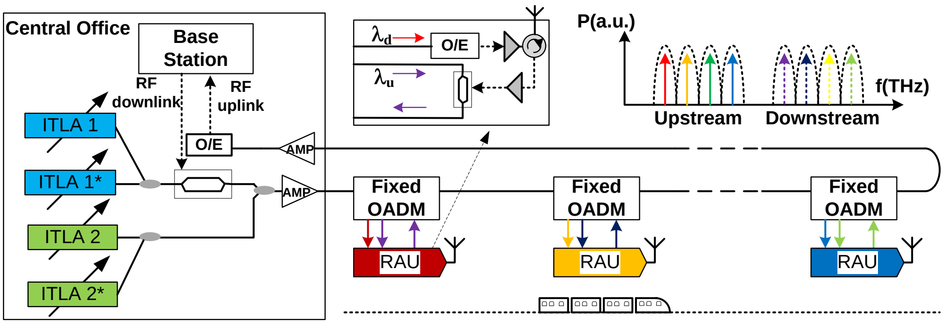

Fig. 5.8. Reconfigurable optical network architecture for moving cells by employing integrable tunable laser assemblies and fixed optical add/drop multiplexers, and remotely-fed RAUs.

5.3.2. Moving Cell Architecture Employed ITLA

The schematic representation of the proposed architecture, called alternate wavelength steering architecture (AWSA), is depicted in Fig. 5.8. There are two pairs of integrable tunable laser assemblies (ITLAs) which are specified by multisource agreement (MSA) within optical internetworking forum (OIF) [148]. The ITLA is selected because it is a standardized device for WDM networks that has the advantage of market volume, thus lower cost. The first pair (*ITLA1* and *ITLA1**) is employed for downstream transmission. When an ITLA is tuned to an RAU that cover the passing train, the other ITLA is disabled and pre-tuned to the next RAU wavelength. When the train enters the coverage area of the next RAU, the pre-tuned ITLA is enabled and the active ITLA is disabled and prepared for the next cycle. By this scheme, we can control switching time from one RAU to the next by overlapping the switch-on time of the pre-tuned ITLA and switch-off time of the active ITLA.

The wavelength from the downstream ITLA pair is modulated by RF downlink signals using an intensity modulator. The modulated wavelength is then combined with a CW wavelength generated by the second pair of ITLA (*ITLA2*, *ITLA2**) for remote modulation at the RAU. The second pair of ITLA operates also in the alternating scheme similar to the first pair. The modulated and CW wavelength are launched into the optical distribution network (ODN) and dropped by the targeted OADM. The CW wavelength is modulated by the uplink RF signal by an intensity modulator and added back onto the ODN.

There are two options for the upstream wavelength returning to the CO. In the reflection choice, the upstream wavelength can reflect back to the same path by which it has reached the RAU. However, the signal is exposed to reflections from the CW transmission e.g., Rayleigh

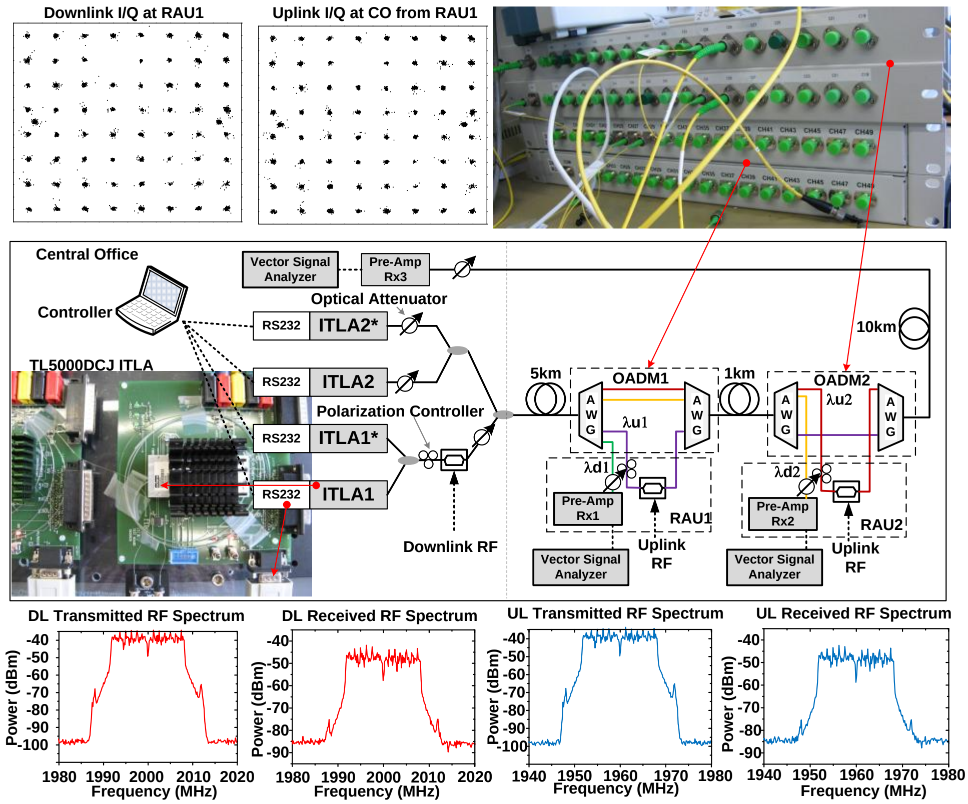

Fig. 5.9. Experimental setup with two OADMs associated with two RAUs and four pc-controlled ITLAs at the central office.

backscattering in the fiber, and reflections in OADMs. Furthermore, the wavelength from different RAUs travels through different path lengths and number of OADMs leading to a fluctuation in received optical power. Therefore, the move-forward option is adopted in which the upstream wavelength continues transmitting through the rest of OADMs and returns to the CO via another fiber path after the last OADM. This method avoids the reflection from CW transmissions and also the fluctuation of received power of the upstream wavelength. From the point where the CW is launched to the ODN and the point where the upstream wavelength is received at the CO, the upstream wavelength of any RAU experiences similar loss (gain if amplifiers are used in the field) to the other since they travel through the same path length and all OADMs.

One of the advantages of having remotely-fed RAUs is that the RAU can be activated and deactivated by controlling the lasers in the CO without any further action in the RAU. If the RAU uses a local laser for upstream transmission, the CO has to signal the RAU to switch the laser off on time in order to avoid interference. The train tracking algorithm is used to activate the right RAU at the right time by controlling only the ITLA array at the CO. If the base station allows multiple-input-multiple-output (MIMO) operation, two or more consecutive RAUs can be activated simultaneously as named moving chain cells in [147]. To realize such schemes, we need to install more ITLAs at the CO with the number determined by the number of simultaneously active RAUs.

5.3.3. Proof of Concept Experiment

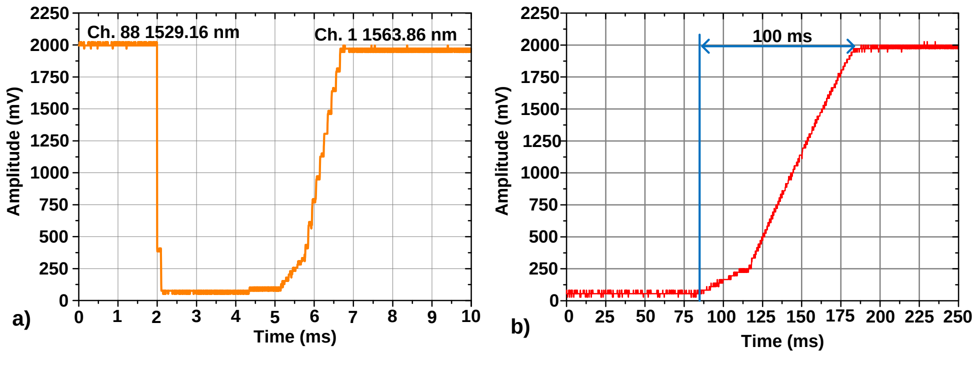

Fig. 5.10. a) Oclaro TL5000DCJ ITLA wavelength switching time, b) Laser enabling time.

The proof of concept experiment setup for AWSA is shown in Fig. 5.9 in which an array of ITLAs is controlled from a computer. The downstream wavelength is modulated by the downlink OFDM (orthogonal frequency division multiplexing) signal centered at 2 GHz using a 10-GHz LiNbO3 intensity modulator. The OFDM signal has 53 subcarriers in which the subcarrier indices -26 and 26 are two pilot carriers using BPSK (binary phase shift keying) and the other subcarriers except zero carry a 54 Mbps pseudo random bit sequence of 2^{-23}-1

(PRBS-23) using 64-QAM. The choice of 54 Mbps is due to the capability of the vector signal generator (R&S SMU-200A). Basically, the architecture is transparent to any signal format and bit rate. The downstream and the upstream CW wavelength reach the first OADM after traveling through 5-km standard SMF fiber. The OADM, constructed by two C-band 16-channel 200-GHz-spaced array waveguide gratings (AWGs), drop λd_1 (1562.23 nm) and λu_1 (1549.32 nm). The CW λu_1 is modulated by the uplink OFDM signal in the same format as the downlink, centered at 1.96 GHz using another 10-GHz intensity modulator. After modulation, λu_1 is added back to the ODN and travels through the second OADM to return to the CO. If the *RAU2* is activated, λd_2 (1560.61 nm) and λu_2 (1547.72 nm) pass through the first OADM to be dropped by the second OADM. The λu_2 is modulated by the uplink signal and is added back into the ODN to return to the CO.

The experiment employs Oclaro TL5000DCJ ITLA, which can cover 88 wavelengths from 1529.16 nm (channel 88) to 1563.86 nm (channel 1) in the 50-GHz grid. The ITLA wavelength switching characteristic is shown in Fig. 5.10.a) where the laser is tuned from channel 88 to channel 1 in three phases. The laser completely switches off in 92 ns in the first phase and then it enters a dark tuning period of 2.944 ms in the second phase. In the last phase, the laser switches on to the new wavelength in 1.516 ms. The switching time is tested over a large number of combinations of source and destination wavelengths in which a negligible variation in switching time is observed.

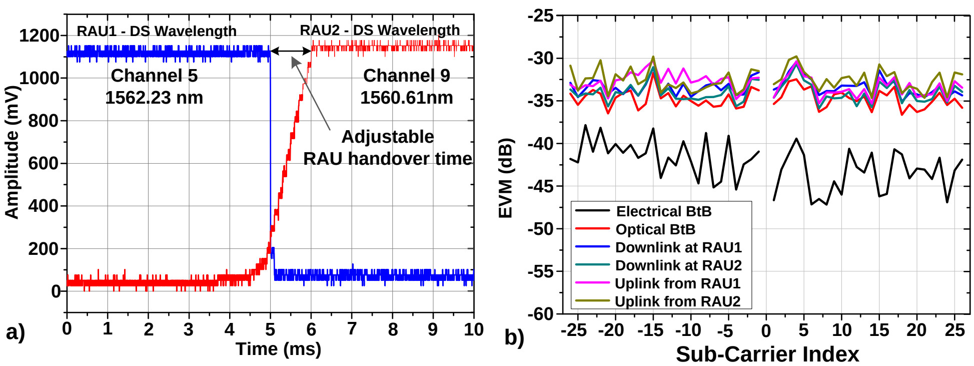

Fig. 5.11. a) Ajustable RAU handover time by overlaping ITLA wavelength switching time, b) Average EVM vs. subcarrier index in various mesurement cases.

As described in the previous section, one laser in a pair of ITLAs is disabled, pre-tuned to the next RAU, and enabled when the RF signal is handed to that RAU. However, the TL5000DCJ laser enabling time is 100 ms as shown in Fig. 5.10.b) which is much longer than the wavelength switching time as the tuning has to be executed more slowly in order to comply with the ramped power versus frequency mask specification. Therefore, I adopted a solution in which the laser is virtually disabled by tuning to an unused wavelength to exploit the short laser switch-on phase of 1.516 ms. In that state, the output of the laser cannot be detected in any RAU.

The time trace of downstream wavelengths at RAU1 and RAU2 during the handover period is shown in Fig. 5.11.a). In time t_0, ITLA1 is programmed to switch from channel 5 (λd_1) to channel 88 (the virtually disabled wavelength) to disable *RAU1*. In time t_S (3.5 ms before t_0), the ITLA1* was programmed to switch from channel 88 to channel 9 (λd_2). In this case, the RAU handover time of 1ms is achieved. The handover time can be adjusted by the offset between t_S and t_0 to yield the desired value.

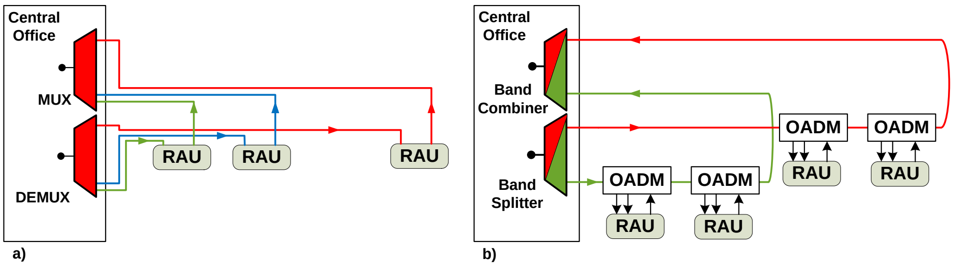

Fig. 5.12. a) Complete parallelized configuration to avoid cascaded OADM, b) Hybrid configuration to compromise between the insertion loss and the fiber count.

To evaluate the impairment introduced by the optical path to RF signals, the EVM of each subcarrier excluding the handover period is measured and shown in Fig. 5.11.b). The electrical back-to-back case has the lowest EVM while the results from the optical cases are close in performance. Among the optical cases, the lowest curve is the optical back-to-back which shows 7.8 dB average penalty in comparison to the electrical back-to-back. Since the other optical cases are very close to the optical back-to-back, we conclude that the optical modulation and detection of RF signals are the dominant impairment source not the transmission through the system. In all transmission cases, the average EVM performance of all carriers is around -34 dB (2 %) providing adequate margin for air transmission within the standards.

To scale up the system with a number of OADMs, the dominant constraint is the optical budget since each OADM introduces a certain insertion loss to the express channels. For instance, the OADM in the experiment introduces 3.5 dB insertion loss. A careful design of dual OADM can reduce the insertion loss to 1.4 dB as shown in [149] which is still substantial when cascaded. To increase the optical budget, we can use optical amplifiers in the field or parallelize the system. An AWG can be used at the CO instead of cascading OADMs to route wavelengths to RAUs as shown in Fig. 5.12.a). However, much more fibers should be deployed in the field, which may not desirable. A band splitter at the CO and OADMs in the field may be a compromised solution between parallel and serial as depicted in Fig. 5.12.b). The band splitter splits the optical spectrum to several sub-bands and each sub-band is conducted by one fiber to a series of OADMs, which is a subset of all OADMs in the system. Optical channel crosstalk by cascading OADMs is another constraint but not dominant since only the wavelengths which address the same RAU, are present at one time. These wavelengths can be selected to have a large spectral spacing to further mitigate crosstalk.

The length of trains, train speeds, Doppler effect, multiple trains, and opposing trains should be taken into account in the system design in a practical implementation. The length of trains and trains speeds determine the spacing between RAUs, the distance between the RAU to the railway, and the employed wireless technology, e.g. WiMax allows up to 250 km/h without significant performance degradation [150] . The Doppler effect is mainly addressed by the wireless technology but can be mitigated by the position of RAU. The longer perpendicular distance between the RAU and the railway, the smoother Doppler frequency shift is experienced. Multiple and opposing trains can be served by multiple systems or the one system by different radio frequencies and additional ITLAs at the OLT. The max reach of moving cell system is largely determined by the maximum tolerable delay of the employed wireless technologies, e.g., 50 km for WiMax.

5.3.4. Conclusions

In this section, a new architecture for moving cell applications is described. The RAU can be activated and deactivated by controlling the optical sources at the CO without any further operations at the RAU. A pair of standardized and mass-produced tunable lasers was employed not only because of cost but also to yield controllable RAU handover time. The proposed system was demonstrated by transmitting downlink and uplink OFDM signal with 53 subcarriers carrying 54Mb/s data. The EVM performance of downlink and uplink signal from both RAUs was -34 dB (~2%, $EVM_{dB} = 20\log_{10}(EVM_{\%}/100)$). The system scalability is also discussed in which power budget was identified as the dominant constraint. To overcome the constraint, the discussion suggested using amplifiers in the field to increase the power budget or parallelize the system to reduce the number of cascaded OADMs, thus the power loss budget requirement.

5.4. Conclusions

This chapter presented two application-specific architectures in which ARON has been designed for dynamic allocation of cell capacities and AWSA has been designed for moving cell applications. The ARON architecture performs wavelength reconfigurability at the RN to allow light-weight ONU/RAUs while cost of the active remote node is shared by the whole population of ONU/RAUs. AWSA, on the other hand, performs wavelength reconfigurability in the central office by leveraging an important characteristic of moving cell application in which RAUs are activated sequentially. Tunable lasers at the central office steer their wavelengths to activate the desired RAU. The address of RAUs is fully encoded by dropped wavelengths, thus no additional wavelength routing and wavelength selection are required.

Both architectures are proof-of-concept demonstrated to study the effect of wavelength reconfigurability and the optical path on the quality of radio signal. Measurements in terms of EVM and wavelength reconfiguration time have been made verify the technical feasibility of proposed architectures in which the EVM penalty and the reconfigurable time are 1% and 450 ns at most, respectively in the ARON experiment and 0.5% and 1ms (adjustable), respectively in the AWSA experiment.

CHAPTER 6

SUMMARY AND OUTLOOK

The modern society is an information society in which businesses stop running and the daily life of individuals completely changes when people get disconnected. Optical access networks have helped more people going online with higher speeds at lower prices. Optical access networks themselves have gone through several evolution phases in which the capacity has been pushed higher and higher by increasing the line rate with the extension of reach and split factor. The latest level has reached 10 Gbps which is the cost turning point meaning that the time dimension is no longer cost-effective for capacity scaling. At this point, wavelength division multiplexing is recognized to be an alternative cost-effective dimension. In fact, the wavelength dimension was added to the legacy TDM-PON in the latest decision of the FSAN consortium for NG-PON2.

In the legacy TDM-PON, all ONUs flexibly share the network aggregate bandwidth by the dynamic timeslot assignment. When the wavelength dimension is added, wavelength reconfigurability is required to allow all ONUs flexibly share the network aggregate bandwidth by the dynamic wavelength and timeslot assignment. Flexibly sharing the network bandwidth is essential to cope with more dynamic traffic patterns and to be in line with the concept of offering services anywhere and anytime.

The history of access networks has proved that cost is the foremost and biggest obstacle for any technology to enter the territory of access networks. Wavelength reconfigurability, however, typically is associated with wavelength tuning at the ONU which is not yet a low cost solution. The wavelength tuning cost is mainly dictated by the cost of tunable transceivers but also by the cost of network-wide wavelength calibration and control. Therefore, the main target of this thesis is to take wavelength reconfigurability over the cost obstacle. A top-down approach was adopted by starting from the architectural design and posing fundamental questions on wavelength reconfigurability.

In the first step in Chapter 2, the natural question was how to reduce the cost of existing architectures. The degree of flexibility is proposed to indicate how flexible a network is. An important conclusion is that networks with a limited flexibility can achieve a large part of the benefits that can be achieved by networks with full flexibility. The limited flexibility can be implemented with a lower cost than the full flexibility by reducing the power loss budget and wavelength tuning range. In the $F=2$ network, meaning that ONUs can move only between two pre-planned wavelengths, wavelength tuning can be avoided by employing two low-cost non-tunable transceivers. Other limitedly-flexible networks, e.g., $F=4$ can be implemented possibly without wavelength tuning but the use of a higher number of fixed transceivers may dismiss the cost advantage over wavelength tuning.

The use of dual fixed transceivers allows to remove the cumbersome wavelength tuning leading to the next question: Could we design an $F=2$ architecture employing dual transceivers but retaining the capability of network-wide bandwidth distribution? Chapter 3 answered the question by proposing the concept of cyclically-linked flexibility. The ONU population is partitioned into groups, each is served by two wavelength channels. Adjacent groups have a wavelength channel in common to create a linked structure of ONU groups and the last group is linked to the first group to form a cyclic configuration. By the cyclically-linked structure, a free bandwidth block can be moved around wavelength channels by rearranging occupied bandwidth blocks. Therefore, the main difference between the cyclically-linked flexibility and the full flexibility is that the free block is moved to meet the requesting ONU instead of moving the requesting ONU to meet the free block.

Moving the free block, certainly, could be impossible and may involve many other in-service ONUs reallocations. Therefore, performance of the cyclically-linked flexibility is mainly dependent on the employed bandwidth rearrangement algorithm. In the traffic scenarios, where connection sizes are small, connection blocking probabilities of the cyclically-linked flexibility and the full flexibility are almost the same. The differences in blocking probabilities are noticeable in the traffic scenarios with large connection sizes. When the connection sizes are in the range of 100 and 900 Mbps, the cyclic-linked flexibility can accommodate 5.5% less offered load in comparison to the full flexibility at the level of 1% blocking.

Nevertheless, the proposed swap-based algorithm shows a promising performance in which the rearrangement efficiency η_{re}, indicating the chance for a rearrangement to be successful, is higher than 72% and can be 100% in moderate load levels. The impact to other ONUs is minimal when a rearrangement operation involves between 2 to 4 reallocations of ONUs in average. The other approach for the rearrangement algorithm, the fit-based algorithm, even achieves higher rearrangement efficiency but at the expense of higher impact to in-service ONUs. Fortunately, the dual transceiver allows the make-before-break wavelength handover to avoid service interruption during reallocations. Therefore, the impacted ONUs experience no degradation on quality of service.

The promising advantages of the cyclically-linked flexibility bring the next question: How to implement the cyclically-linked flexibility by a physical architecture? Chapter 4 answered the question by proposing a family of physical architectures in which each member was designed for a certain scenario. PRO-Access realizes the cyclically-linked flexibility by a passive RN, a carefully-designed wavelength plan, and dual remotely-seeded transceivers. The outside plant is passive with only 3-dB extra power budget in comparison to the static WDM-TDM PON and the ONU is wavelength-agnostic. The architecture is proof-of-concept demonstrated with symmetric 10 Gbps down/up transmission. This architecture is applicable for new deployments or disruptive upgrades with a maximum of 20-km reach since the RN configuration is not compliant to current power-splitter-based RNs and the remote-seeded ONU method is not suitable for long-reach.

To address long-reach scenarios, WCL-Access was proposed in which wavelength converters are used in the RN and a dual low-cost transceiver, which is similar to current PON transceivers, is employed in the ONU. The wavelength-converted RN located in the distributed central office allows reusing current deployments of both access and metro sections. The increased RN cost was proved to be well spread out to ONUs in order to have a comparable or lower cost per user in comparison to the amplifier-based Broadcast-and-Select long-reach PON. The WCL-Access architecture is more cost-effective when there are more than 16 ONUs per branch in the average estimation and 56 ONUs per branch in the high estimation.

NG-PON2 is expected to have the first deployment before 2015 which still uses the power-splitter-based outside plant to stack four TDM-PONs with wavelength reconfigurability as an option. To address this short time frame, PSB-Access or the cyclically-linked NG-PON2 was proposed in which the outside plant is compliant with current power-splitter-based deployments. The cyclically-linked structure is realized by the pluggable passive wavelength selector at the ONU. Although there is no difference in terms of power loss budget compared to the fully flexible Broadcast-and-Select using tunable transceivers, the cyclically-linked NG-PON2 can perform wavelength reconfigurability without wavelength tuning. Blocking probability performance between the cyclically-linked NG-PON2 and the wavelength-tuned NG-PON2 is almost the same in various traffic scenarios. The rearrangement efficiency η_{re} is 100% for most cases because the probability for a rearrangement attempt to be unsuccessful is smaller when the number of wavelength channels is reduced. In the case of four wavelength channels, the performances of cyclically-linked flexibility and of the full flexibility show no significant difference.

The fourth architecture exploits the concept of cyclically-linked flexibility beyond the main purpose of wavelength reconfigurability. The cyclically-linked protection can be regarded as a modified type C protection by engaging multiple standardized PONs to protect each other. The impact of a feeder fiber cut in busy hours is demonstrated to be completely absorbed by joining 16 PONs. The extra burden is smoothly spread out to other PONs by a bandwidth rearrangement operation thanks to the cyclically-linked structure. The cyclically-linked protection has the same physical parts as the type C protection but no standby capacity is needed since a large pool of active capacity is formed in order to protect its members. Therefore, the cyclically-linked protection is a novel and cost-effective method for ultra-resilient access networks.

Wavelength reconfigurability was considered in the context of transporting digital streams before Chapter 5. Therefore, the proposed architectures described in Chapter 4 can be used for mobile backhaul or fronthaul with digitized RF signals, e.g., CPRI transport. In some specific scenarios, a native support of RF signals with wavelength reconfigurability is desirable. Chapter 5 addresses this issue by proposing two application-specific reconfigurable architectures. The ARON architecture was designed for the dynamic cell capacity assignment in densely-populated areas by a wavelength-routed RN based on the SOA-array. The small capacity reallocation time is achieved thanks to the fast switching of SOA gates. A complete downlink and uplink experiment was carried out to demonstrate that the reallocation time is as small as 450 ns and there is a negligible impact to the existing channel.

The second architecture aims to provide a high-speed and reliable Internet connection for train passengers by the concept of moving cells. The AWSA architecture uses the method of wavelength steering in which the tunable laser at the central office tunes its wavelength to follow the train. The architecture avoids the use of a fast tunable laser by using two slow and mass-produced tunable lasers working in an alternating mode. The remote antenna unit can be activated and deactivated simply by controlling lasers at the central office. The handover time between two antenna units is adjustable by setting appropriate timings for the laser pair. A proof of concept experiment was conducted with two remote antenna units and bidirectional transmission of 54 Mbps OFDM signals at 2 GHz band. The EVM degradation contributed by the optical path is proved to be small i.e., at most 2%. Practical considerations such as train speeds and Doppler effect were discussed in which train speeds and Doppler effect mitigation are mainly determined by the employed wireless technology, e.g., 250 km/h for WiMAX but also by the position of RAU towers.

The power saving achieved by turning off unused capacity in off-peak hours can be conducted by all proposed architectures. The concrete saving figures were provided in Chapter 2 for *F=2* limited flexibility is applicable for the PRO-Access, the WCL-Access, the PBS-Access, and the cyclically-linked protection architecture. The ARON and the AWSA architecture also can save power in a similar fashion by reducing the number of active subcarriers in light traffic conditions.

The NG-PON2 standard is expected to specify ONU wavelength handover signaling procedures (OLT-ONU interface) and general limiting parameters such as handover time to ensure interoperability. The standard will not specify any particular physical implementation and wavelength and timeslot assignment algorithm. It is similar to what has been done on dynamic bandwidth assignment (DBA) in current TDM-PON standards. Signaling procedures for DBA and convergence times have been specified but the implementation in the circuit level and the DBA algorithm are left for the industry. Therefore, the cyclically-linked NG-PON2 can be considered as a particular implementation for wavelength reconfigurable NG-PON2 which already emerges at the horizon.

Looking beyond NG-PON2, wavelengths naturally are still the most cost-effective dimension for capacity scaling since 4 wavelengths is a small number in the-state-of-the-art WDM technology. The evolution of line rate in access networks will be repeated with the wavelength count. At this time, PRO-Access and WCL-Access come to the stage since they are scalable in terms of wavelength count and user count. PRO-Access needs more work on the integration of the dual remotely-fed transceiver while WCL-Access needs more work on the integration of wavelength converters. Nevertheless, all proposed architectures including RoF architectures require industrial support to reach and go beyond the prototype stage in order to continue the battle with competing technologies. In the prototype stage, more work should be carried out to analyze the reconfiguration impact for various kinds of services, especially real-time ones.

The cyclically-linked protection has a slightly different position since it is applicable directly in current TDM PON standards. It also can be applied to WDM-TDM PONs, e.g., NG-PON2. The implementation of cyclically-linked protection heavily involves the network planning stage because fiber routes need to be planned in order to form the cyclically-linked structure. The cyclically-linked protection can be used without any change in current standards since it is the same as standardized type C protection from the ONU's perspective and the cooperative operation of line cards is not in the scope of PON standards.

In the future, TDM could be replaced by another per-wavelength sharing technique such as OFDM to further increase the spectral efficiency. The cyclically-linked flexibility and its architectures are still applicable since bandwidth blocks in the bandwidth map, in principle, can be realized by any per-wavelength multiplexing technique. In the physical layer, bandwidth blocks can be timeslots in TDM, subcarriers in OFDM, or others. Bandwidth granularity in OFDM by subcarriers may be larger than in TDM by timeslots resulting larger a bandwidth unit block in the bandwidth map. The DBA algorithm and its sub-algorithms should be adapted to allow smooth reallocations of subcarriers among ONUs.

Overall, the work reported in this thesis successfully solves the cost-prohibitive problem of wavelength reconfigurability. Instead of following conventional approaches, it explores a new direction to implement wavelength reconfigurability by which it brings the idea of a flexible WDM-TDM access optical network closer to reality.

APPENDIX A – OPNET SIMULATION

A.1. OPNET Discrete Event Simulation

The OPNET modeler is a widely-used and commercial network simulator which is aimed for analyzing and designing communication networks, devices, protocols, and applications. It is used by many network operators, system integrators, and academia including British Telecom, NEC, and Intel. The modeler is based on discrete-event simulation in which the operation of the simulated system is represented as a chronological sequence of events. Each event occurs at an instant in time and impacts on the state of the system. In OPNET, a frequent event is the

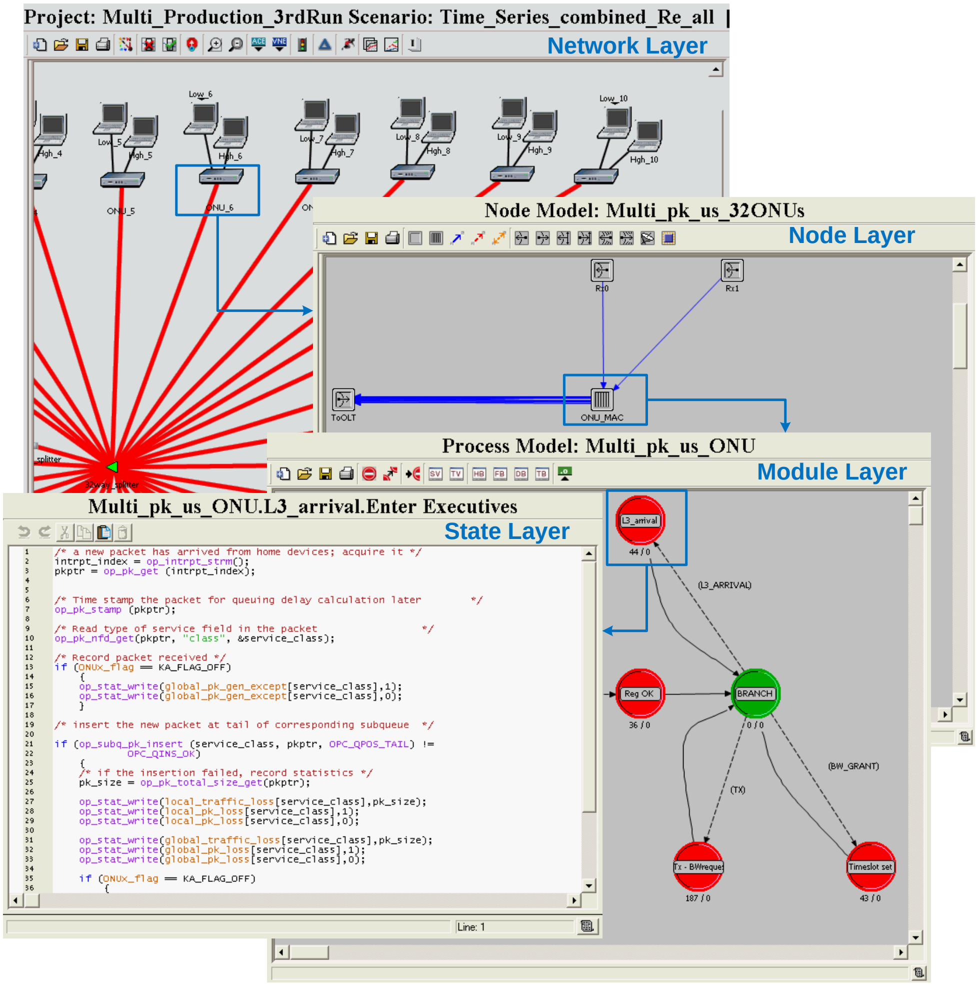

Fig. A.1. OPNET Modeler hierarchical structure, the lowest layer is implemented by C/C++ codes to define to detail behaviors of the device.

packet arrival to a module which will handle the packet in a defined way. For example, the packet can be examined to get the sender address and subsequently placed in a queue. Therefore, OPNET can simulate the behavior of any network device or any network of connected devices in detail.

To facilitate the model development, the discrete-event simulator is organized in a hierarchical structure including the network layer, the node layer, the module layer, and the state layer as shown in Fig. A.1. The network layer is an intuitive representation of network topology which is composed of nodes and links. A node is then defined in the node layer as the composition of modules and connections. The module is defined by a finite-state machine which is composed by states and conditional transitions. At an instant of time, the current state of the module stays in one and only one state in the finite-state machine. When an event occurs at the module, e.g. a packet arrival, the exit executive of the current state is executed. The exit executive is defined in the state layer by C/C++ programming. After the exit executive is completed, the module transits to the next state with the matching transition condition. Upon arriving the next state, the enter executive of the next state is executed. After this executive is completed, the module current state is changed to the next state and the module waits for the next event to occur.

The OPNET modeler is provided with a large library of nodes and protocols based on current standards. New nodes and protocols can also developed if they are not based on current standards by defining the node structure, the finite-state machine of each module in the node structure, and the executives of each finite-state machine. The OPNET modeler license is free for educational institutions with renewal every 6 months.

A.2. Reconfigurable WDM-TDM Optical Access Network Model

The model for reconfigurable WDM-TDM optical access network is built without using the existing nodes in the OPNET model library. For this thesis, the node models were developed including the OLT, the 32-way power splitter/combiner, the ONU, and the bursty packet source. The DBA node and configuration settings node were also developed for upgradability and to avoid cumbersome manual parameter settings, respectively. The data plane and control plane of the model will be described in this Section.

In the data plane, each ONU is connected by a bursty packet generator as shown in Fig. A.2. Each packet is generated with a header and a payload. The header includes AllocID, ONUID, and the destination address (the OLT address) and the payload is a dummy Ethernet packet with the size uniformly distributed between 64 to 1518 bytes. The packet is forwarded to the ONU to be placed in a queue. The MAC module forms the upstream burst frame by taking packets in the head of the queue. The size of the burst and sending time is instructed by the OLT though the control plane. The burst structure is based on XG-PON framing in the ITU-T G.987.3 recommendation. The upstream burst is forwarded to the assigned wavelength in the WDM link. The upstream burst travels through the two 32-way combiners. The combiner is able to generate an alarm signal if there is any collision among upstream bursts (overlap on the time domain in the same wavelength). This feature can ensure the correct operation for the system, especially for DBA development. When the burst reaches the OLT, it is de-capsulated to get individual packets. Each packet is examined for statistics and discarded later on. In each step in the packet flow, statistics can be collected such as queuing delay and packet size.

To support the collision-free operation in the data plane, the control plane is established. The ONU registers and performs pre-simulation configurations with the OLT through this plane. During the course of operation, the two important transactions between the ONU and the OLT are the connection establishment and the bandwidth assignment as shown in Fig. A.3. When the ONU wants to send packets for a certain AllocID, it first sends a connection establishment request to the OLT with the AllocID and the connection size. The OLT processes the request to accept or reject and responds to the ONU. To forward packets, the ONU sends a bandwidth request every scheduling round of 125 μs. The ONU will receive a

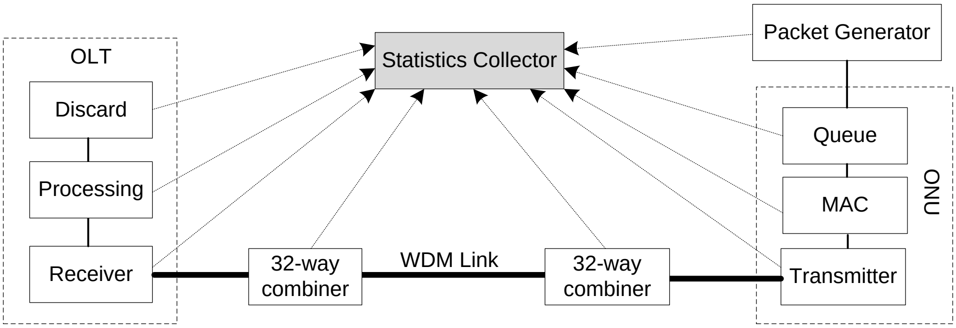

Fig. A.2. Packet life cycle in the reconfigurable WDM-TDM optical access model

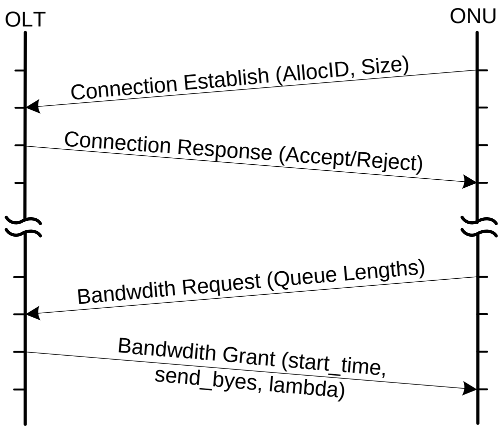

Fig. A.3. Signaling messages between the OLT and the ONU for connection establishment and packet forwarding bandwidth grant after three rounds which includes start time, granted bytes, and granted wavelength. Three-round time is accounted for transmission delays between the ONU and the OLT and the processing time of the DBA at the OLT.

ABBREVIATIONS

ADSL	Asymmetric Digital Subscriber Line
APD	Avalanche Photodiode
API	Application Programming Interfaces
APON	Asynchronous transfer mode Passive Optical Network
ARON	Active Routing Optical access Network
ASE	Amplified Spontaneous Emission
AWG	Arrayed Waveguide Grating
AWSA	Alternate Wavelength Steering Architecture
BLS	Broadband Light Source
BPL	Broadband Powerline
BPON	Broadband Passive Optical Network
BPSK	Binary Phase Shift Keying
BtB	Back-to-Back
CAPEX	Capital Expenditure
CLBP	Cyclically-Linked Bandwidth Pool
CO	Central Office
CPE	Consumer Premise Equipment
CPRI	Common Public Radio Interface
CW	Continuous Wave
CWDM	Coarse Wavelength Division Multiplexing
DAS	Distributed Antenna System
DBA	Dynamic Bandwidth Allocation
DDAS	Dynamic Distributed Antenna System
DEMUX	Demultiplexer
DOCSIS	Data Over Cable Service Interface Specification
DS	Downstream
DSL	Digital Subscriber Line
DWDM	Dense Wavelength Division Multiplexing
EDFA	Erbium-Doped Fiber Amplifier
EFM	Ethernet in the First Mile study group
EMI	Electromagnetic Interference
EPON	Ethernet Passive Optical Network
FBG	Fiber Bragg Grating
FEC	Forward Error Correction
FSAN	Full Service Access Network consortium
FSR	Free Spectral Range
FTTB	Fiber to the Building/Basement
FTTC	Fiber to the Curb/Cabinet
FTTH	Fiber to the Home
FTTN	Fiber to the Node
FTTP	Fiber to the Premises
FWX	Four Wave Mixing
GEM	GPON Encapsulation Method
GPON	Gigabit-capable Passive Optical Network

HD	High Definition
HFC	Hybrid Fiber Coax
IM/DD	Intensity Modulation / Direct Detection
ISP	Internet Service Provider
ITLA	Integrable Tunable Laser Assembly
LCoS	Liquid Chrystal on Silicon
LTE	Long-Term Evolution
MIMO	Multiple Input Multiple Output
MUX	Multiplexer
NG-PON	Next Generation Passive Optical Network
NRZ	Non-Return to Zero
OADM	Optical Add/Drop Multiplexer
OBSAI	Open Base Station Architecture Initiative
ODN	Optical Distribution Network
OFDM	Orthogonal Frequency Division Multiplexing
OLT	Optical Line Terminal
ONT	Optical Network Terminal
ONU	Optical Network Unit
OPEX	Operational Expenditure
P2P	Peer-to-Peer
PON	Passive Optical Network
PRBS	Pseudorandom Bit Sequence
PRO-Access	Passive –components-based Reconfigurable Optical Access network
PSB-Access	Passive-Splitter-Based Reconfigurable Optical Access network
PSTN	Public Switch Telephone Network
QAM	Quadrature Amplitude Modulation
RAU	Remote Antenna Unit
REAM	Reflective Electro-Absorption Modulator
RF	Radio Frequency
RN	Remote Node
RSOA	Reflective Semiconductor Optical Amplifier
SLA	Service Level Agreement
SMF	Single Mode Fiber
SOA	Semiconductor Optical Amplifier
SONET/SDH	Synchronous Optical Network/Synchronous Digital Hierarchy
TDM	Time Division Multiplexing
TDMA	Time Division Multiple Access
TFF	Thin Film Filter
US	Upstream
VDSL2	Very high Digital Subscriber Line 2
VOA	Variable Optical Attenuator
WCL-Access	Wavelength-Converted Long-reach Reconfigurable Optical Access network
WSS	Wavelength Selective Switch
XGM	Cross Gain Modulation
XG-PON	10Gbps Passive Optical Network
XPM	Cross Phase Modulation

REFERENCES

[1] "Cisco Visual Networking Index: Forecast and Methodology, 2010–2015," Cisco White Paper, Jun. 2011.

[2] "Cloud computing," *Wikipedia - The Free Encyclopedia*, Aug-2012. [Online]. Available: http://en.wikipedia.org.

[3] "Internet Traffic," *Wikipedia - The Free Encyclopedia*, Aug-2012. [Online]. Available: http://en.wikipedia.org.

[4] "Cisco Visual Networking Index: Usage Study," Cisco White Paper, Oct. 2010.

[5] "Cisco Visual Networking Index: Global Mobile Data Traffic Forecast Update, 2011–2016," Cisco White Paper, Feb. 2012.

[6] U. Paul, A.P. Subramanian, M.M. Buddhikot, and S.R. Das, "Understanding Traffic Dynamics in Cellular Data Networks," in *Proc. of Int. Conf. on Computer Commun. (INFOCOM 2011)*, 2011, pp. 882–890.

[7] Federal Communication Commission (FCC), "What is Broadband?," Feb-2010. [Online]. Available: http://www.broadband.gov/about_broadband.html/. [Accessed: 26-Aug-2012].

[8] "Very high speed digital subscriber line transceivers 2 (VDSL2)." ITU-T Recommendation G.993.2, Dec-2011.

[9] "Broadband Performance." The Federal Communications Commision (http://broadband.gov/), Feb-2010.

[10] "DSL Technology Evolution." The Broadband Forum (http://www.broadband-forum.org), Jan-2009.

[11] G. Andreas, L. Christoph, and L. Ralph Leppla, "Power efficiency of optical versus electronic access networks," in *Proc. of European Conf. and Exhibit. on Opt. Commun. (ECOC2008)*, Brussels, 2008, p. Tu.4.A.2.

[12] S. Bhaumik, D. Chuck, G. Narlikar, and G. Wilfong, "Energy-efficient design and optimization of wireline access networks," in *Proc. of Int. Conf. on Computer Commun. (INFOCOM 2011)*, 2011, pp. 451–455.

[13] "CURRENT Group Says Goodbye to BPL Industry," *Smart Grid News*, Feb-2008. [Online]. Available: http://www.smartgridnews.com.

[14] "Can 4G challenge FTTH as a business alternative?," FTTH council Europe / Durrants Gorkana group, Jun. 2012.

[15] M. Kawahata, "The Hi-OVIS Optical Communication System," in *Proc. of 9th European Microwave Conf.*, 1979, pp. 83–88.

[16] K. Chang, and E. Hara, "Fiber-Optic Broad-Band Integrated Distribution-Elie and Beyond," *IEEE J. on Sel. Areas on Commun.*, vol. 1, no. 3, pp. 439–44, Apr. 1983.

[17] J. Fox, D. Fordham, R. Wood, and D. Ahern, “Initial Experience with the Milton Keynes Optical Fiber Cable TV Trial,” *IEEE Trans. on Commun.*, vol. 30, no. 9, pp. 2155–2162, Sep. 1982.

[18] J. Kanzow, “BIGFON: Preparation for the Use of Optical Fiber Technology in the Local Network of the Deutsche Bundespost,” *IEEE J. on Sel. Areas on Commun.*, vol. 1, no. 3, pp. 436–439, Apr. 1983.

[19] C. Veyres, and J.J. Mauro, “Fiber to the home: Biarritz (1984) . . . Twelve cities (1988),” in *Proc. of IEEE Int. Conf. on Commun. (ICC’88)*, 1988, vol. 2, pp. 874–878.

[20] Paul W. Shumate, “Fiber-to-the-Home: 1977–2007,” *J. Lightw. Technol.*, vol. 26, no. 9, pp. 1093–1103, 2008.

[21] “Media Access Control Parameters, Physical Layers, and Management Parameters for Subscriber Access Networks.” IEEE Standard 802.3ah, Sep-2004.

[22] Ton Koonen, “Fiber to the Home/Fiber to the Premises: What, Where, and When?,” *Proceedings of the IEEE*, vol. vol. 94, no. 5, pp. 911 – 934, May 2006.

[23] A. Luvison, “The architecture of full services access network,” in *Proc. of Opt. Fiber Commun. Conf. (OFC’98)*, 1998, pp. 130–131.

[24] “Gigabit-capable passive optical networks (GPON): General characteristics.” ITU-T Recommendation G.984.1, Mar-2008.

[25] “Gigabit-capable Passive Optical Networks (GPON): Transmission convergence layer specification.” ITU-T Recommendation G.984.3, Mar-2008.

[26] “10-Gigabit-capable passive optical networks (XG-PON): General requirements.” ITU-T Recommendation G.987.1, Jan-2010.

[27] “Physical Layer Specifications and Management Parameters for 10 Gb/s Passive Optical Networks.” IEEE Standard 802.3av, Otc-2009.

[28] “North American FTTH Status - March 31, 2011.” FTTH Council Americas, Mar-2011.

[29] M. Abrams, Y. Fujimoto, V. O’Byrne, and D. Piehler, “FTTP deployments in the United States and Japan-equipment choices and service provider imperatives,” *J. Lightw. Technol.*, vol. 23, no. 1, pp. 236 – 246, Jan. 2005.

[30] F. Escher, H. Foisel, A. Templin, B. Nagel, and M. Adamy, “Enabling Broadband Communication, Deutsche Telekom FTTH Deployment,” in *Proc. of Opt. Fiber Commun.Conf. and Expo. and the National Fiber Opt. Engineers Conf. (OFC/NFOEC 2012)*, 2012, p. NTh3E.2.

[31] Fabrice Bourgart, “Preparing the future of optical access at FT,” in *Proc. of Opt. Fiber Commun.Conf. and Expo. and the National Fiber Opt. Engineers Conf. (OFC/NFOEC 2009)*, 2009.

[32] Chang-Hee Lee et al., “WDM-PON experiences in Korea [Invited],” *J. of Opt. Netw.*, vol. 6, no. 5, pp. 451–464, 2007.

[33] J. Park, G. Y. Kim, H. J. Park, and J. H. Kim, "FTTH Deployment Status & Strategy in Korea: GW-PON Based FTTH Field Trial and Reach Extension Strategy of FTTH in Korea," in *Proc. of Global Telecom. Conf. (GLOBECOM 2008)*, 2008, pp. 1 – 3.

[34] Martin Maier, "WDM Passive Optical Networks and Beyond: the Road Ahead [Invited]," *J. Opt. Commun. Netw.*, vol. 1, no. 4, pp. C1 – C16, 2009.

[35] B. Tromborg, H. Olesen, P. Xing, and S. Saito, "Transmission line description of optical feedback and injection locking for Fabry-Perot and DFB lasers," *IEEE J. of Quantum Electronics*, vol. 2, no. 11, pp. 1875–1889, Nov. 1987.

[36] S.-J. Park, C.H. Lee, K.T. Jeong, H.J. Park, J.G. Ahn, and K.H. Song, "Fiber-to-the-home services based on wavelength-division-multiplexing passive optical network," *J. Lightw. Technol.*, vol. 22, no. 11, pp. 2582 – 2591, Nov. 2004.

[37] J. Kani, F. Bourgart, A. Cui, A. Rafel, M. Campbell, Russell Davey, and S. Rodrigues, "Next-Generation PON—Part I: Technology Roadmap and General Requirement," *IEEE Commun. Mag.*, vol. 47, no. 11, pp. 43–49, Nov. 2009.

[38] F. J. Effenberger, H. Mukai, S. Park, and T. Pfeiffer, "Next-Generation PON—Part II: Candidate Systems for Next-Generation PON," *IEEE Commun. Mag.*, vol. 47, no. 11, pp. 50–57, Nov. 2009.

[39] P. Chanclou, A. Cui, F. Geilhardt, H. Nakamura, and D. Nesset, "Network operator requirements for the next generation of optical access networks," *IEEE Network Journal*, vol. 26, no. 2, pp. 8–14, Mar. 2012.

[40] D.P. Shea, and Mitchell, "A 10-Gb/s 1024-Way-Split 100-km Long-Reach Optical-Access Network," *J. Lightw. Technol.*, vol. 25, no. 3, pp. 685 – 693.

[41] "Deliverable 2.1 - Requirements for European next-generation optical access networks." Optical Access Seamless Evolution (OASE) European PF7 Project, Sep-2010.

[42] H. Rohde, S. Smolorz, E. Gottwald, and K. Kloppe, "Next generation optical access: 1 Gbit/s for everyone," in *Proc. of 35th European Conf. and Exhibit. on Opt. Commun. (ECOC2009)*, p. 10.5.5.

[43] "Google Fiber Blog." [Online]. Available: http://googlefiberblog.blogspot.nl. [Accessed: 31-Aug-2012].

[44] "Google Fiber." [Online]. Available: http://fiber.google.com/plans/residential/. [Accessed: 31-Aug-2012].

[45] "Common Public Radio Interface Specification V5.0." CPRI Industrial Consortium, Sep-2011.

[46] "BTS System Referecne Document." Open Base Station Architecture Initiative, 2006.

[47] Ed Harstead, "Technologies for NGPON2: Why I think 40G TDM PON (XLG-PON) is the clear winner." NG-PON2 workshop - Opt. Fiber Commun.Conf. and Expo. and the National Fiber Opt. Engineers Conf. (OFC/NFOEC 2012), Mar-2012.

[48] H.-D. Jung, N.-C. Tran, C. Okonkwo, E. Tangdiongga, and T. Koonen, "10Gb/s Bi-Directional Symmetric WDM-PON System Based on POLMUX Technique with

Polarization Insensitive ONU," in *Proc. of Opt. Fiber Commun.Conf. and Expo. and the National Fiber Opt. Engineers Conf. (OFC/NFOEC 2010)*, 2010, p. JThA27.

[49] J. Mora, B. Ortega, J. Capmany, and F. Grassi, "Bidirectional optical access netwok based on PolMUX tecnique using centralized light sources," in *Proc. Int. Topical Meeting on Microwave Photonics (MWP'09)*, 2009, pp. 1–4.

[50] Sang-Yuep Kim, "Single and multi-carrier coherent detection using DSP technologies for future optical access systems," in *Proc. of 9th Int. Conf. on Opt. Internet (COIN2010)*, 2010, pp. 1–3.

[51] C.W. Chow, C.H.Yeh, C.H. Wang, C.L. Wu, S. Chi, and C. Lin, "Studies of OFDM signal for broadband optical access networks," *J. on Sel. Areas in Commun.*, vol. 28, no. 6, pp. 800 – 807, Aug. 2010.

[52] Josep Prat, "OFDMA-PON: A Solution for Next Generation Converged Access Networkin." NG-PON2 workshop - Opt. Fiber Commun.Conf. and Expo. and the National Fiber Opt. Engineers Conf. (OFC/NFOEC 2012), Mar-2012.

[53] X.Q. Jin, J.L. Wei, R.P. Giddings, T. Quinlan, S. Walker, and J.M. Tang, "Experimental Demonstrations and Extensive Comparisons of End-to-End Real-Time Optical OFDM Transceivers With Adaptive Bit and/or Power Loading," *IEEE Photonics Journal*, vol. 3, no. 3, pp. 500 – 511, Jun. 2011.

[54] "Deliverable D2.2 - Techno-economical analysis for the identified capacity upgrade, dynamic capacity allocation, aggregate transport of wired-wireless signals and infrastructure convergence solutions." Architectures for fLexible Photonic Home and Access networks (ALPHA) European PF7 project, Dec-2008.

[55] G. Talli, P.D. Townsend, "Hybrid DWDM-TDM long-reach PON for next-generation optical access," *J. Lightw. Technol.*, vol. 24, no. 7, pp. 2827–2834, 2006.

[56] P. Ossieur, C. Antony, A. Naughton, S. Porto, N. A. Quadir, A. M. Clarke, and P.D. Townsend, "Hybrid DWDM-TDMA PONs for Next Generation Access," in *Proc. of Opt. Fiber Commun.Conf. and Expo. and the National Fiber Opt. Engineers Conf. (OFC/NFOEC 2012)*, 2012, p. OW1B.7.

[57] Domaniç Lavery, Maria Ionescu, Sergejs Makovejs, Enrico Torrengo, and Seb J. Savory, "A long-reach ultra-dense 10 Gbit/s WDM-PON using a digital coherent receiver," *Optics Express*, vol. 18, no. 25, pp. 25855–25860, 2010.

[58] J.D. Reis, D.M. Neves, and A.L. Teixeira, "Density and Guard Band in Migration Scenarios to Coherent Ultra-Dense WDM," in *Proc. of Global Telecom. Conf. (GLOBECOM 2011)*, 2011, pp. 1–5.

[59] "Gigabit-capable passive optical networks (GPON): Long reach." ITU-T Recommendation G.984.7, Jul-2010.

[60] M. Fricke, "Examining the Evolution of the Access Network Topology," in *Proc. of Global Telecom. Conf. (GLOBECOM 2009)*, 2009, pp. 1–3.

[61] D.P. Shea, and J.E. Mitchell, "Long-Reach Optical Access Technologies," *IEEE Network Journal*, vol. 21, no. 5, pp. 5–11, Sep. 2007.

[62] D.P. Shea, and J.E. Mitchell, "Operating Penalties in Single-Fiber Operation 10-Gb/s, 1024-Way Split, 110-km Long-Reach Optical Access Networks," *IEEE Photonics Techno. Letters*, vol. 18, no. 23, Dec. 2006.

[63] R. Glatty, P. Guignard, and P. Chanclou,, "Flexible Optical Access Network with SOA Amplification," in *Proc. Int. Conf. on Commun.*, 2008, pp. 5182 – 5185.

[64] D. Nesset, R. Gorena, M. Potter, and M. Yates, "Economic Study Comparing Raman Extended GPON and Mid-span GPON Reach Extenders," in *Proc. of Opt. Fiber Commun.Conf. and Expo. and the National Fiber Opt. Engineers Conf. (OFC/NFOEC 2010)*, 2010, p. NMC2.

[65] K.-O. Kim, K.-H. Doo, and S.-S. Lee, "Implementation of OEO based reach extender for 60km long reach GPON," in *Proc. of 9th Int. Conf. on Opt. Internet (COIN2010)*, 2010, pp. 1–3.

[66] Peter Vetter, "Directions for Energy Efficient Optical Access," 2nd Annual Workshop on Photonic Technologies for Access and Biophotonics - Standford Univ., Jan-2011.

[67] P. Chanclou et al., "Technical options for NGPON2 beyond 10G PON," in *Proc. of 37th European Conf. and Exhibit. on Opt. Commun. (ECOC2011)*, 2011, p. We.9.C.3.

[68] Shunji Kimura, "An Operator's View," NG-PON2 workshop - Opt. Fiber Commun.Conf. and Expo. and the National Fiber Opt. Engineers Conf. (OFC/NFOEC 2012), Mar-2012.

[69] "A broadband optical access system with enhanced survivability." ITU-T Recommendation G.983.5, Jan-2002.

[70] "Which way forward? Next-generation PON and the future of fiber." Alcatel-Lucent White Paper, 2010.

[71] N. Cvijetic, "OFDM for Next-Generation Optical Access Networks," *J. Lightw. Technol.*, vol. 30, no. 4, pp. 384–398, Feb. 2012.

[72] J. Armstrong, "OFDM for Optical Communication," *J. Lightw. Technol.*, vol. 27, no. 3, pp. 189–204, Feb. 2009.

[73] Michael Eiselt, "Tunable WDM-PON," NG-PON2 workshop - Opt. Fiber Commun.Conf. and Expo. and the National Fiber Opt. Engineers Conf. (OFC/NFOEC 2012), Mar-2012.

[74] Kerry Litvin, "Self-Seeded WDM PON," NG-PON2 workshop - Opt. Fiber Commun.Conf. and Expo. and the National Fiber Opt. Engineers Conf. (OFC/NFOEC 2012), Mar-2012.

[75] Byeong Whi Kim, "DWDM-PON Solutions This Year," NG-PON2 workshop - Opt. Fiber Commun.Conf. and Expo. and the National Fiber Opt. Engineers Conf. (OFC/NFOEC 2012), Mar-2012.

[76] Jun Shan Wey, "UDWDM PON – the Clear Technology Winner for NG-PON2," NG-PON2 workshop - Opt. Fiber Commun.Conf. and Expo. and the National Fiber Opt. Engineers Conf. (OFC/NFOEC 2012), Mar-2012.

[77] Ezra Ip, Alan Pak Tao Lau, Daniel J. F. Barros, and Joseph M. Kahn, "Coherent detection in optical fiber systems," *Optics Express,* vol. 16, no. 2, pp. 753–791, Jan. 2008.

[78] T. Koonen, T., T. Muys, C. van der Plaats, S.M.H. de Groot, H.J.J.N. Kenter, I.G.M.M Niemegeers, and F.N.C. Slothouber, "TOBASCO: an innovative approach for upgrading CATV fiber-coax networks for broadband interactive services," *IEEE Communications Magazine*, vol. 35, no. 4, pp. 76 – 81, 1997.

[79] Y. Luo, X. Zhou, F. Effenberger, X. Yan, G. Peng, Y. Qian, and Y. Ma, "Time and Wavelength Division Multiplexed Passive Optical Network (TWDM-PON) for Next Generation PON Stage 2 (NG-PON2)," *J. Lightw. Technol.*, vol. PP, no. 99, Aug. 2012.

[80] "The race for NGPON 2 heats up as two contenders stand out." [Online]. Available: http://blogs.informatandm.com/4120/the-race-for-ngpon-2-heats-up-as-two-contenders-stand-out/. [Accessed: 31-Aug-2012].

[81] Peter Vetter, "Tutorial Next Generation Optical Access Technologies," in *Proc. of 38th European Conf. and Exhibit. on Opt. Commun. (ECOC2012)*, 2012, p. Tu.3.G.1.

[82] Frank Effenberger, "XG-PON1 versus NG-PON2: Which One Will Win?," in *Proc. of 38th European Conf. and Exhibit. on Opt. Commun. (ECOC2012),* 2012, p. Tu.4.B.1.

[83] N.-C. Tran, T. Koonen, C. Okonkwo, E. Tangdiongga, "Limited Flexibility: a Cost-Effective Trade-off for Reconfigurable WDM-TDM Optical Access Networks," in *Proc. of 37th European Conf. and Exhibit. on Opt. Commun. (ECOC2011),* 2011, p. We.9.C.4.

[84] N.C Tran, E. Tangdiongga, C.M. Okonkwo, H.D. Jung, and A.M.J Koonen, "Flexibility Level Adjustment in Reconfigurable WDM-TDM Optical Access Networks," *J. Lightw. Technol.*, vol. 30, no. 15, pp. 2542–2550.

[85] N.M.M.K. Chowdhury, and R. Boutaba, "Network virtualization: state of the art and research challenges," *IEEE Commun. Mag.*, vol. 47, no. 7, pp. 20–26, Jul. 2009.

[86] R. Nejabati, E. Escalona, P. Shuping, and D. Simeonidou, "Optical network virtualization," in *Proc. of 15th Int. Conf. on Optical Network Design and Modeling (ONDM 2011),* 2011, pp. 1–5.

[87] V. Sivaraman, C. Russell, I.B. Collings, and A. Radford, "Architecting a national optical fiber open-access network: The Australian Challenge," *IEEE J. Network*, vol. 26, no. 4, pp. 4–10, Aug. 2012.

[88] T. Koonen, K. Steenbergen, F. Janssen, and J. Wellen, "Flexibly Reconfigurable Fiber-Wireless Network using Wavelength Routing Techniques: The ACTS Project AC349 PRISMA," *J. of Photonic Netw. Commun.*, vol. 3, no. 3, pp. 297–306, 2001.

[89] G. Puerto, J. Mora, B. Ortega, and J. Capmany, "Selective Multicast in a Dynamic Wavelength Router for DWDM Converged Wired/Wireless Access Networks," in *Proc. of Opt. Fiber Commun.Conf. and Expo. and the National Fiber Opt. Engineers Conf. (OFC/NFOEC 2010)*, 2010, p. OWQ3.

[90] N.-C. Tran, H.-D. Jung, C. Okonkwo, E. Tangdiongga, and T. Koonen, "ARON: A SOA Array-based WDM-TDM Reconfigurable Optical Access Network," in *Proc. of Future Network & Mobile Summit 2010*, Florence, Italy, 2010, pp. 1–7.

[91] G. Das, B. Lannoo, D. Colle, M. Pickavet, M., and P. Demeester, “A hybrid WDM/TDM PON architecture using wavelength selective switches,” in *Proc. of 4th Int. Sym. on Adv. Netw. and Telecom. Sys.*, 2010, pp. 52–54.

[92] N.-C. Tran, H.-D. Jung, C. Okonkwo, E. Tangdiongga, and T. Koonen, “A 10 Gb/s passive-components-based WDM-TDM reconfigurable optical access network architecture,” in *Proc. of Opt. Fiber Commun. Conf. and Expo. and the National Fiber Opt. Engineers Conf. (OFC/NFOEC 2011)*, 2011, p. OThT1.

[93] R. Glatty, P. Guignard, and P. Chanclou, “Flexibility in Access Networks□: a Novel WDMA/TDMA Scheme for Passive Optical Networks,” in *Proc. of Opt. Fiber Commun.Conf. and Expo. and the National Fiber Opt. Engineers Conf. (OFC/NFOEC 2007)*, 2007, p. JThA77.

[94] P. J. Urban, B. Huiszoon, R. Roy, M. M. de Laat, F. M. Huijskens, E. J. Klein, G. D. Khoe, A. M. J. Koonen, and H. de Waardt, “High-Bit-Rate Dynamically Reconfigurable WDM–TDM Access Network,” *J. Opt. Commun. Netw.*, vol. 1, no. 2, pp. A143 – A158, Jul. 2009.

[95] P.J. Urban, F.M. Huijskens, G.D. Khoe, A.M.J Koonen, and H. de Waardt, “Reconfigurable WDM/TDM Access Network Providing 10-Gb/s/ Over 27-km SSMF With Colorless ONU,” *IEEE Photonics Technol. Letters*, vol. 21, no. 23, pp. 1758–1760, Dec. 2009.

[96] P. Ossieur et. al., “Demonstration of a 32 × 512 Split, 100 km Reach, 2 × 32 × 10 Gb/s Hybrid DWDM-TDMA PON Using Tunable External Cavity Lasers in the ONUs,” *J. Lightw. Technol.*, vol. 29, no. 24, pp. 3705–3718, Dec. 2011.

[97] “One-way transmission time.” ITU-T Recommendation G.114, May-2003.

[98] “TR 22.976 - Study on Release 2000 services and capabilities.” Third Generation Partnership Project (3GPP), Jun-2000.

[99] L. Hsueh, M.S. Rogge, S. Yamamoto, and L.G. Kazovsky, “A highly flexible and efficient passive optical network employing dynamic wavelength allocation,” *J. of Lightw. Techno.*, vol. 23, no. 1, pp. 277 – 286, 2005.

[100] C. Bock, J. Prat, and S.D. Walker, “Hybrid WDM/TDM PON Using the AWG FSR and Featuring Centralized Light Generation and Dynamic Bandwidth Allocation,” *J. of Lightw. Technol.*, vol. 23, no. 12, p. 3981, 2005.

[101] A.M.J. Koonen, N.-C. Tran, E. Tangdiongga,, “The Merits of Reconfigurability in WDM-TDM Optical In-Building Networks,” in *Proc. of Opt. Fiber Commun.Conf. and Expo. and the National Fiber Opt. Engineers Conf. (OFC/NFOEC 2011)*, 2011, p. JWA63.

[102] “TRAMMS IP Traffic report no 2,” Traffic Measurements and Models in Multi-Service Networks (TRAMMS) Project, Jun-2008.

[103] “FTTH/B Panorama Europe at December 2011.” FTTH Council Europe, Dec-2011.

[104] “88-channel 50GHz AWG Datasheet.” Enablence Technologies Inc., 2010.

[105] N.-C. Tran, C. Okonkwo, E. Tangdiongga, H.D. Jung, and A.M.J. Koonen, "CLBP Flexibility: an Architectural Approach for Reconfigurable Optical WDM-TDM Access Networks," *J. Opt. Commun. Netw.*, To be appeared early 2013.

[106] Pat Iannone, and Ken Reichman, "Strategic and Tactical Uses for Extended PON," Opt. Fiber Commun.Conf. and Expo. and the National Fiber Opt. Engineers Conf. (OFC/NFOEC 2008), Mar-2008.

[107] Tatiana Yakusheva, "The Way Forward Towards Next Generation Converged Access Network," 38th European Conf. and Exhibit. on Opt. Commun. (ECOC2012), Sep-2012.

[108] M.J. Wale, "Options and trends for PON tunable optical transceivers," in *Proc. of 37th European Conf. and Exhibit. on Opt. Commun. (ECOC2011)*, 2011.

[109] S.H. Lee, A. Wonfor, R.V. Penty, I.H. White, G. Busico, R. Cush, R., and M. Wale, "Athermal colourless C-band optical transmitter for passive optical networks," in *Proc. of 36th European Conf. and Exhibit. on Opt. Commun. (ECOC2010)*, 2010, p. Mo.1.B.2.

[110] W. Pohlmann, and T. Pfeiffer, "Demonstration of wavelength-set division multiplexing for a cost effective PON with up to 80 Gbit/s upstream bandwidth," in *Proc. of 37th European Conf. and Exhibit. on Opt. Commun. (ECOC2011)*, 2011, p. We.9.C.1.

[111] N.D. Whitbread et. al., "AlGaInAs-InP C-band tunable DS-DBR laser for semi-cooled operation at 55°C," in *Proc. of 34th European Conf. and Exhibit. on Opt. Commun. (ECOC2008)*, 2008, p. We.3.C.4.

[112] M. Roppelt, M. Eiselt, K. Grobe, and J.-P Elbers, "Tuning of an SG-Y Branch Laser for WDM-PON," in *Proc. of Opt. Fiber Commun.Conf. and Expo. and the National Fiber Opt. Engineers Conf. (OFC/NFOEC 2012)*, 2012, p. OW1B.4.

[113] M. Roppelt, F. Pohl, K. Grobe, M. Eiselt, and J. Elbers, "Tuning methods for uncooled low-cost tunable lasers in WDM-PON," in *Proc. of Opt. Fiber Commun.Conf. and Expo. and the National Fiber Opt. Engineers Conf. (OFC/NFOEC 2011)*, 2011, p. NTuB1.

[114] R. Murano, W.F. Sharfin, M. Cahill, and J. Wernlund, "Tunable GPON receivers enable phased migration to 1Gb/s per subscriber," in *Proc. of Opt. Fiber Commun.Conf. and Expo. and the National Fiber Opt. Engineers Conf. (OFC/NFOEC 2009)*, 2009, p. NME4.

[115] R. Murano, and M.J.L. Cahill, "Low Cost Tunable Receivers for Wavelength Agile PONs," in *Proc. of 38th European Conf. and Exhibit. on Opt. Commun. (ECOC2012)*, 2012, p. We.2.B.3.

[116] J. R. Martijn et. al., "Monolithic AWG-based Discretely Tunable Laser Diode With Nanosecond Switching Spee," *IEEE Photonics Technol. Letters*, vol. 21, no. 13, pp. 905–907, Jul. 209AD.

[117] "(XG-PON): Transmission convergence (TC) layer specification." ITU-T Recommendation G.987.3, Otc-2010.

[118] W.E. Leland, M.S. Taqqu, W. Willinger, and D.V. Wilson, "On the self-similar nature of Ethernet traffic (extended version)," *IEEE/ACM Trans. on Networking*, vol. 2, no. 1, pp. 1–15, Feb. 1994.

[119] W. Willinger, M.S. Taqqu, R. Sherman, and D.V. Wilson, “Self-similarity through high-variability: statistical analysis of Ethernet LAN traffic at the source level,” *IEEE/ACM Trans. on Networking*, vol. 5, no. 1, pp. 71–86, Feb. 1997.

[120] A. Holt, “Long-range dependence and self-similarity in WWW proxy cache references,” *IEE Proc. on Commun.*, vol. 147, no. 6, pp. 317–321, Dec. 2000.

[121] N.-C. Tran, H.-D. Jung, C. Okonkwo, E. Tangdiongga, and T. Koonen, “PROaccess: A Passive-Components-based Reconfigurable WDM-TDM Optical Access Network,” in *Proc. of the Future Network & Mobile Summit 2011*, Warsaw, Poland, 2011, pp. 1–7.

[122] P. J. Urban, A. M. J. Koonen, G. D. Khoe, and H. de Waardt, “Mitigation of Reflection-induced Crosstalk in a WDM Access Network,” in *Proc. of Opt. Fiber Commun.Conf. and Expo. and the National Fiber Opt. Engineers Conf. (OFC/NFOEC 2008)*, 2008, p. OThT3.

[123] D. C. Kim et. al., “10 Gbps SOA-REAM using Monolithic Integration of Planar Buried-Heterostructure SOA with Deep-Ridge Waveguide EA Modulator for Colourless Optical Source in WDM-PON,” in *Proc. of 37th European Conf. and Exhibit. on Opt. Commun. (ECOC2011)*, Geneva, 2011, pp. 1–3.

[124] J. Bauwelinck, B. Schrenk, C. Kazmierski, J.A. Lazaro, J. Prat, and X.Z. Qiu, “Multi-Operability and Dynamic Bandwidth Allocation in PONs with Electrically Reconfigurable SOA/REAM-Based ONUs,” in *Proc. of 37th European Conf. and Exhibit. on Opt. Commun. (ECOC2010)*, Torino Italy, 2010, p. Th.10.B.4.

[125] Y. Lin, N. Rahmanian, S.H. Kim, G.P. Nordin, C. Topping, D.W. Smith, and J. Ballato, “Ultracompact AWG Using Air-Trench Bends With Perfluorocyclobutyl Polymer Waveguides,” *J. of Lightw. Technol.*, vol. 26, no. 17, pp. 3062–3070, Sep. 2008.

[126] E. Ciaramella, “Wavelength Conversion and All-Optical Regeneration: Achievements and Open Issues,” *J. Lightw. Technol.*, vol. 30, no. 4, pp. 572–582, Feb. 2012.

[127] Y. Awaji, H. Furukawa, B.J. Puttnam, N. Wada, P. Chan, and R. Man, “Burst-mode optical amplifier,” in *Proc. of Opt. Fiber Commun.Conf. and Expo. and the National Fiber Opt. Engineers Conf. (OFC/NFOEC 2010)*, 2010, p. OThI4.

[128] J. S. Barton et. al., “10 Gb/s wavelength conversion using a widely tunable series push-pull photocurrent-driven transmitter,” *IEEE Photonics Technol. Letters*, vol. 17, no. 9, pp. 1902–1904, Sep. 2005.

[129] M.N. Sysak et al., “Single-chip wavelength conversion using a photocurrent-driven EAM integrated with a widely tunable sampled-grating DBR laser,” *IEEE Photonics Technol. Letters*, vol. 16, no. 9, pp. 2093–2095, Sep. 2004.

[130] X. Yin et al., “A 10Gb/s APD-Based Linear Burst-Mode Receiver with 31dB Dynamic Range for Reach-Extended PON Systems,” in *Proc. of 38th European Conf. and Exhibit. on Opt. Commun. (ECOC2012)*, 2012, p. Tu.1.B.5.

[131] K. Zhou, M. Dubov, C. Mou, L. Zhang, V.K. Mezentsev, and I. Bennion, “Line-by-Line Fiber Bragg Grating Made by Femtosecond Laser,” *IEEE Photonics Technol. Letters*, vol. 22, no. 12, pp. 1190–1192, Aug. 2010.

[132] “MEL - OFC2012 brochures.” MEL Inc., Mar-2012.

[133] D. Payne, “Evolvable, sustainable, low power optical network architectures,” in *Proc. of 37th European Conf. and Exhibit. on Opt. Commun. (ECOC2011)*, 2011, p. We.8.C.1.

[134] N.-C. Tran, C. Okonkwo, E. Tangdiongga, and T. Koonen, “Cost-effective and Scalable Architecture for Moving Cell Application Employing Integrable Tunable Laser Assembly,” in *Proc. of Opt. Fiber Commun. Conf. and Expo. and the National Fiber Opt. Engineers Conf. (OFC/NFOEC 2012)*.

[135] A.R. Mishra, *Fundamentals of Cellular Network Planning and Optimisation: 2G/2.5G/3G... Evolution to 4G*. Wiley-Interscience, 2004.

[136] J.C. Attard and J.E. Mitchell, “Optical network architectures for dynamic reconfiguration of full duplex, multiwavelength, radio over fiber,” *J. of Opt. Netw.*, vol. 5, no. 6, pp. 435–444, 2006.

[137] T. Koonen, A. Ng’oma, M.G. Larrode, F. Huijskens, I.T. Monroy, and G.-D. Khoe, “Novel Cost-Efficient Techniques for Microwave Signal Delivery in Fibre-Wireless Networks,” in *Proc. of 37th European Conf. and Exhibit. on Opt. Commun. (ECOC2004)*, 2004.

[138] S-E. Elayoubi, O. Ben Haddada, and B. Fouresti´e, “Performance evaluation of frequency planning schemes in OFDMA-based networks,” *IEEE Trans. on Wireless Commun.*, vol. 7, no. 5, pp. 1623–1633, May 2008.

[139] D. L. Perez, A. Juttner, J. Zhang, “Dynamic Frequency Planning Versus Frequency Reuse Schemes in OFDMA Networks,” in *Proc. of Vehicular Technol. Conf. (VTC2009)*, 2009, pp. 1–5.

[140] Can Desem, “Optical Interference in Subcarrier Multiplexed Systems with Multiple Optical Carriers,” *IEEE J. of Sel. Areas in Commun.*, vol. 8, no. 7, pp. 1290 – 1295, Sep. 1990.

[141] M.D. McKinley et al., “EVM Calculation for Broadband Modulated Signals,” in *Proc. of ARFTG Microwave Measurement Conf.*, 2004, pp. 45–52.

[142]“Preliminary datasheet - 60-R-EAM-1550.” CIP Technologies, 2009.

[143] H. Wang, A. Wonfor, K.A Williams, RV. Penty, and I.H. White, “Demonstration of a Lossless Monolithic 16x16 QW SOA Switch,” in *Proc. of 37th European Conf. and Exhibit. on Opt. Commun. (ECOC2009)*, 2009, pp. 1–2.

[144] A. Albores-Mejia et al., “160 Gbit/s line-rate data routing through monolithic multi-stage optical switch circuit,” *Electronics Letter*, vol. 46, no. 17, pp. 1209–1211, Aug. 2010.

[145] Bart Lannoo, Didier Colle, Mario Pickavet, and Piet Demeester, “Radio-over-Fiber-Based Solution to Provide Broadband Internet Access to Train Passengers,” *IEEE Commun. Mag.*, pp. 56–62, Feb. 2007.

[146] C.-H. Yeh et al., “Theory and Technology for Standard WiMAX Over Fiber in High Speed Train Systems,” *J. Lightw. Technol.*, vol. 28, no. 16, pp. 2327–2336, Aug. 2010.

[147] Y.-T. Hsueh, M.-F. Huang, M. Jiang, Y. Shao, K. Kim, and G.-K. Chang, “A Novel Wireless over Fiber Access Architecture Employing Moving Chain Cells and RoF

Technique for Broadband Wireless Applications on the Train Environment," in *Proc. of Opt. Fiber Commun.Conf. and Expo. and the National Fiber Opt. Engineers Conf. (OFC/NFOEC 2011)*, p. OWT3.

[148] J. Hutchins and Karl Gass, "Integratable Tunable Laser Assembly Multi Source Agreement." Optical Internetworking Forum (OIF), 15-Jun-2004.

[149] "100GHz Dual Channel OADM (3x3)." AC Photonics Inc., 2010.

[150] A. Rottinghaus, R. Hariharan, Xingang Guo, A. Rangarajan, R. Avivi, A. Busch, and B. Conner, "Supporting High Speed on WiMAX: From Theory to Practice," in *Proc. of Vehicular Technol. Conf. (VTC2011)*, 2011, pp. 1–6.

List of Publications

Journals

[1] **N.C Tran**, J. Bauwelinck, E. Tangdiongga, C.M. Okonkwo, and A.M.J Koonen, "*Long-Reach Reconfigurable TWDM Optical Access Network without Wavelength Tuning based on Cyclic-Linked Flexibility*," J. of Opt. Commun. and Netw., in preparation.

[2] **N.C Tran**, J. Bauwelinck, E. Tangdiongga, and A.M.J Koonen, "*Demonstration of Long-Reach PON Using 10Gb/s 3R Burst-Mode Wavelength Converter for Metro-Access Convergence,"* Photonics Technol. Letters, submitted, Feb. 2013

[3] **N.C Tran**, E. Tangdiongga, C.M. Okonkwo, and A.M.J Koonen, *"CLBP Flexibility: an Architectural Approach for Reconfigurable Optical WDM-TDM Access Networks,"* J. of Opt. Commun. and Netw., accepted, Jan. 2013.

[4] **N.C Tran**, E. Tangdiongga, C.M. Okonkwo, H.D. Jung, and A.M.J Koonen, *"Flexibility Level Adjustment in Reconfigurable WDM-TDM Optical Access Networks,"* J. of Lightw. Technol., vol. 30, no. 15, pp. 2542-2550, 2012.

[5] **N.C. Tran,** H.D. Jung, C.M. Okonkwo, E. Tangdiongga, and A.M.J Koonen, *"Dynamically delivering radio signals by the active routing optical access network,"* Photonics Technol. Letters, vol. 24, no. 3, pp. 182-184, 2012.

[6] M.K. Hong, **N.C. Tran,** Y. Shi, Y., E. Tangdiongga, S.K. Han, and A.M.J. Koonen, *"10-Gb/s transmission over 20-km single fiber link using 1-GHz RSOA by discrete multitone with multiple access,"* Optics Express, vol. 19, no. 26, B486-B495, 2011.

Conferences

[7] **N.C. Tran,** C.M. Okonkwo, E. Tangdiongga, and A.M.J Koonen, *"Cost-effective and scalable architecture for moving cell application employing integrable tunable laser assembly,"* in Proc. of Opt. Fiber Commun.Conf. and Expo. and the National Fiber Opt. Engineers Conf. (OFC/NFOEC 2012), pp. OTu2H.7, 4-8 Mar. 2012, Los Angeles, California.

[8] A.M.J. Koonen, Y. Shi, **N.C. Tran,** C.M. Okonkwo, H.P.A Boom, and E. Tangdiongga, *"A perspective from Europe on in-home networking,"* in Proc. of Opt. Fiber Commun.Conf. and Expo. and the National Fiber Opt. Engineers Conf. (OFC/NFOEC 2012), pp. Nth1D, 4-8 Mar. 2012, Los Angeles, California. (Invited)

[9] S.H. Zou, C.M. Okonkwo, Z.Z. Cao, **N.C. Tran**, and E. Tangdiongga, and A.M.J. Koonen, *"Dynamic Optical Routing and Simultaneous Generation of Millimeter-Wave Signals for In-Building Access Network,"* in Proc. of Opt. Fiber Commun.Conf. and Expo. and the National Fiber Opt. Engineers Conf. (OFC/NFOEC 2012), pp. OTh3G, 4-8 Mar. 2012, Los Angeles, California.

[10] **N.C. Tran,** A.M.J. Koonen, C.M. Okonkwo, and E. Tangdiongga, *"Limited Flexibility: a Cost-Effective Trade-off for Reconfigurable WDM-TDM Optical Access*

Networks," in Proc. of 37th European Conf. and Exhibit. on Opt. Commun. (ECOC2011), pp. We.9.C.4, 18 - 22 Sep. 2011, Geneva, Switzerland.

[11] M.K. Hong, **N.C. Tran,** Y. Shi, E. Tangdiongga, and A.M.J Koonen, *"10Gb/s Transmission over 20km Single Fiber Link using 1GHz RSOA by Discrete Multitone with Multiple Access,"* in Proc. of 37th European Conf. and Exhibit. on Opt. Commun. (ECOC2011), pp. Th.11.C3, 18 - 22 Sep. 2011, Geneva, Switzerland.

[12] **N.C. Tran,** E. Tangdiongga, and A.M.J. Koonen, "*PROaccess : a passive-components-based reconfigurable WDM-TDM optical access network,*" in Proc. of the Future Netw. & Mobile Summit, 15 - 17 Jun. 2011, Warsaw, Poland.

[13] A.M.J. Koonen, C.M. Okonkwo, Y. Shi, H.P.A. Boom, **N.C. Tran**, E. Tangdiongga, "*Recent research advancements in in-building optical networks,"* in Proc. of the 13th Int. Conf. on Transparent Opt. Netw. (ICTON), pp. Tu.A5.1, 26-30 Jun. 2011, Stockholm, Sweden. (Invited)

[14] **N.C. Tran**, H.D. Jung, C.M. Okonkwo, E. Tangdiongga, and A.M.J. Koonen, *"A 10 Gb/s passive-components-based WDM-TDM reconfigurable optical access network architecture,"* in Proc. of Opt. Fiber Commun.Conf. and Expo. and the National Fiber Opt. Engineers Conf. (OFC/NFOEC 2012), pp. OThT1, 6-10 Mar. 2011, Los Angeles, California.

[15] S.T. Abraha, **N.C. Tran**, C.M. Okonkwo, H.S. Chen, E. Tangdiongga, and A.M.J. Koonen, *"Service multicasting by all-optical routing of 1 Gb/s IR-UWB for in-building networks,"* in Proc. of Opt. Fiber Commun.Conf. and Expo. and the National Fiber Opt. Engineers Conf. (OFC/NFOEC 2012), pp. JWA68, 6-10 Mar. 2011, Los Angeles, California.

[16] A.M.J. Koonen, N**.C. Tran**, and E. Tangdiongga, *"The Merits of Reconfigurability in WDM-TDM Optical In-Building Networks,"* in Proc. of Opt. Fiber Commun.Conf. and Expo. and the National Fiber Opt. Engineers Conf. (OFC/NFOEC 2011), p. JWA63, 6-10 Mar. 2011, Los Angeles, California.

[17] H.D. Jung, **N.C. Tran**, E. Tangdiongga, and A.M.J. Koonen, *"New architecture for reconfigurable WDM-PON networks based on SOA gating array,"* in Proc. of the 9th Int. Conf. on Opt. Internet (COIN), 11-14 Jul. 2010, Jeju, South Korea.

[18] **N.C. Tran**, H.D. Jung, C.M. Okonkwo, E. Tangdiongga, and A.M.J. Koonen, "*ARON: A SOA array-based WDM-TDM reconfigurable optical access network"* in Proc. of the Future Netw. & Mobile Summit 2010, 16-18 Jun. 2010, Florence, Italy.

[19] H.D. Jung, **N.C. Tran**, C.M. Okonkwo, E. Tangdiongga, A.M.J Koonen, *"10Gb/s bi-directional symmetric WDM-PON system based on POLMUX technique with polarization insensitive ONU,"* in Proc. of Opt. Fiber Commun. Conf. and Expo. and the National Fiber Opt. Engineers Conf. (OFC/NFOEC 2010), pp. JThA27, 21-25 Mar. 2010, San Diego, California.

ACKNOWLEDGEMENT

A wise man once said: “When you are around, it is just a place to stay but when you leave, it becomes a part of your soul”. I have been with the Electro-Optical Communication (ECO) group for four years and the moment is just around the corner.

First of all, I would like to thank my promoter Prof. Ton Koonen for giving me the opportunity to conduct my research in the ECO group at Eindhoven University of Technology. This is a unique chance to work in a world-leading group with knowledgeable colleagues ranging across many disciplines. I am very grateful to him for his guidance which not only kept me on track but also allowed room to stimulate my creativity. During the course of my PhD, I have been supervised by Dr. Hyun-Do Jung, Dr. Eduward Tangdiongga, and Dr. Chigo Okonkwo. I am thankful to Hyun-Do for his valuable instructions, especially on setting up an experiment in which collecting equipments seems to be the most challenging part. I would like to thank Eduward for his valuable comments and advice which helped to strengthen my results. I am very grateful to Chigo for the fruitful discussions and for his effort to correct my poor English.

I would like to thank my PhD examination committee members who accepted to be in the committee in spite of their very tight schedule.

I am thankful to my peer PhD candidates Aaron, Abhinav, Davide, Haoshuo, Heije, Jim, Jun, Karen, Kotian, Moon, Nikos, Pang, Pinxiang, Prometheus, Roy, Solomon, Stefano, Vlado, and Yan. Together with them, I have gone through all the emotional phases of a PhD candidate from frustration and desperation to optimism and cheerfulness. I will never forget our lunch conversations, our international dinners, and our joyful trips to the conferences.

I received a lot of support from the group-mates, secretaries, technicians, friends, students, and APLHA project members. It is simply impossible to mention all of you by name here. Without you, my experiments would never work, my simulations would never run, and my life would be much more difficult.

I am deeply indebted to my family for their unconditional love, support, and inspiration. My special thanks go to Huyen, my beloved wife and Lien, my little daughter.

ABOUT THE AUTHOR

Nguyen-Cac (Karl) TRAN was born in Hanoi, Vietnam, on June 18^{th}, 1982. He received his B.Eng. degree in Electronics and Telecommunications from Hanoi University of Technology in 2005. He worked for Vietnam Telecoms National from Aug. 2005 to Mar. 2006. He completed his M.Sc. in Korea University, South Korea under the Korean Government IITA grant between Mar. 2006 to Feb. 2008. His Master's thesis reported a study on ROADM-enable optical metro network designs to natively support Ethernet services. Following that, he started to work for Panasonic R&D Center, Vietnam as a scientific assistant to the director.

In April 2009, he started working towards the Ph.D. degree at Eindhoven University of Technology in the framework of the European ALPHA project. The research is focused on reconfigurable optical access networks to support convergent wired and wireless services. He proposed a concept of cyclically-linked flexibility that can perform wavelength reconfigurability without wavelength tuning. The concept was realized into four different physical architectures, each addressing a different deployment scenario. He also proposed reconfigurable architectures to natively support radio signal delivery. His works are very much appreciated by the industry.

He has published and presented significant results in top scientific journals (PTL, JLT, and JOCN) and at major international conferences (OFC/NFOEC and ECOC). He is a member of the IEEE and serves actively as a reviewer for IEEE and OSA journals.